

# Microscopic radiation damage in semiconductor detectors

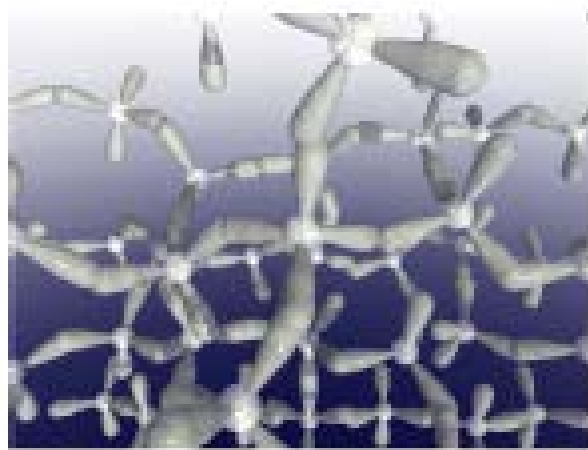
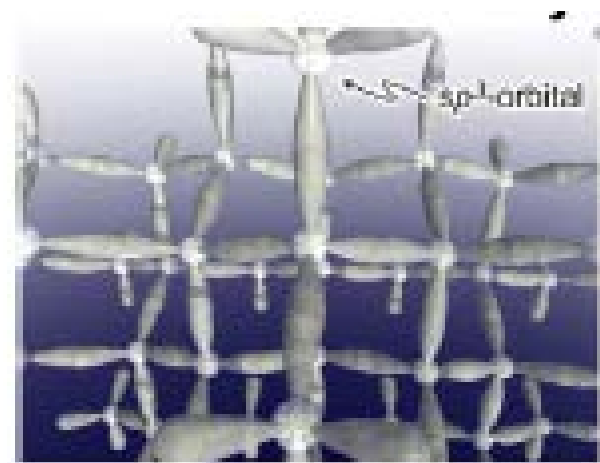
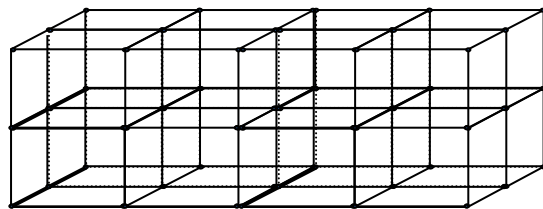
M. Bruzzi  
INFN Sezione Firenze  
Università di Firenze, Italy

# Outline

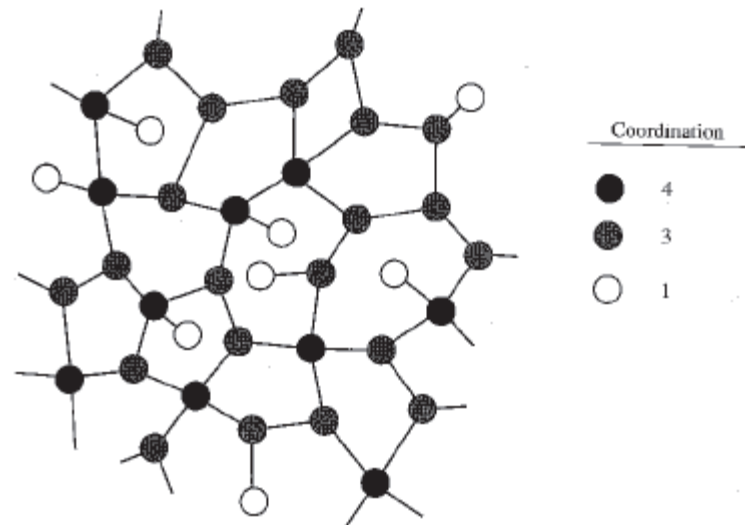
- Introduction to crystals and defects
- Microscopic radiation damage
- Defect spectroscopy in semiconductors
- Defect engineering strategies
- Influence of deep levels on device properties
  - Detector for high energy physics experiments
  - Dosimeters for clinical radiotherapy applications

# Solid-state structures

**Crystalline : Long-range order and periodic structure**

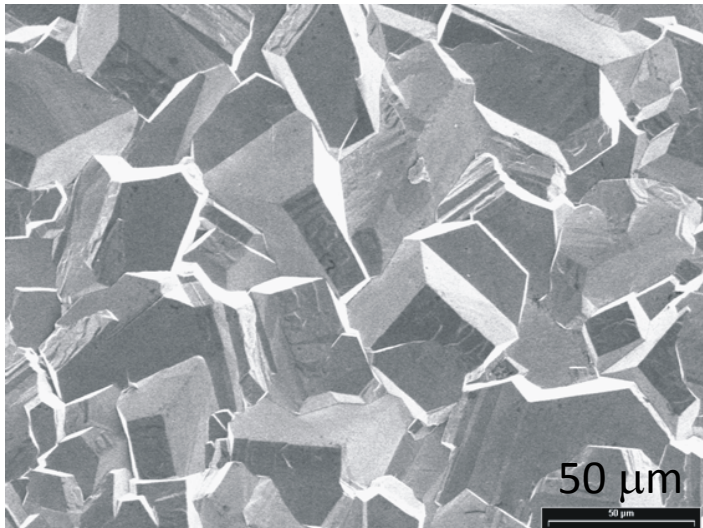


**Amorphous:** short-range ordered structure. Energetically higher than the corresponding ordered structure.

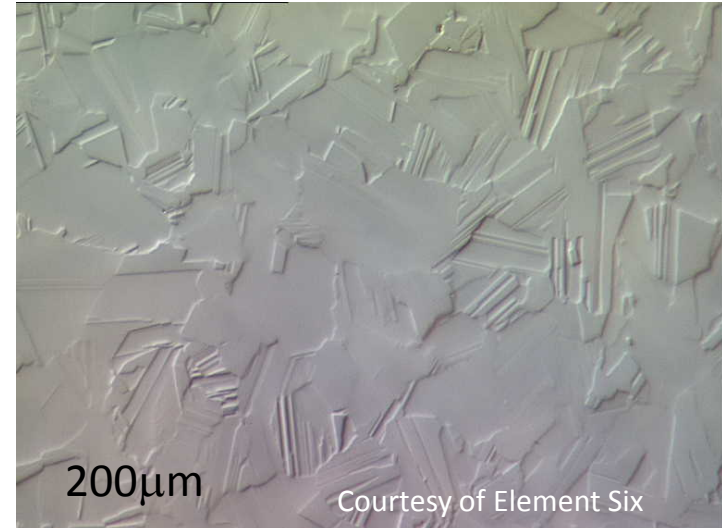


# Polycrystalline structures

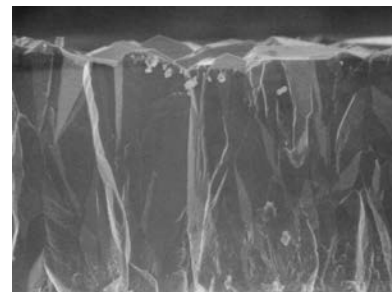
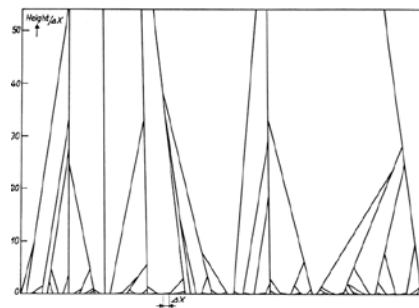
## example: synthetic (Chemical Vapour Deposited) Diamond



After polishing and  
Material removal



- Columnar growth – increased quality at growth side



CVD diamond made in Florence

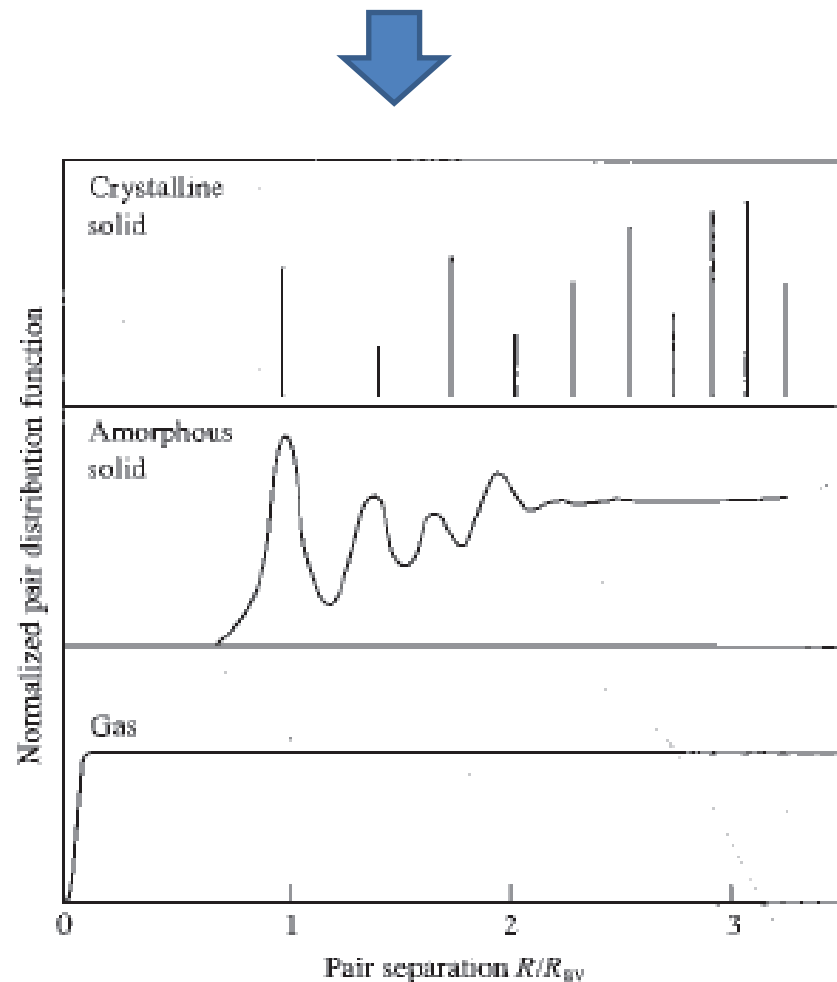
## Microscopic Disorder: short and long range order

Distribution function of the average distance  $R$  between pairs of atoms in the material.

Gas: Relative positions completely random  
→ distribution function constant;

Crystalline solid: only certain values of  $R$  are possible → distribution is different from zero only for a set of discrete  $R$

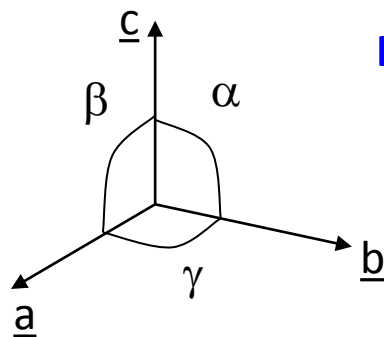
Amorphous solid: a short range order is present due to coordination through bondings → distribution function shows broaden peaks corresponding to first  $R$  values of the corresponding crystalline lattice, for higher  $R$  tends to be constant.



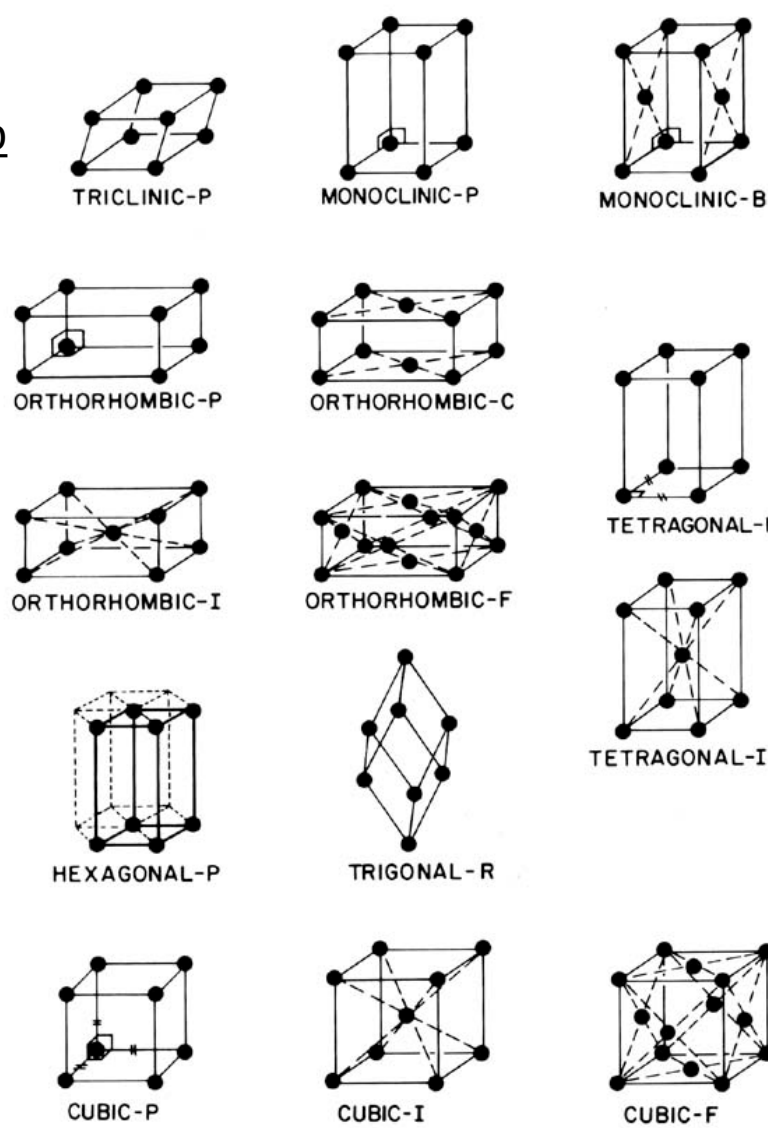
# Crystalline Structures

## Primitive lattices (7)

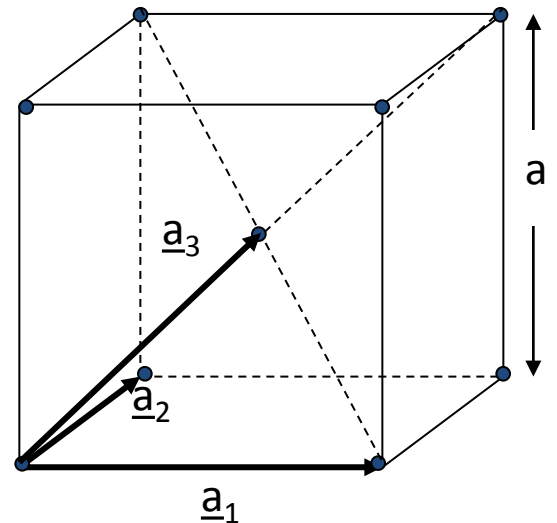
|                                |                                                                        |
|--------------------------------|------------------------------------------------------------------------|
| <b>Triclinico</b>              | $a \neq b \neq c \quad \alpha \neq \beta \neq \gamma$                  |
| <b>Monoclinico</b>             | $a \neq b \neq c$<br>$\alpha = \beta = 90^\circ \neq \gamma$           |
|                                | $\alpha = \gamma = 90^\circ \neq \beta$                                |
| <b>Ortorombico</b>             | $a \neq b \neq c \quad \alpha = \beta = \gamma = 90^\circ$             |
| <b>Tetragonale</b>             | $a = b \neq c$<br>$\alpha = \beta = \gamma = 90^\circ$                 |
| <b>Esagonale</b>               | $a = b \neq c$<br>$\alpha = \beta = 90^\circ \quad \gamma = 120^\circ$ |
| <b>Romboedrico o trigonale</b> | $(a = b = c; \alpha = \beta = \gamma \neq 90^\circ)$                   |
| <b>Cubico</b>                  | $a = b = c$<br>$\alpha = \beta = \gamma = 90^\circ$                    |



## Bravais lattices (14)



## Body centered cubic lattice



(bcc)

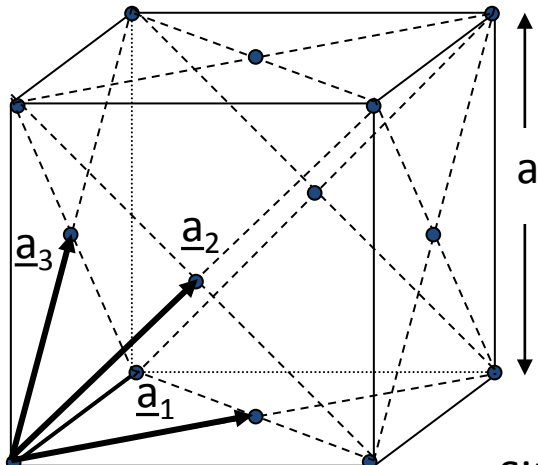
$$\underline{a}_1 = a \underline{u}_x$$

$$\underline{a}_2 = a \underline{u}_y$$

$$\underline{a}_3 = a/2 (\underline{u}_x + \underline{u}_y + \underline{u}_z)$$

$$\text{Sites per cell} = 8/8 + 1 = 2$$

## Face centered cubic lattice



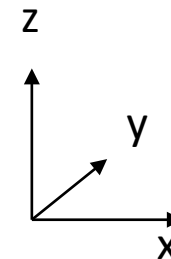
(fcc)

$$\underline{a} = a/2 (\underline{u}_x + \underline{u}_y)$$

$$\underline{b} = a/2 (\underline{u}_x + \underline{u}_z)$$

$$\underline{c} = a/2 (\underline{u}_y + \underline{u}_z)$$

$$\text{Sites per cell} = 8/8 + 6/2 = 4$$

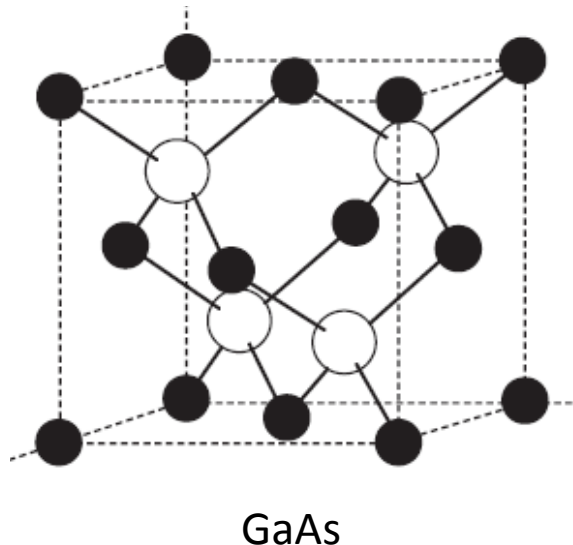
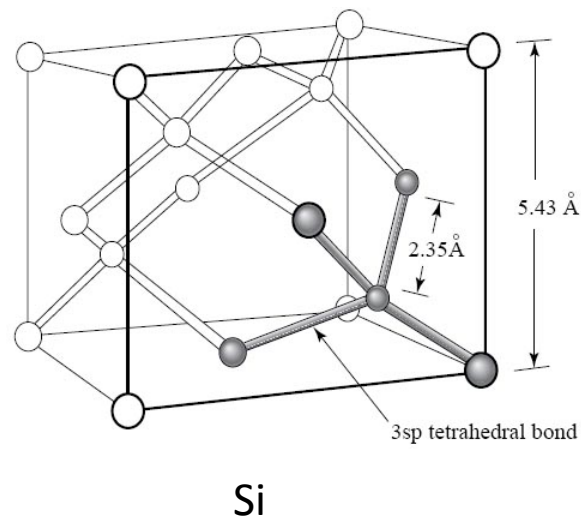


| BCC | FCC |
|-----|-----|
|     | Ar  |
| Fe  | Ag  |
| Li  | Al  |
| W   | Au  |
| Na  | Ca  |
| K   | Cu  |
| Cr  | Pb  |

## Lattice with basis: Diamond

FCC with base 2:  $(0; a/4 (u_x + u_y + u_z))$ .

Two FCC lattices interpenetrated by  $\frac{1}{4}$  of the body diagonal



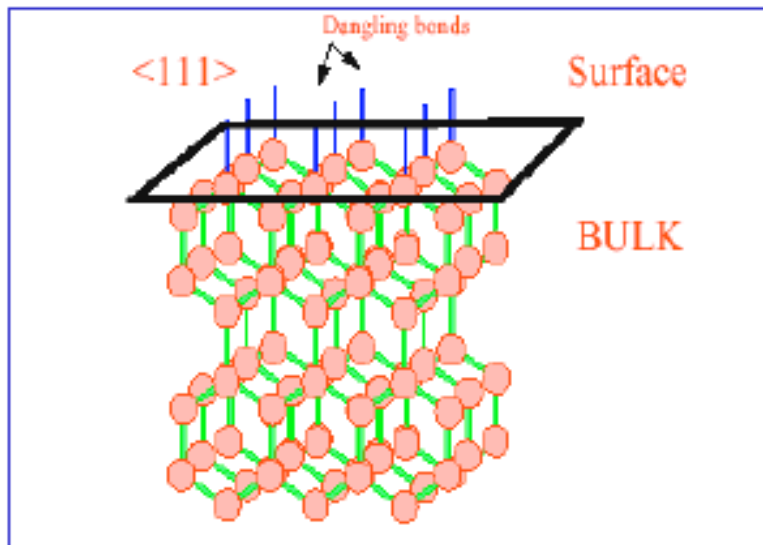
| Material      | $a (\text{\AA})$ |
|---------------|------------------|
| C ( diamond ) | 3.57             |
| Si            | 5.43             |
| Ge            | 5.66             |
| $\alpha$ -Sn  | 6.49             |
| ZnS           | 5.41             |
| SiC           | 4.35             |
| GaAs          | 5.65             |

## Surface Damage and Effect of the crystal orientation

Trap and Oxide charge densities  $D_{it}$  and  $N_{ox}$  at the Si-SiO<sub>2</sub> interface

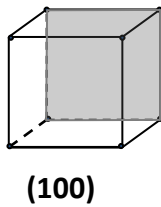
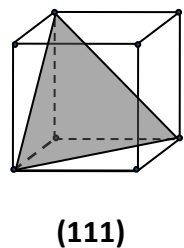
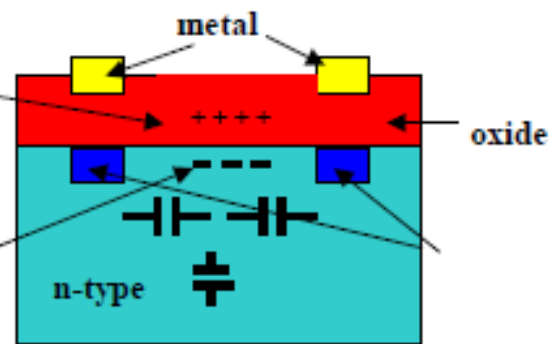
More available dangling bonds at the crystal surface  
in <111> than <100>  $\Rightarrow D_{it<111>} \gg D_{it<100>}$

$$D_{it} = \frac{1}{q} \cdot \frac{dQ_{it}}{dE}$$



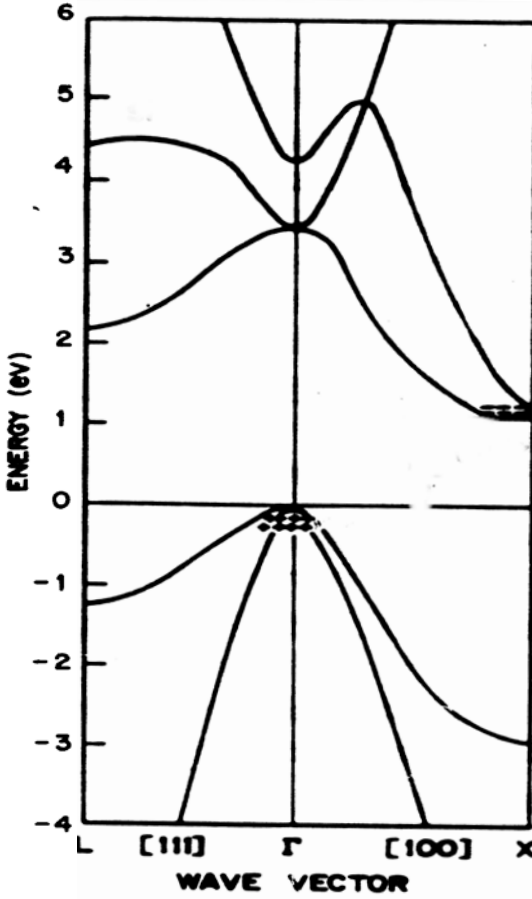
Positive interface charges  $N_{ox}$

Electron layer at the silicon-oxide affecting  $C_{int}$  and  $C_{back}$

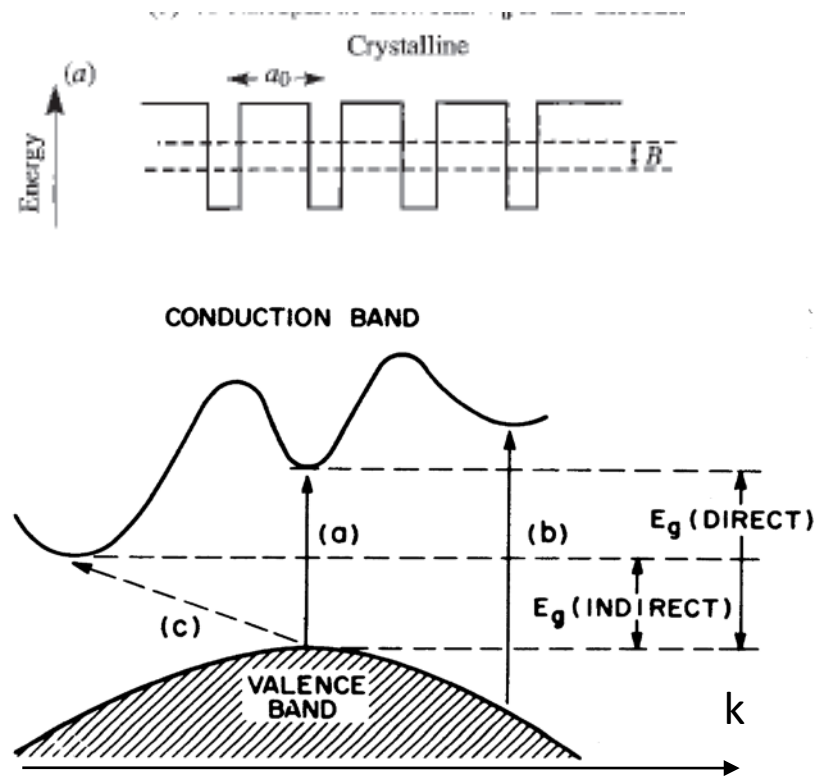


# Bande di energia nei semiconduttori cristallini

Una delle proprietà fondamentali di un semiconduttore / isolante è la presenza del band gap che separa la banda di valenza occupata da quella di conduzione vuota (  $T = 0K$ ). Dalla teoria del potenziale periodico debole il gap risulta come conseguenza della periodicità della struttura cristallina.



Silicio



**GAP DIRETTO** (GaAs) il massimo della banda di valenza  $E_v$  ed il minimo della banda di conduzione  $E_c$  si trovano a stesso  $k$

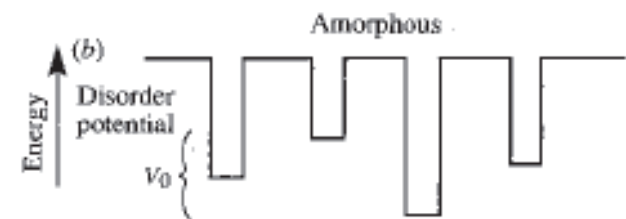
**GAP INDIRETTO:** Si, Ge.

## Struttura elettronica dei semiconduttori amorfi

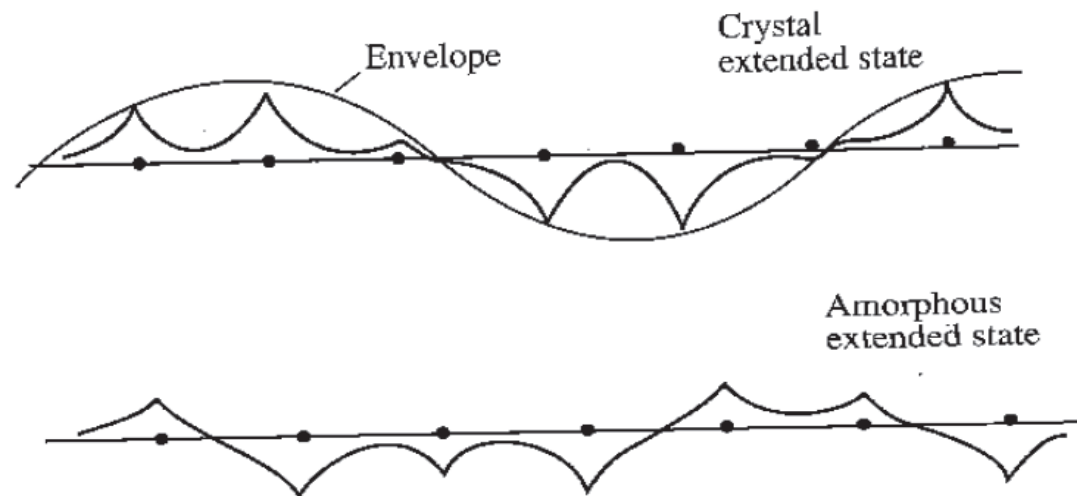
Il cristallo perfetto è descritto con un array di buche di potenziale uguali, lo stato amoro è mostrato come lo stesso array a cui è aggiunto un potenziale casuale con ampiezza media  $V_0$  (modello di Anderson, 1958).

Le funzioni d'onda elettroniche in un reticolo periodico sono date dal teorema di Bloch :

$$\Phi(\underline{r}) = u_k(\underline{r}) \exp(i\underline{k} \cdot \underline{r})$$



$u_k(\underline{r}) = u_k(\underline{r} + \underline{R})$  ha la periodicità del reticolo. Sussiste quindi una relazione di fase costante nei diversi siti reticolari, la funzione d'onda ha un momento ben definito,  $\underline{k}$ , e si estende attraverso tutto il cristallo.



L'effetto del disordine nel materiale amoro causa uno scattering molto frequente tra stati di Bloch

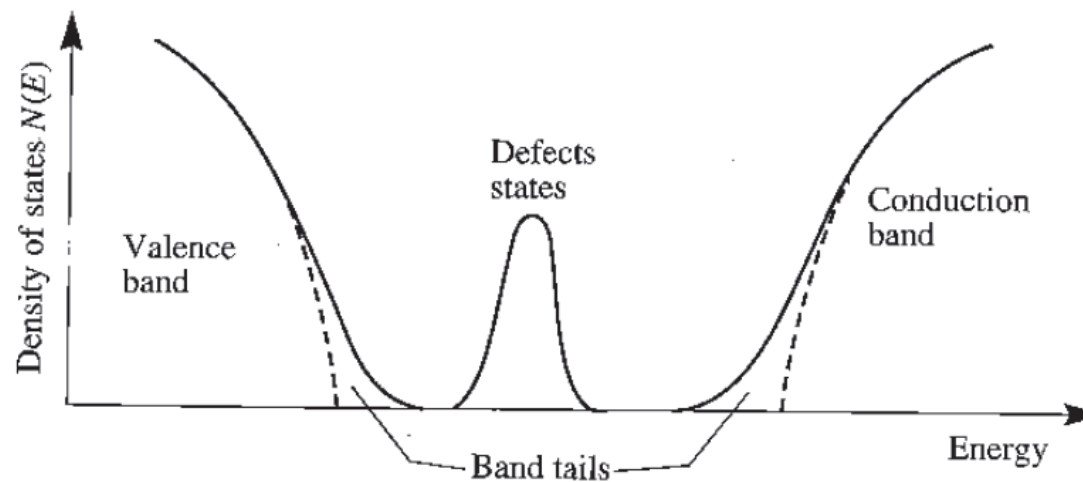
→ l'onda perde di coerenza su distanze dell'ordine di uno o due siti reticolari.

Lo scattering dovuto ai difetti nel materiale amorofo causa grande incertezza nel momento elettronico:

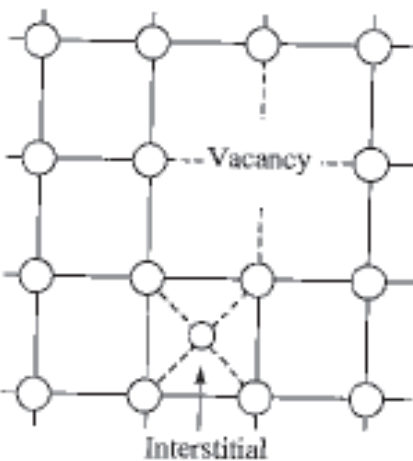
$$\Delta x \Delta p \approx h \quad \rightarrow \Delta k \approx \frac{2\pi}{\Delta x} \approx \frac{2\pi}{a} \approx k$$

$\Delta k \approx k \rightarrow$  *il momento k nel materiale amorofo non si conserva nelle transizioni elettroniche.*

- 1) Le bande di energia degli amorfi non vengono descritte da relazioni di dispersione  $\epsilon, k$  ma in termini di distribuzione delle densità di stati  $N(\epsilon)$ .
- 2) Si perde la distinzione tra gap diretto e indiretto.
- 3) Il disordine riduce la mobilità dei portatori a causa del frequente scattering producendo un profondo effetto di localizzazione delle funzioni d'onda.



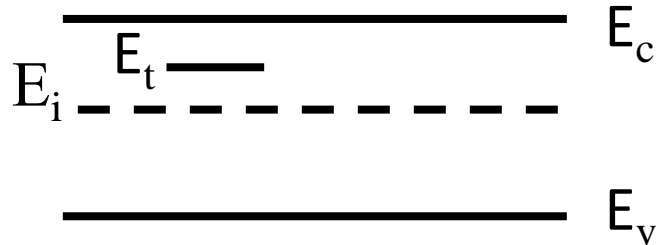
## Defects in a crystalline solid

| Lattice Disorder                                                                                                                                              | Impurities                                                                                                                                                                                                                                             |
|---------------------------------------------------------------------------------------------------------------------------------------------------------------|--------------------------------------------------------------------------------------------------------------------------------------------------------------------------------------------------------------------------------------------------------|
|                                                                               | <p><b>Point defects</b></p> <ul style="list-style-type: none"><li>o Vacancy</li><li>o interstitial</li></ul> <p><b>Point Defects</b></p> <ul style="list-style-type: none"><li>o <b>substitutional (e.g. Dopants)</b></li><li>o interstitial</li></ul> |
| <p><b>Linear defects</b></p> <ul style="list-style-type: none"><li>o <b>dislocations</b></li></ul>                                                            | <p><b>Bulk defects</b></p> <ul style="list-style-type: none"><li>o precipitates</li></ul>                                                                                                                                                              |
| <p><b>Extended defects</b></p> <ul style="list-style-type: none"><li>o <b>grain boundaries</b></li><li>o <b>Interfaces</b></li><li>o <b>Surface</b></li></ul> |                                                                                                                                                                                                                                                        |

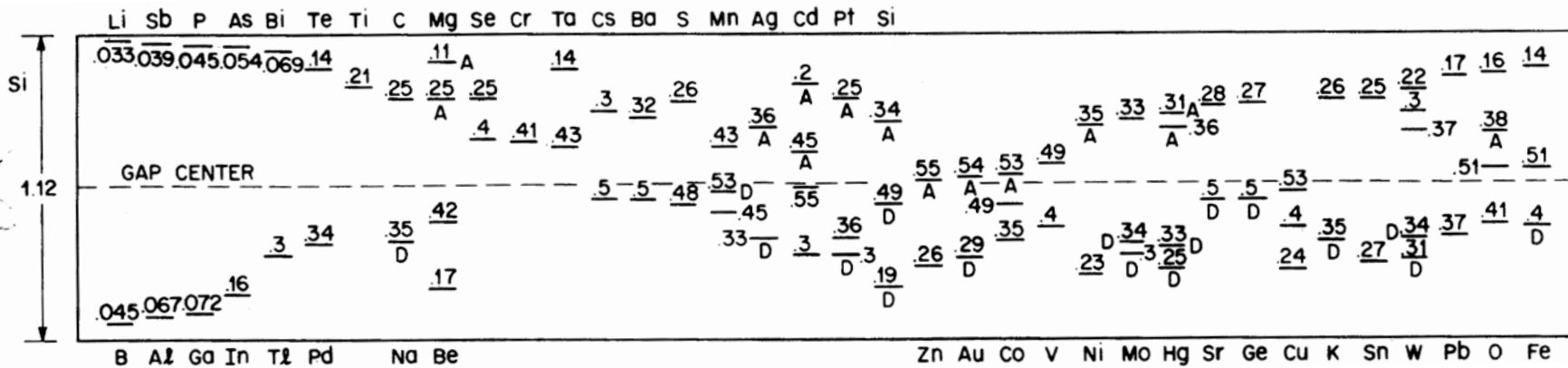
# Electrical activity of Defects

Relevant Parameters:

- $E_t$  energy within bandgap from conduction/valence band
- $\sigma_n, \sigma_p$  cross section for capture of electron/hole
- $N_t$  defect concentration in bulk or interface



## Example : Energy Levels of impurities in Si



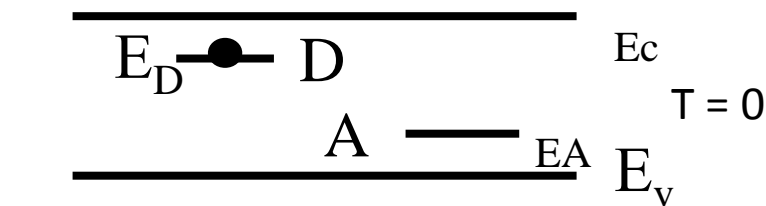
Da: S. M. Sze, Physics of Semiconducor Devices, Wiley & Sons, Singapore, 1981

## Shallow levels

### The hydrogen-like model

Donor (e.g. P in Si) is seen as a complex Si + H, an hydrogen atom is added at a site of the silicon lattice.

$$E_{Dn} = -\frac{e^4 m^*}{2(\epsilon_0 \epsilon_r)^2 \hbar^2} \frac{1}{n^2} \approx 10\text{-}60\text{meV}$$



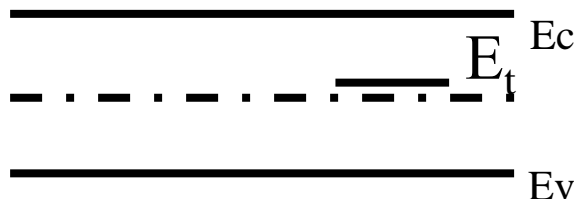
→ fully ionized at moderate temperatures → Doping

$$a^*_n = \frac{\epsilon_0 \epsilon_r \hbar^2}{m^* e^2} n^2 \quad a_0 = 0.529 \text{ \AA Bohr radius, } a_{\text{Si}} \sim 30 \text{ \AA ; } a_{\text{Ge}} \sim 80 \text{ \AA}$$

→ delocalized wave functions

### Deep levels

- Energetic level close to midgap,
- Localised wave functions
- May participate to doping / compensation as well as to generation / recombination processes.
- Can trap generated e/h thus reducing the detector signal
- Trap occupancy strongly determined by working conditions ( e.g. current, temperature, electric field .. ).

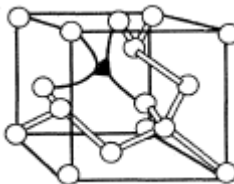


## Semiconductor s proposed for detector applications

| Property                             | Si                  | Diamond             | Diamond             | 4H SiC              |
|--------------------------------------|---------------------|---------------------|---------------------|---------------------|
| Material                             | MCz, FZ, epi        | Polycrystal         | single crystal      | epitaxial           |
| E <sub>g</sub> [eV]                  | 1.12                | 5.5                 | 5.5                 | 3.3                 |
| E <sub>breakdown</sub> [V/cm]        | 3·10 <sup>5</sup>   | 10 <sup>7</sup>     | 10 <sup>7</sup>     | 2.2·10 <sup>6</sup> |
| μ <sub>e</sub> [cm <sup>2</sup> /Vs] | 1450                | 1800                | >1800               | 800                 |
| μ <sub>h</sub> [cm <sup>2</sup> /Vs] | 450                 | 1200                | >1200               | 115                 |
| v <sub>sat</sub> [cm/s]              | 0.8·10 <sup>7</sup> | 2.2·10 <sup>7</sup> | 2.2·10 <sup>7</sup> | 2·10 <sup>7</sup>   |
| Z                                    | 14                  | 6                   | 6                   | 14/6                |
| ε <sub>r</sub>                       | 11.9                | 5.7                 | 5.7                 | 9.7                 |
| e-h energy [eV]                      | 3.6                 | 13                  | 13                  | 7.6                 |
| Density [g/cm3]                      | 2.33                | 3.515               | 3.515               | 3.22                |
| Displacem. [eV]                      | 13-20               | 43                  | 43                  | 25                  |
| e-h/μm for mips                      | ~80                 | 36                  | 36                  | 55                  |
| Max ccd [μm]                         | >500                | 300                 | 800                 | 55                  |
| Max wafer φ                          | 6"                  | 6"                  | ~1.4cm              | 2"                  |
| Commercial                           | yes                 | limited             | limited             | limited             |
| CERN R&Ds                            | RD50, RD39          | RD42                | RD42                | RD50                |

# Native Defects in Silicon

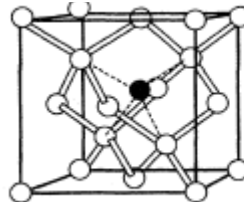
**Vacancy** : empty lattice site V.



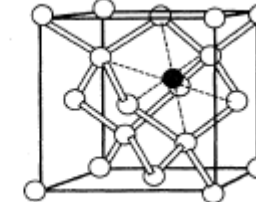
Point defects and dopant diffusion in silicon

P. M. Fahey,\* P. B. Griffin, and J. D. Plummer

**Self-interstitial** : a silicon atom that resides in one of the interstices of the silicon lattice.

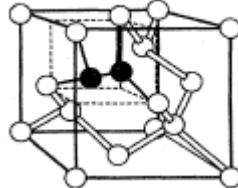


Tetrahedral Interstitial



Hexagonal Interstitial

**Interstitialcy** : two atoms in non-substitutional positions configured about a single substitutional lattice site.



**Oxygen**: as interstitial, up to  $10^{18}\text{cm}^{-3}$  in Cz Si, (in Float Zone  $[\text{O}_i] \sim 10^{15}\text{cm}^{-3}$ ), electrically inert. It can give rise to **shallow thermal donors (TDs)** small clusters of atoms formed at the early stages of oxygen aggregation, if  $[\text{O}_i] \sim 10^{17}\text{cm}^{-3}$  or higher.

**Carbon**: usually a **substitutional**,  $\text{C}_s$  electrically inert  $[\text{C}_s] \sim 10^{16}\text{cm}^{-3}$  .

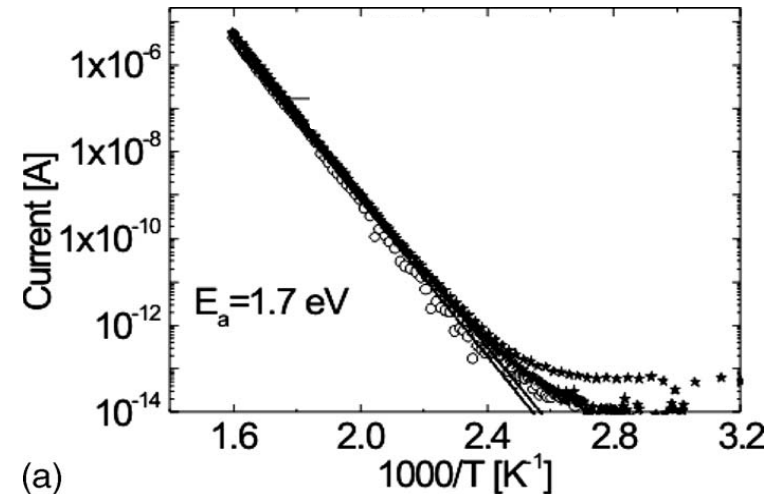
Native defects in silicon have too small concentrations to be visible to analytical techniques as electron paramagnetic resonance, deep-level transient spectroscopy..).

## Native Defects in Diamond

Nitrogen abundant since an impurity diffusing in the material during growth. Nitrogen defect can be either **single substitutional impurity** or in **aggregated form**. The single substitutional nitrogen is an **electron donor**, **1.7 eV below the conduction band edge**.

Example of electrical conduction activated by substitutional N HPHT single crystal diamond (Sumitomo) with  $[N] = 1.7 \times 10^{19}$  N-traps/cm<sup>3</sup>

R. Mori et al. JAP, 2009



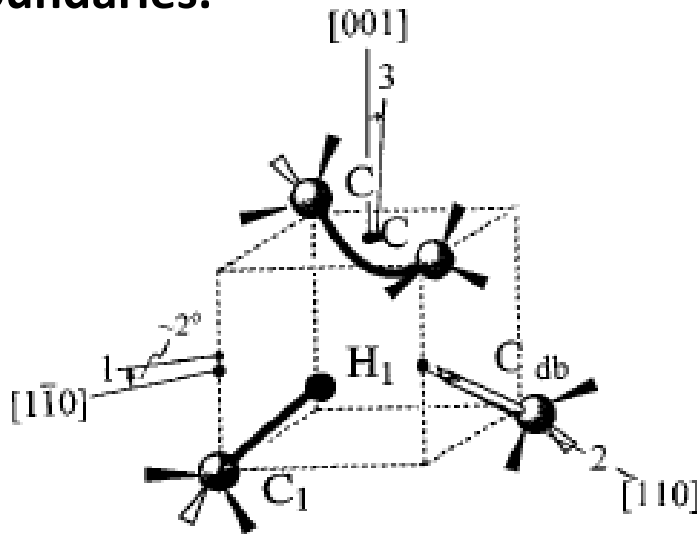
Other defects due to dangling bonds ( mostly in grain boundaries ), silicon, boron, hydrogen.

### Charge Character of defects in diamond : general trends

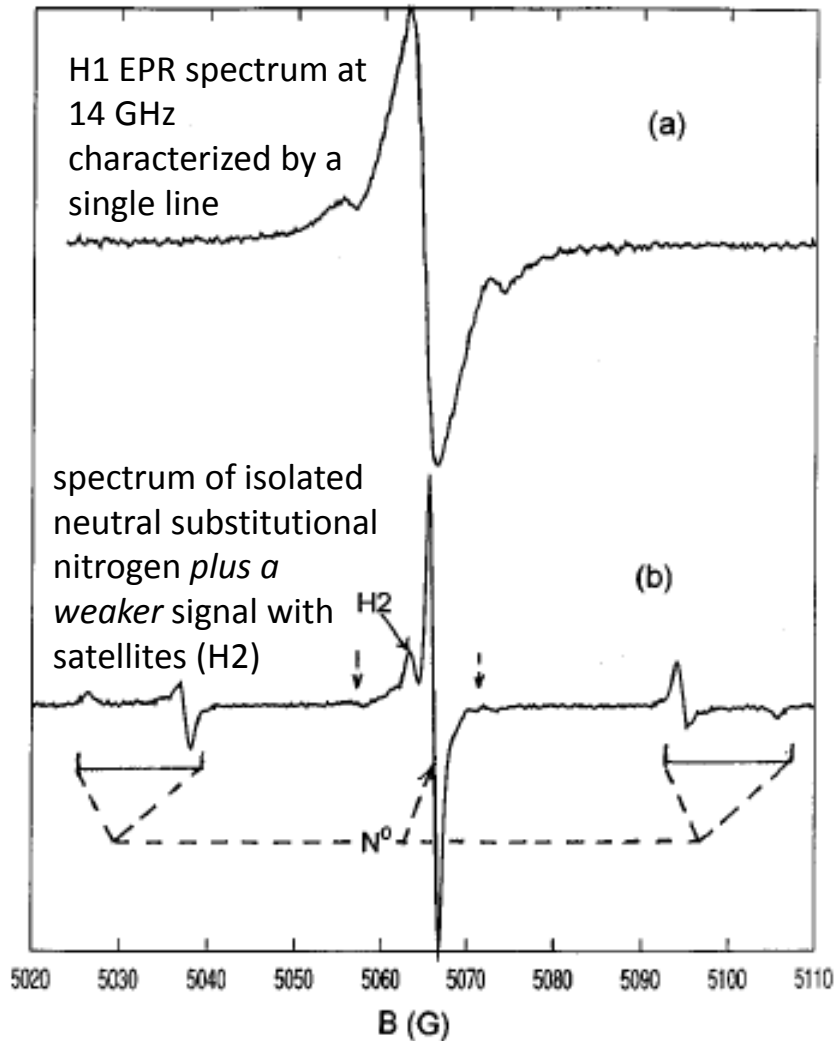
Diamond has a naturally slightly p-type character. As a general trend substitutional chalcogen impurities yield to relatively deep donor levels and dangling bonds yield to deep acceptor states.

## 2. Hydrogen related defects

H1: A single hydrogen atom in a vacancy. Hydrogen is hypothesized to passivate most of the dangling bonds in defective regions as grain boundaries.

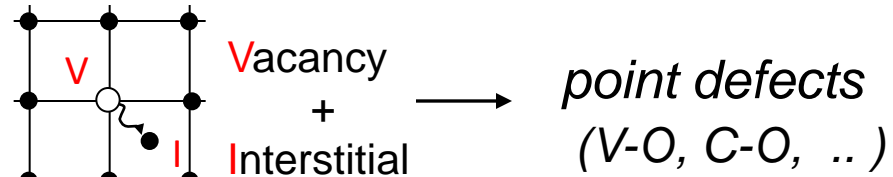


Defects H1 and H2 arise from two distinct electrically active defects produced when a single hydrogen atom enters a stretched bond at a grain boundary, or other extended misfit region in the polycrystalline CVD material. H forms a bond with one of the carbons, producing an electrically active dangling bond on the other as the two carbons relax backward.



# Radiation Damage – Microscopic Effects

particle → Si →  $E_K > 25 \text{ eV}$



$E_K > 5 \text{ keV}$

point defects and clusters of defects

## ◆ $^{60}\text{Co}$ -gammas

- Compton Electrons with max.  $E_\gamma \approx 1 \text{ MeV}$  (no cluster production)

## ◆ Electrons

- $E_e > 255 \text{ keV}$  for displacement
- $E_e > 8 \text{ MeV}$  for cluster

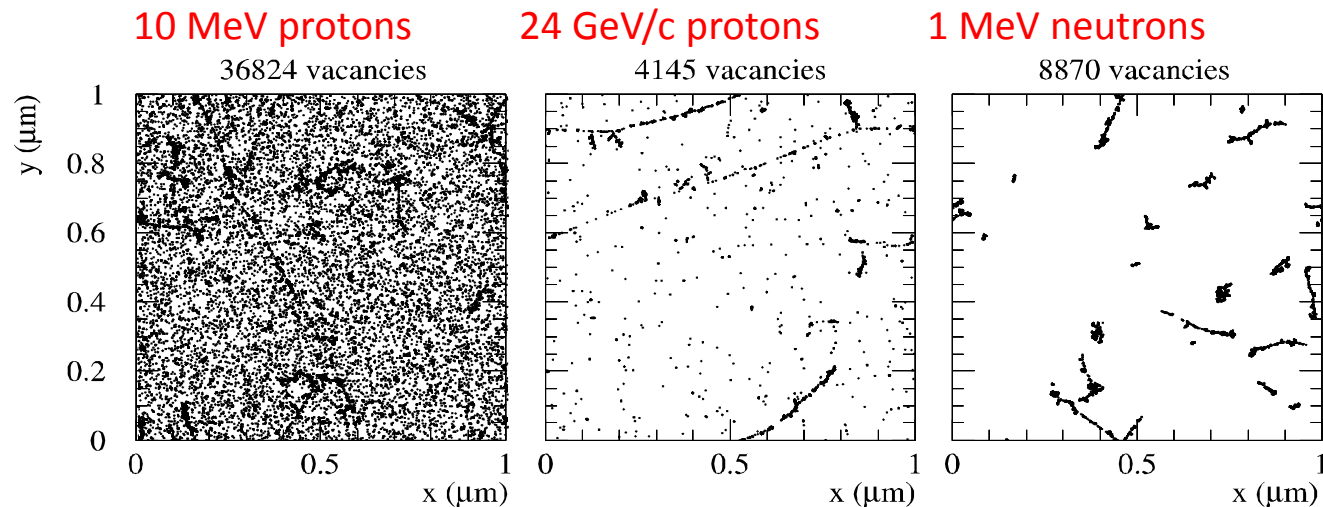
## ◆ Neutrons (elastic scattering)

- $E_n > 185 \text{ eV}$  for displacement
- $E_n > 35 \text{ keV}$  for cluster

Displacement energy - energy needed to displace an atom from the lattice site: 13-20 eV Si, 43eV Diamond .

Initial distribution of vacancies in  $(1\mu\text{m})^3$  after  $10^{14} \text{ particles/cm}^2$

[Mika Huhtinen ROSE TN/2001-02]



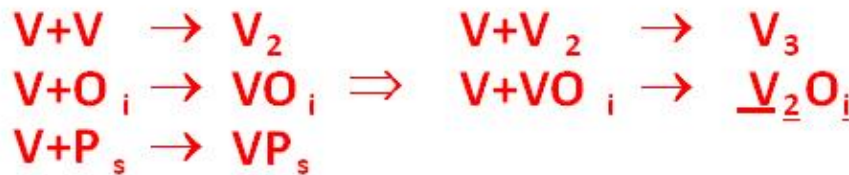
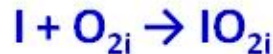
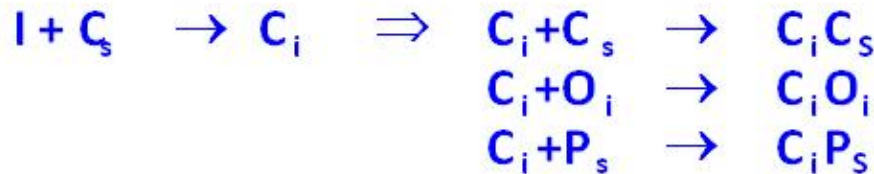
[Mika Huhtinen NIMA 491(2002) 194]

- Secondary defect generation

Dopants : P, B

Main impurities in silicon: Carbon C<sub>s</sub>

Oxygen O<sub>i</sub>



- Initial donor/acceptor (P,B) concentration removal
- formation of stable defects with deep levels acting as compensating centres

## Si - Vacancy related point-defects:

### The A centre

oxygen-doped silicon dominant centers of vacancy capture may be isolated interstitials  $O_i$  and trapping results in the formation of the V-O centre, so-called A centre

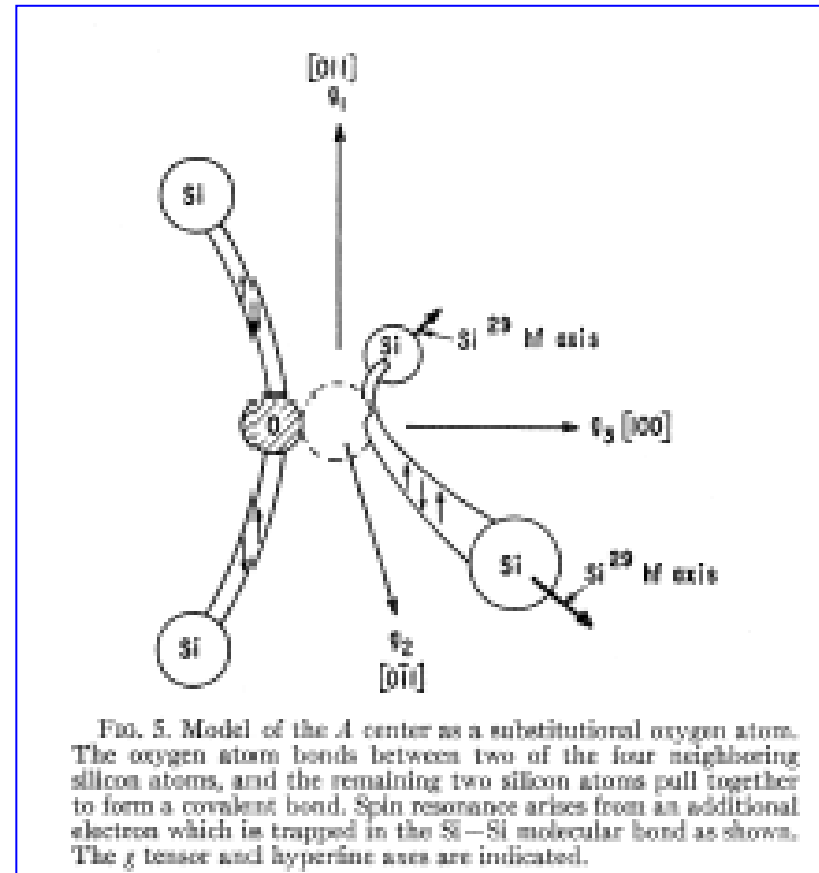
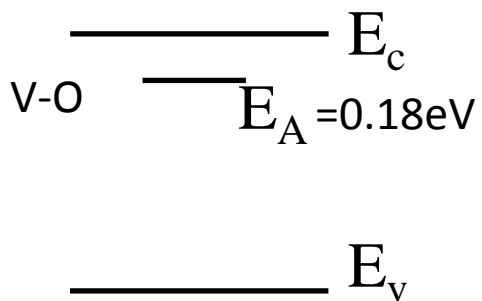


FIG. 5. Model of the  $A$  center as a substitutional oxygen atom. The oxygen atom bonds between two of the four neighboring silicon atoms, and the remaining two silicon atoms pull together to form a covalent bond. Spin resonance arises from an additional electron which is trapped in the  $Si-Si$  molecular bond as shown. The  $g$  tensor and hyperfine axes are indicated.

V-O defect (A centre)

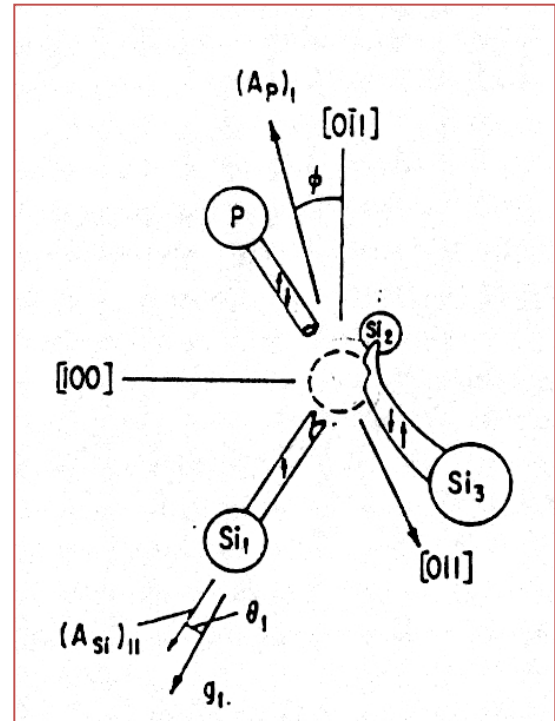
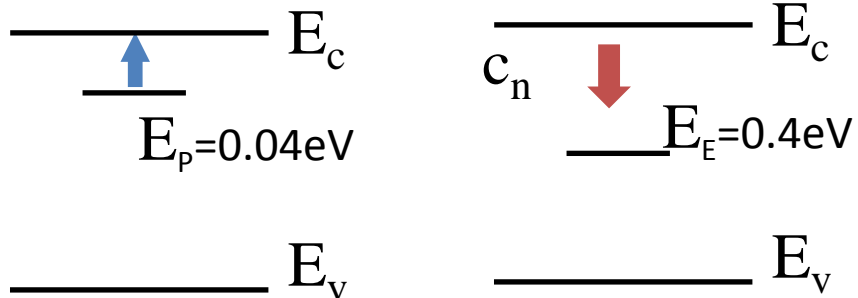
Watkins, Corbett: Phys.Rev.,121,4, (1961),1001

## Si - Vacancy related point-defects:

### The E centre

In Phosphorous doped Si vacancy is also trapped by P to create the P-V defect, the so-called E centre.

This changes the doping of the crystal, removing the doping atom P and creating an acceptor-like energy level at  $E_t = 0.42\text{eV}$   
→ carrier removal → doped semiconductors become almost intrinsic after heavy irradiation

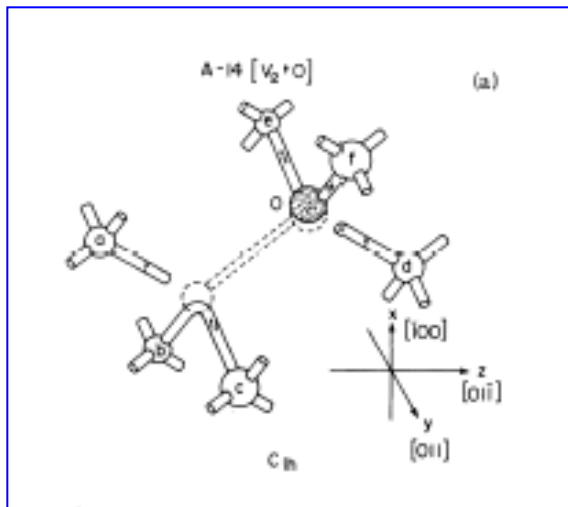


Phosphorous-Vacancy  
P-V (E centre )

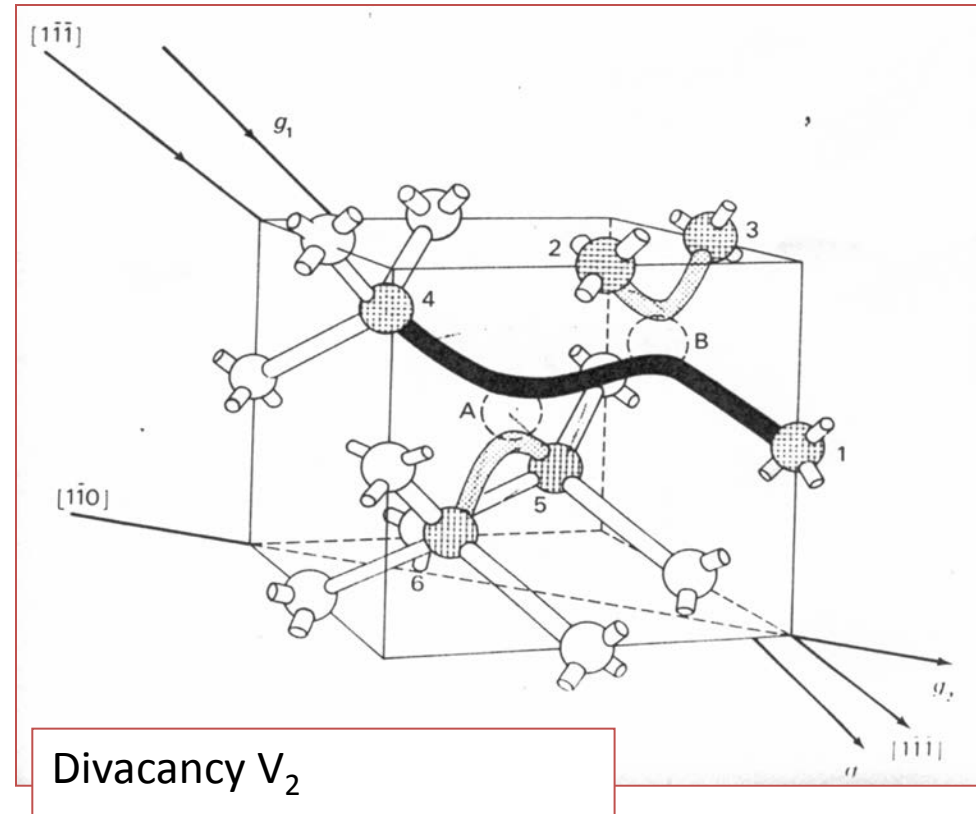
Corbett, Watkins et al, PRB, 60s

## Si - Vacancy related point-defects: Point-defects involving more than one vacancy

Point-defects can involve more than one vacancy, creating deep levels in the Si gap:  $V_2$ ,  $V_2O$ ,  $V_3O$  etc..



$V_2O$  defect

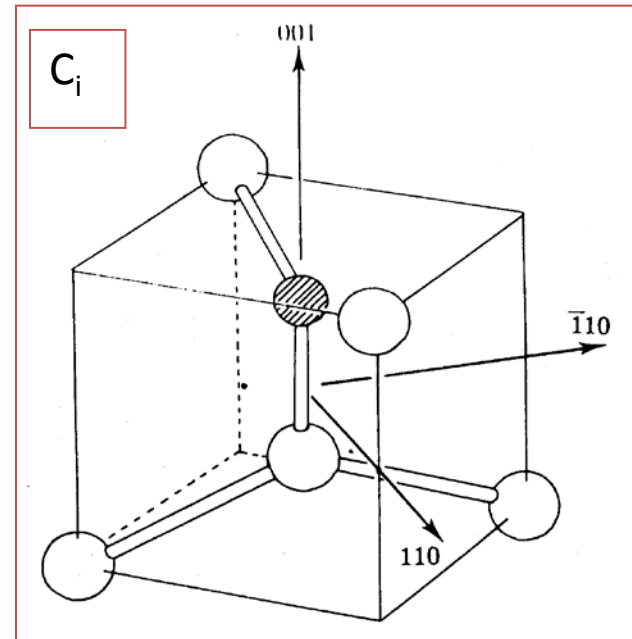
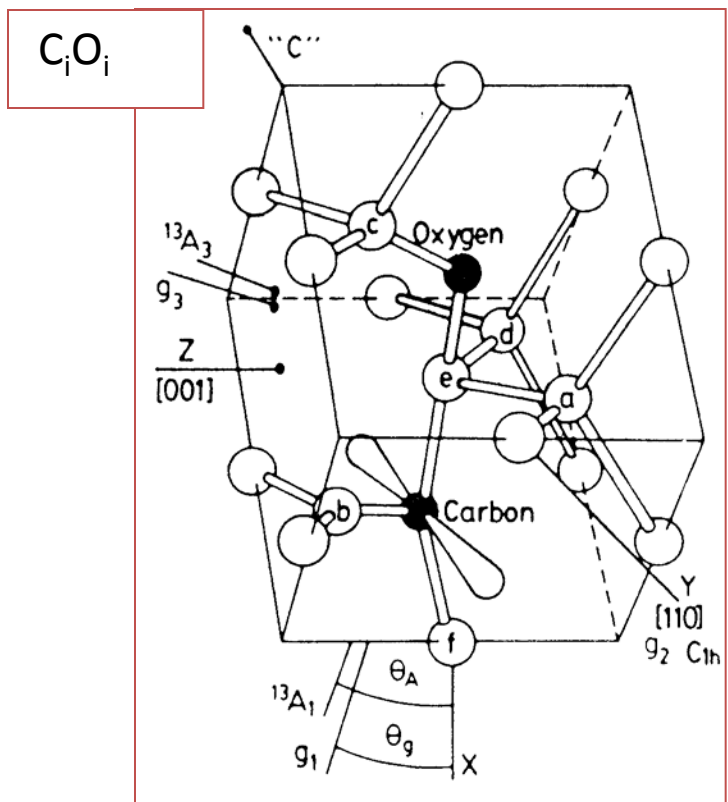


Lee, Corbett: Phys.Rev.B,13,6, (1976),2653

## Radiation Induced Defects related to Carbon and Oxygen

$$\text{FZ } [\text{O}_i] \sim 10^{15} \text{ cm}^{-3}; \text{ CZ } [\text{O}_i] \sim 10^{17} - 10^{18} \text{ cm}^{-3}$$

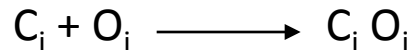
$$[\text{C}_s] \sim 10^{15} \text{ cm}^{-3}$$



Watkins replacement mechanism:



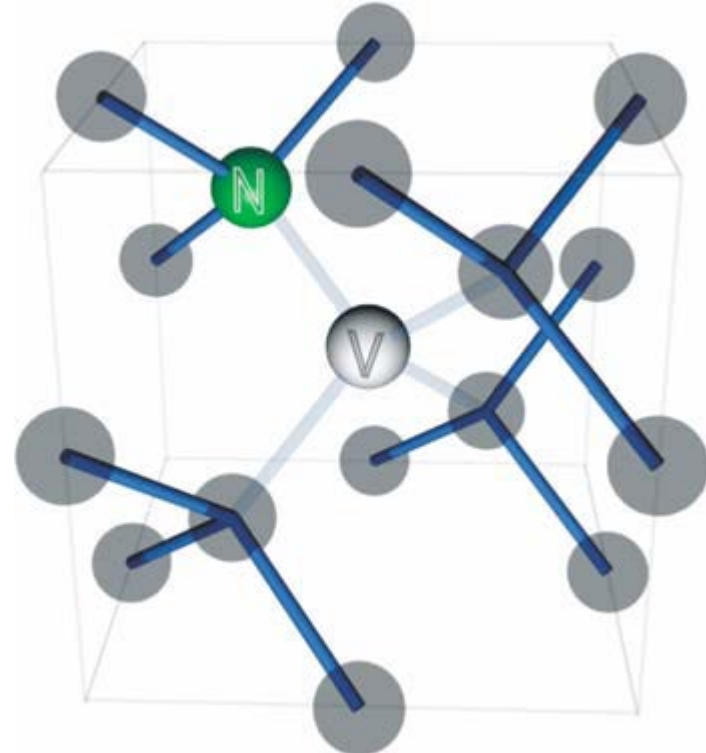
$\text{C}_i$  mobile at 300K



# Vacancy related defects in Diamond

## 1. Nitrogen – Vacancy defect

The nitrogen vacancy defect centre in diamond is traditionally observed in radiation damaged nitrogen rich diamond. It is also named GR1 centre. This defect gives rise to a strong absorption at 1.945 eV (637 nm).



Schematic representation of the nitrogen vacancy (NV) centre structure.

F. Jelezko and J. Wrachtrup: Single defect centres in diamond: A review phys. stat. sol. (a) 203, No. 13, 3207–3225 (2006)

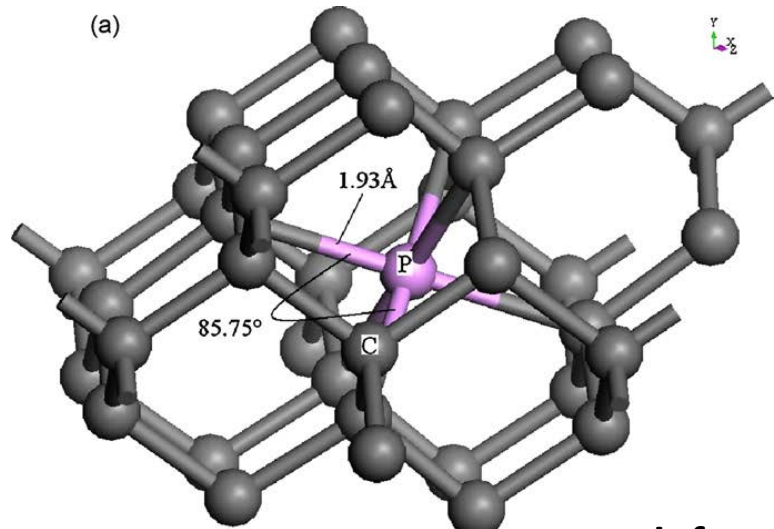
# Interaction of Vacancy with Doping Levels in Diamond

P doped n-type single-crystalline diamond with thermal activation energy of 0.58 eV and highest mobility of 0.35 cm<sup>2</sup>/Vs [Kato et al.].

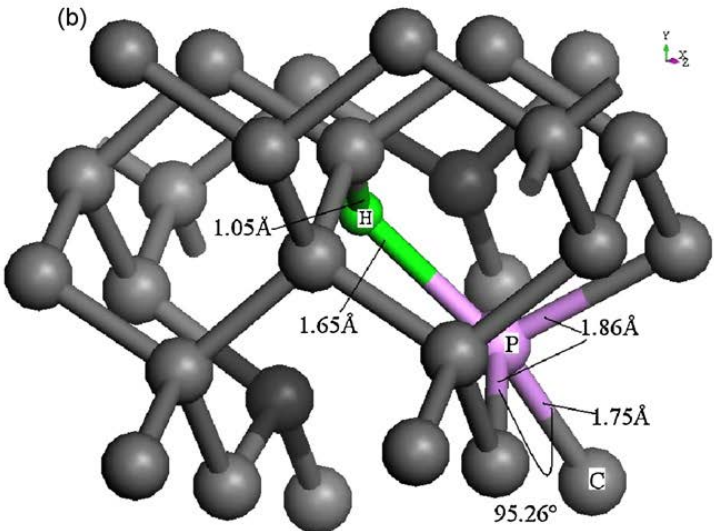
Vacancy and H defects may bind to the neighboring P atom forming PVH related complex to influence the electronic properties of doped diamond [Yan et al.].

P-V , P-V-H ,P-2V-H complexes introduce acceptor levels providing hole carriers in diamond.

H. Kato, S. Yamasaki, H. Okushi, Appl. Phys. Lett. 86 (2005) 222111.  
C.X. Yan et al. Theoretical characterization of carrier compensation in P-doped diamond Applied Surface Science 255 (2009) 3994–4000

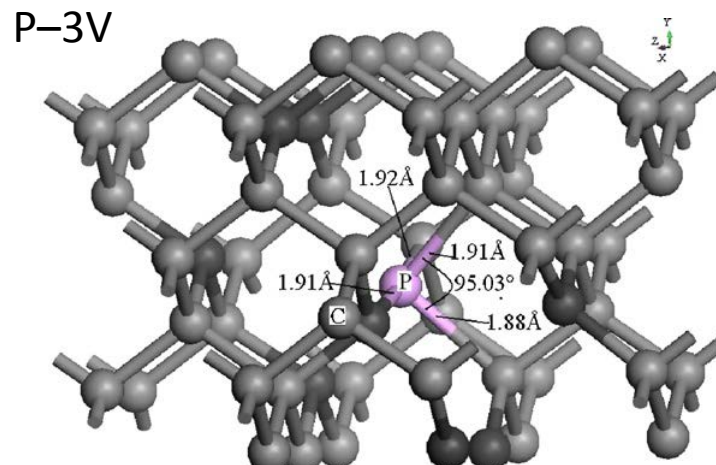
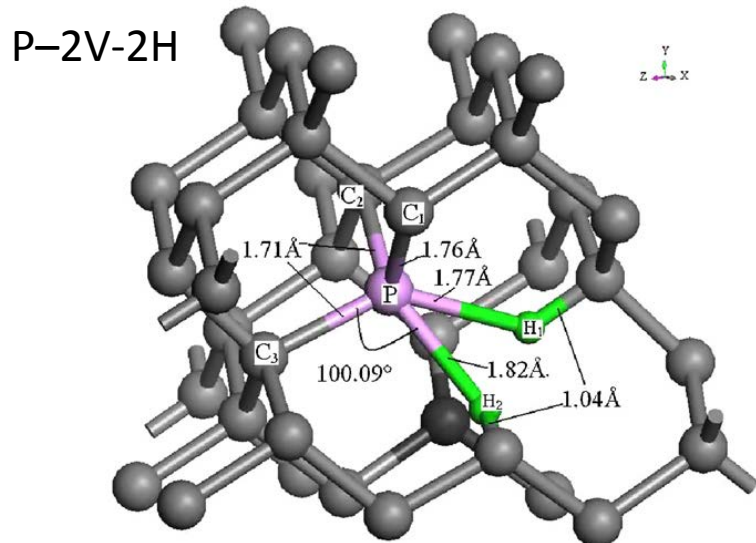


P-V defect



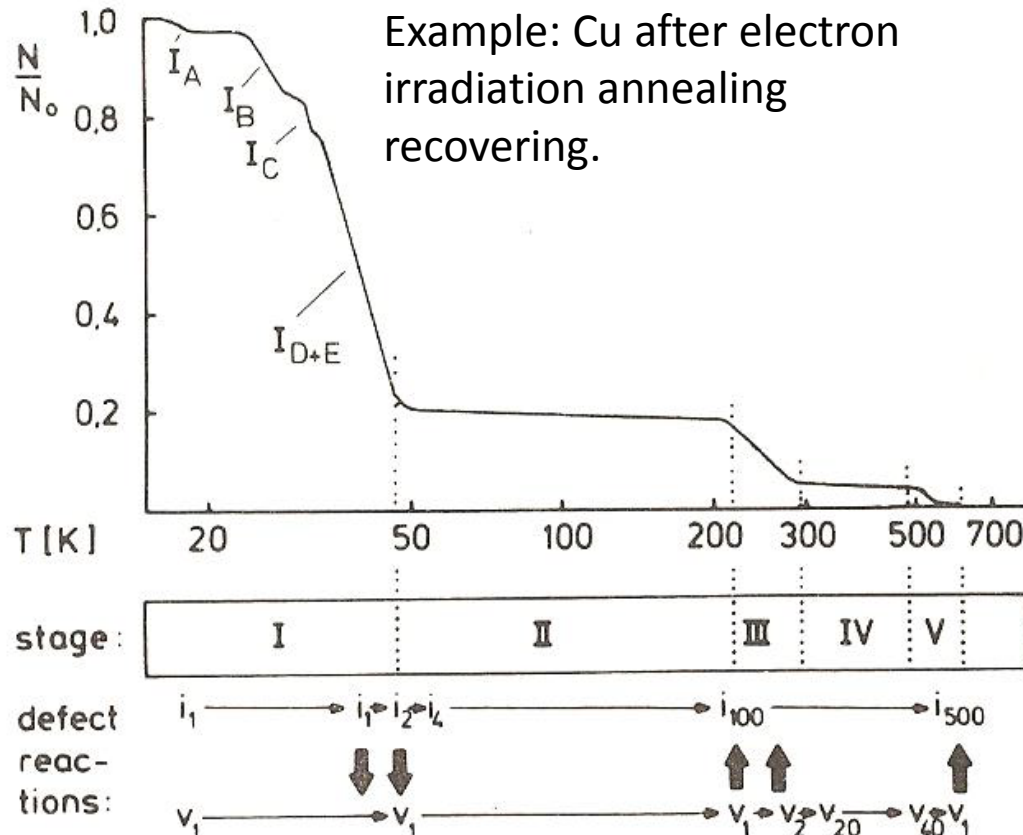
P-V-H complex defect

Divacancy complex P–2V–2H and trivacancy complex P–3V, introduce energy levels near the middle of the band gap, which may serve as **recombination centers**.



## Annealing

Defect configuration can significantly change by heating up the irradiated sample or storing at T higher than that of irradiation.

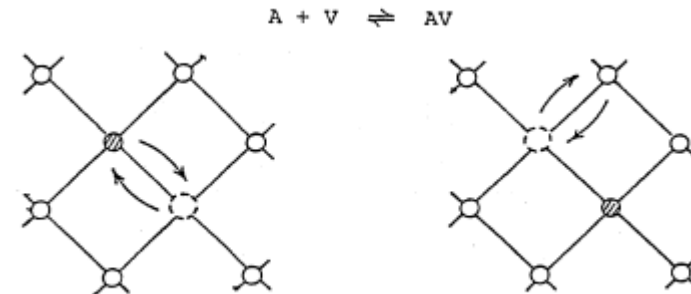


$I_1, V_1$  single vacancy, interstitial  
 $I_2, V_2$  di-interstitials ,divacancies...

- I<sub>A</sub> – I<sub>E</sub> collapse of close to separated Frenkel pairs
- II: formation of clusters as small interstitial loops
- III: vacancies migrate and annihilate at interstitial clusters & vacancy agglomerate in vacancy clusters
- IV: vacancy clusters grow in size
- V: vacancy clusters dissociate thermally and annihilate at interstitial loops: radiation damage is removed

A simple picture of the diffusion mechanisms of dopant impurities in Si is considering that vacancies mediate impurity diffusion via impurity-vacancy pairs.

Self-interstitials may also contribute via the "kick-out" mechanism (i.e., ejection of substitutional impurities into interstitial channels)



VOLUME 54, NUMBER 4

PHYSICAL REVIEW LETTERS

28 JANUARY 1985

TABLE I. Theoretical and experimental activation energies (in electronvolts) for self-diffusion (SD) in intrinsic Si, P diffusion in intrinsic and *n*-type Si, and Al diffusion in intrinsic and *p*-type Si.

| Species    | $Q_{\text{int}}$     | Species        | $Q_{\text{int}}$ | $Q_n$            | Species         | $Q_{\text{int}}$ | $Q_p$ |
|------------|----------------------|----------------|------------------|------------------|-----------------|------------------|-------|
| Theory     |                      |                |                  |                  |                 |                  |       |
| $V^{++}$   | 5.1                  | $(P_s V)^+$    | 3.2              | 3.8              | $(Al_s V)^+$    | 3.9              | 3.2   |
| $V^+$      | 4.7                  | $(P_s V)^0$    | 3.0              | 3.0              | $(Al_s V)^0$    | 3.5              | 3.5   |
| $V^0$      | 4.2                  | $(P_s V)^-$    | 3.2              | 2.6              | $(Al_s V)^-$    | 3.5              | 4.1   |
| $V^-$      | 4.5                  | $(P_s I)^0$    | 5.7              | 5.7              | $(Al_s I)^0$    | 4.0              | 4.0   |
| $I^{++}$   | 5.6                  | $(P_s I)^+$    | 5.1              | 5.1              | $(Al_s I)^{++}$ | 4.3              | 3.0   |
| $I^+$      | 5.5                  | $(P_s I)^-$    | 5.2              | 4.6              | $(Al_s I)^+$    | 3.9              | 3.1   |
| $I^0$      | 5.7                  | $(P_s I)^{--}$ | 5.6              | 4.5              | $(Al_s I)^0$    | 3.9              | 3.9   |
| Experiment |                      |                |                  |                  |                 |                  |       |
| SD         | 4.1–5.1 <sup>a</sup> | P              | 3.7 <sup>b</sup> | 3.1 <sup>b</sup> | Al              | 3.5 <sup>c</sup> | ...   |

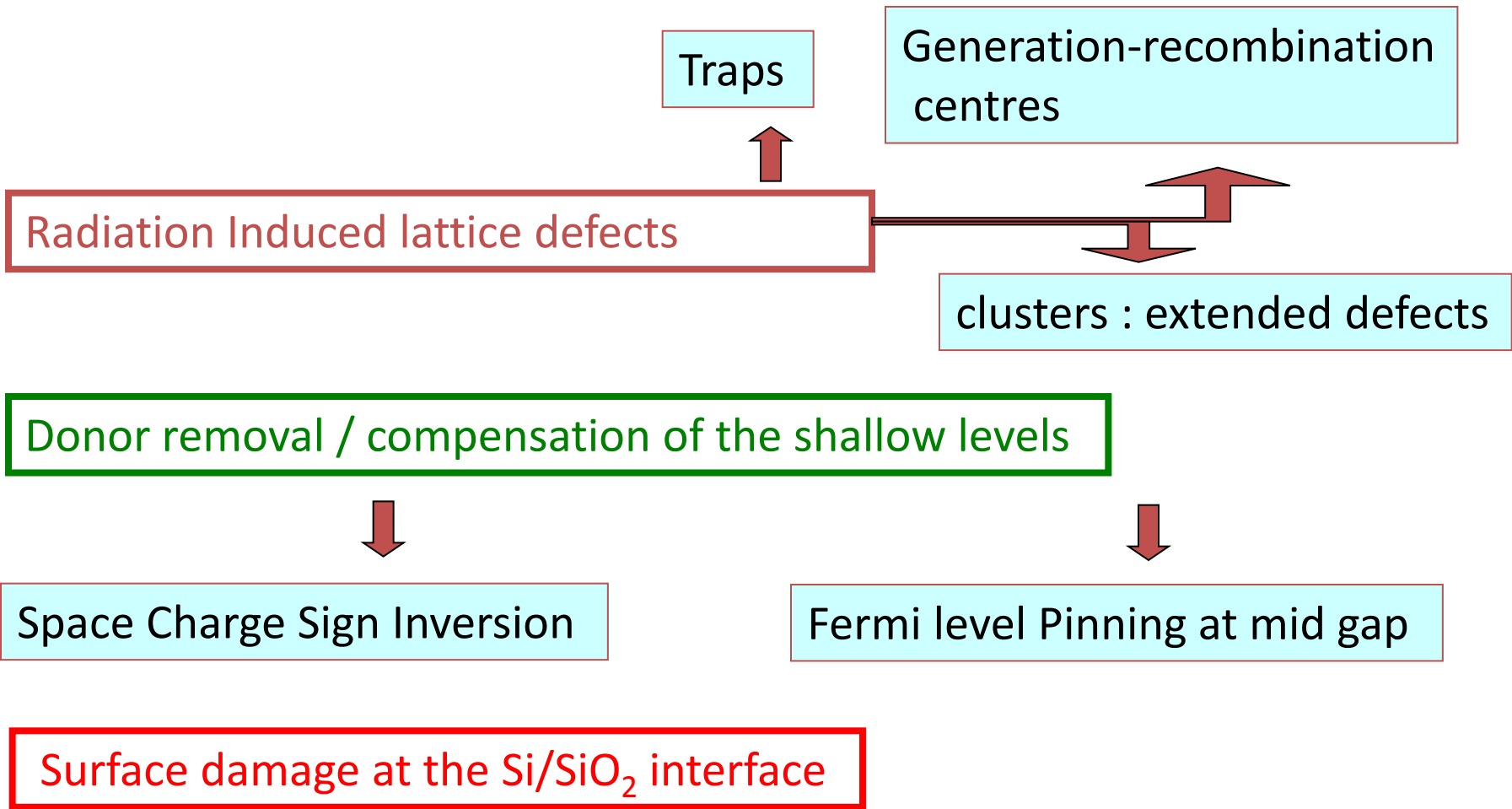
<sup>a</sup>See compilation of experimental values in Ref. 9.

<sup>b</sup>J. S. Makris and B. J. Masters, J. Electrochem. Soc. **120**, 1252 (1973).

<sup>c</sup>C. S. Fuller and J. Ditzenberger, J. Appl. Phys. **27**, 544 (1956).

Note: In diamond, unlike in silicon vacancies and interstitials created are immobile at room temperature.

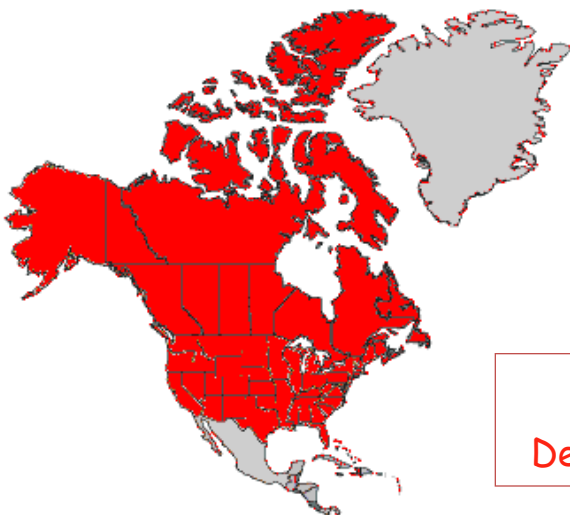
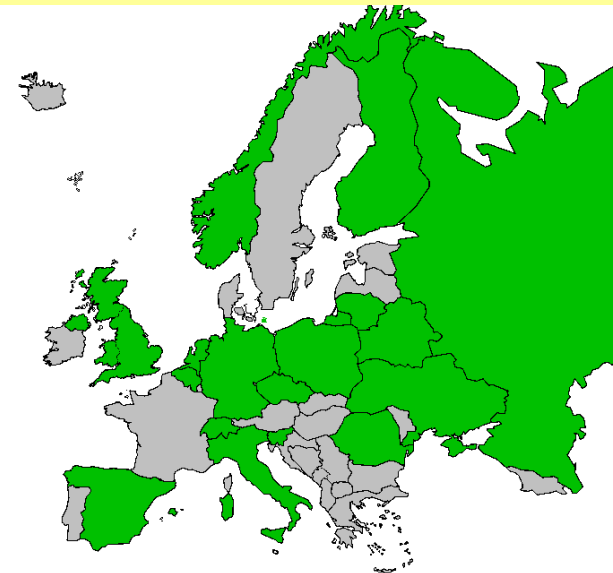
# Radiation induced defects affecting semiconductors properties



# RD50 - Development of Radiation Hard Semiconductor Devices for High Luminosity Colliders

## 38 European institutes

Belarus (Minsk), Belgium (Louvain), Czech Republic (Prague (3x)), Finland (Helsinki, Lappeenranta), Germany (Dortmund, Erfurt, Freiburg, Hamburg, Karlsruhe, Munich), Italy (Bari, Florence, Padova, Perugia, Pisa, Trento), Lithuania (Vilnius), Netherlands (NIKHEF), Norway (Oslo (2x)), Poland (Warsaw(2x)), Romania (Bucharest (2x)), Russia (Moscow, St.Petersburg), Slovenia (Ljubljana), Spain (Barcelona, Valencia), Switzerland (CERN, PSI), Ukraine (Kiev), United Kingdom (Glasgow, Lancaster, Liverpool)



## 8 North-American institutes

Canada (Montreal), USA (BNL, Fermilab, New Mexico, Purdue, Rochester, Santa Cruz, Syracuse)

## 1 Middle East institute

Israel (Tel Aviv)

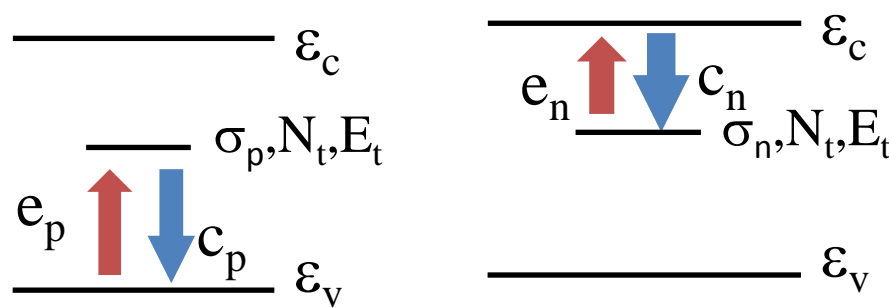
257 Members from 47 Institutes

Detailed member list: <http://cern.ch/rd50>

## Electrical activity of defects

I difetti reticolari sono caratterizzati da livelli energetici posti all'interno del gap proibito. Essi scambiano elettroni e lacune con le bande di conduzione e valenza. Il tasso con cui avvengono questi processi è descritto mediante i **coefficienti di cattura**  $c_n, c_p$  ed **emissione**  $e_n, e_p$  rispettivamente per elettroni/lacune.

Parametri rilevanti di un difetto: livello energetico di energia  $E_t$ , sezione d'urto per la cattura di un elettrone/lacuna  $\sigma_n, \sigma_p$  (esprime la probabilità intrinseca che il difetto catturi un portatore), la concentrazione del difetto nel materiale,  $N_t$ .



Nel determinare i coefficienti bisogna tener conto che gli elettroni sono emessi (le lacune catturate) dai livelli energetici occupati con elettroni ( $n_t$ ), mentre elettroni sono catturati (le lacune emesse) dai livelli vuoti ( $N_t - n_t$ ).

## Capture coefficients

$N_t$  = concentrazione totale di livelli energetici;  $n_t$  = concentrazione di livelli occupati,  
 $n$  = concentrazione di elettroni liberi;  $p$  = concentrazione di lacune libere;  
 $v_n$  = velocità termica media elettronica;  $v_p$  = velocità termica media della lacuna  
 $\sigma_n$  = sezione d'urto per la cattura di un elettrone;  $\sigma_p$  = sezione d'urto per la cattura di una lacuna;

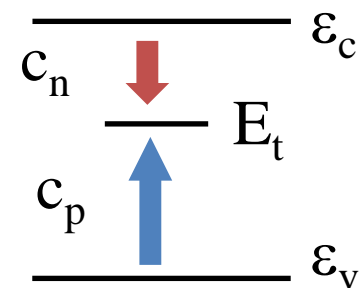
Il difetto non occupato viene esposto ad un flusso di elettroni liberi per unità d'area dato da:  
 $nv_n$ , il numero di elettroni catturati dagli stati vuoti nell'intervallo  $\Delta t$  è:

$$\Delta n_t = \sigma_n v_n n (N_t - n_t) \Delta t.$$

Definiamo coefficiente di cattura  $c_n$ :

$$\frac{\Delta n}{\Delta t} \frac{1}{N_t - n_t} = c_n = \sigma_n v_n n$$

Analogamente per le lacune:  $c_p = \sigma_p v_p p$



## Equilibrio termico: bilancio tra cattura ed emissione

L'occupazione del livello  $n_t/N_t$  è determinato dalla competizione tra processi di cattura ed emissione.

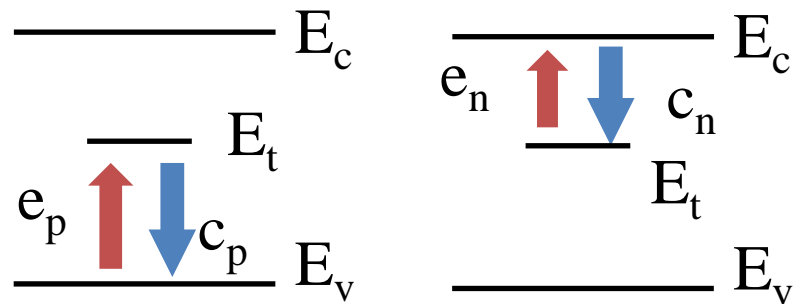
La relazione che descrive il tasso di occupazione del livello è:

$$\frac{dn_t}{dt} = (c_n + e_p)(N_t - n_t) - (e_n + c_p)n_t$$

Caso 1 equilibrio termico - i processi di emissione e cattura devono bilanciarsi sia per gli elettroni che per le lacune:

$$e_n n_t = c_n (N_t - n_t)$$

$$e_p (N_t - n_t) = c_p n_t$$



L'occupazione delle trappole è determinata dai rapporti:

$$\frac{n_t}{N_t} = \frac{c_n}{c_n + e_n} = \frac{e_p}{c_p + e_p}$$

## Coefficienti di emissione

L'occupazione del livello è determinata dalla distribuzione di Fermi-Dirac. Per uno stato profondo (per semplicità assumo non si abbia degenerazione):

$$\frac{n_t}{N_t} = \left[ 1 + \exp\left(\frac{E_t - E_F}{KT}\right) \right]^{-1}$$

Da cui:

$$e_n = c_n \exp\left(\frac{E_t - E_F}{KT}\right)$$

$$e_p = c_p \exp\left(\frac{E_F - E_t}{KT}\right)$$

otteniamo:

$$e_n = \sigma_n v_n N_c \exp\left(-\frac{E_c - E_t}{KT}\right)$$

$$e_p = \sigma_p v_p N_v \exp\left(-\frac{E_t - E_v}{KT}\right)$$

Dato che valgono:

$$n = N_c \exp\left(\frac{E_F - E_c}{KT}\right)$$

$$p = N_v \exp\left(\frac{E_v - E_F}{KT}\right)$$

Quindi i coefficienti di emissione dipendono dalla temperatura con andamento:

$$\longrightarrow e_n(T) \propto T^2 \cdot e^{-\frac{E_c - E_t}{K_B T}}$$

# Trap occupancy

In general emission rates  $G_{n,p}$  are different from capture rates  $R_{n,p}$  so that  $U_{n,p} \neq 0$  :

$$U_n = G_n - R_n = e_n n_t - c_n (N_t - n_t)$$

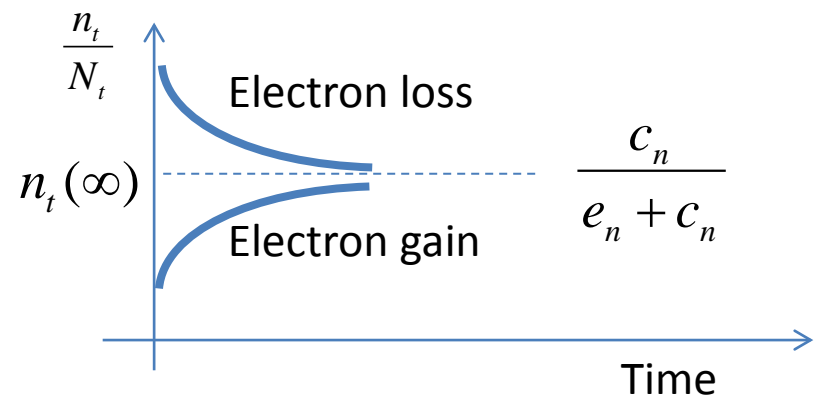
$$U_p = G_p - R_p = e_p (N_t - n_t) - c_p n_t$$

Trap occupation at equilibrium can be inferred considering  $U_n = U_p$  :

$$\frac{n_t}{N_t} = \frac{c_n + e_p}{c_p + e_n + c_n + e_p}$$

Filling factor:  $F = \frac{n_t}{N_t - n_t} = \frac{c_n + e_p}{c_p + e_n}$

Ratio between filled and empty states



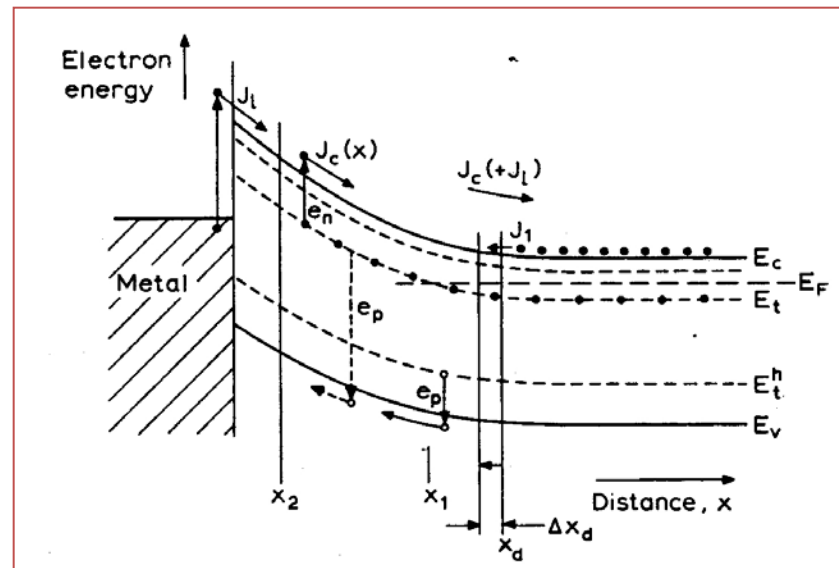
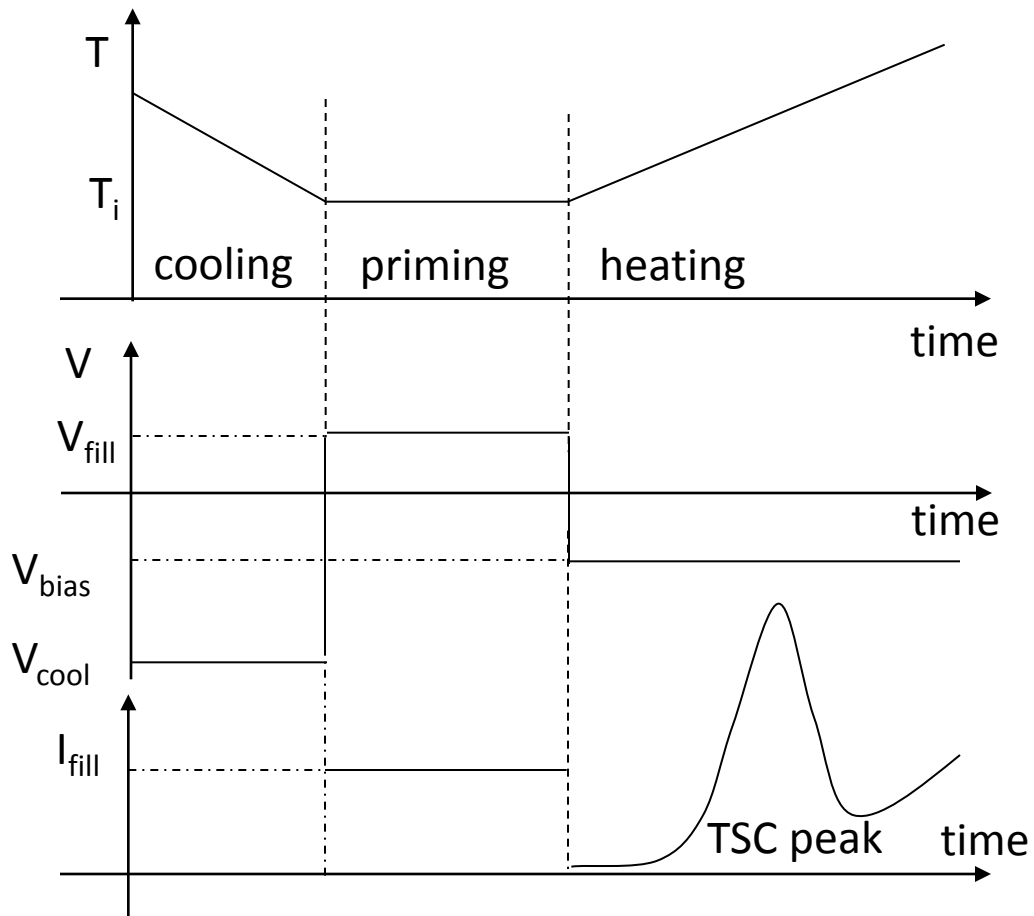
Example: relaxation of the occupancy of an electron trap in n-type material from full and empty initial conditions, to the equilibrium occupancy

# **How to detect electrically active defects ?**

## **Defect Spectroscopy in semiconductors**

- 1. Thermally Stimulated Currents TSC**
- 2. Deep Level Transient Spectroscopy DLTS**
- 3. Photo Induced Current Transient Spectroscopy PICTS**

# Thermally Stimulated Current: TSC

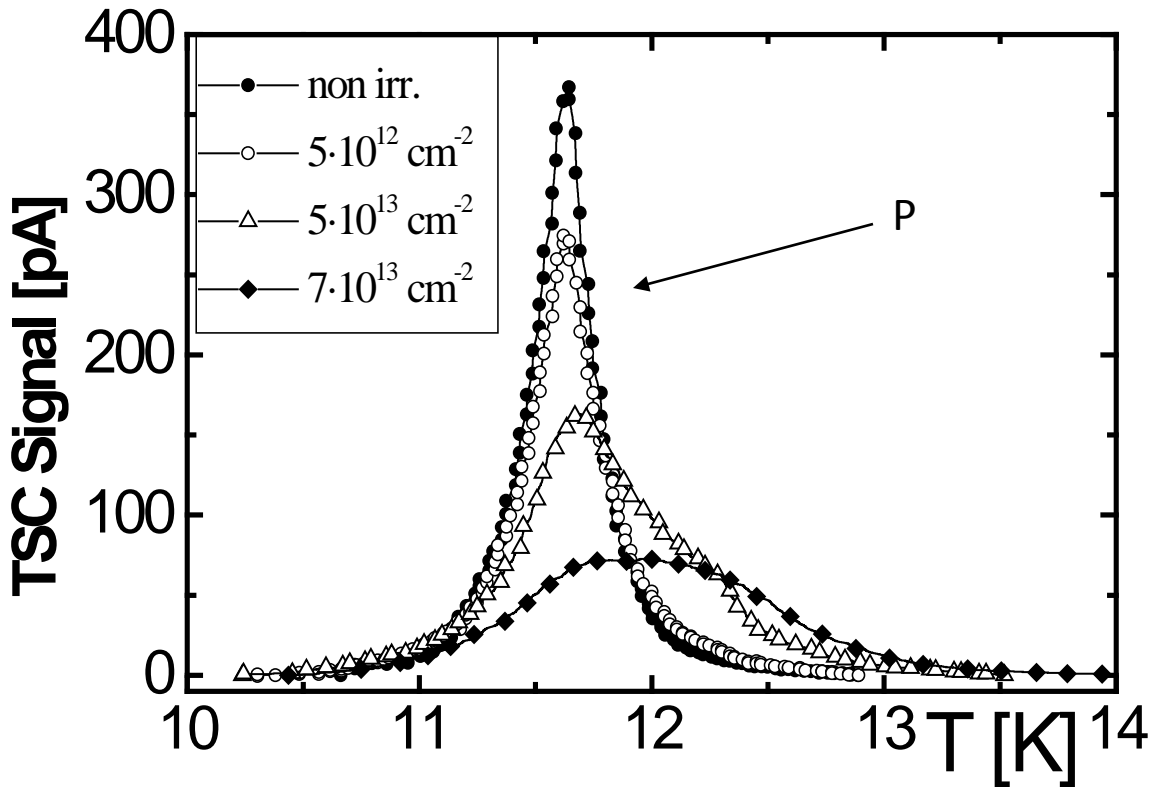


$$\frac{dn_t}{dt} = -e_n \cdot n_t$$

$$e_n = N_c \sigma_n v_{th} \cdot e^{-\frac{E_c - E_t}{KT}}$$

$$I_{TSC}(T) = -\frac{1}{2} q \cdot A \cdot N_t \cdot W \cdot e_n(T) \exp\left(-\frac{1}{b} \int_{T_i}^T e_n(T) dT\right)$$

## Example 1: TSC at Low Temperature to evidence Shallow Donor Removal in n-type Si irradiated with neutrons



J. Phys. D: Appl. Phys. 33 (2000) 299–304. Printed in the UK

PII: S0022-3727(00)06399-3

Thermally stimulated currents  
analysis of the shallow levels in  
irradiated silicon detectors

E Borchi<sup>†‡</sup>, M Bruzzi<sup>†‡</sup>, Z Li<sup>§</sup> and S Pirollo<sup>†‡</sup>

## Example 2: TSC at High Temperature to evidence deep level removal in polycrystalline diamond irradiated with neutrons

- Results:

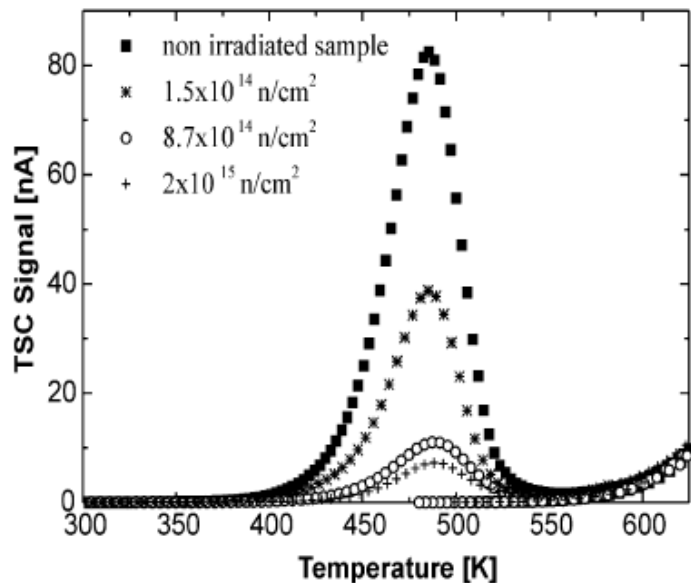


Fig. 1. TSC signal vs. temperature for non-irradiated and irradiated samples, after filling with UV xenon lamp for 20 min. The samples are biased with 100 V. The heating rate is 0.15 K/s. The neutron fluences are indicated in the legend.

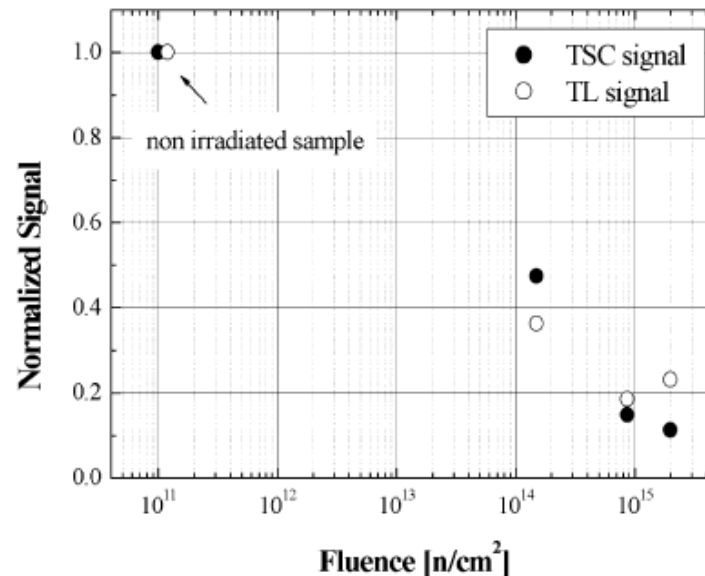
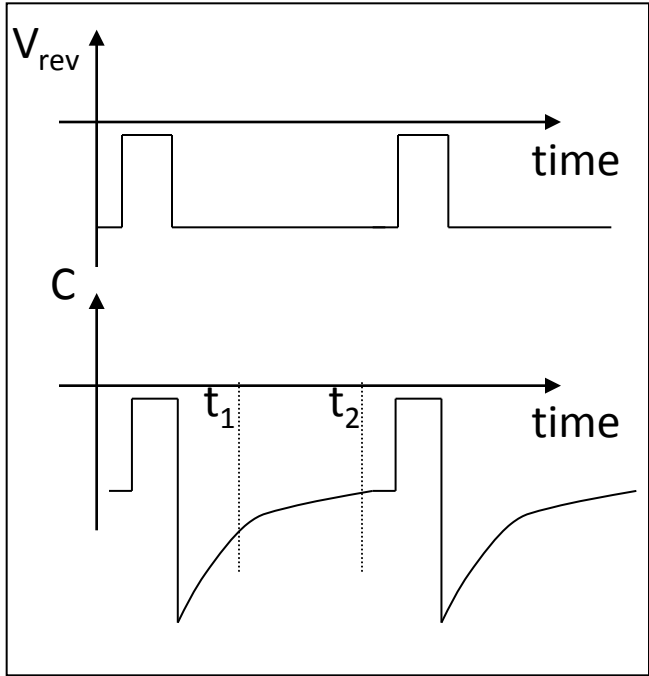


Fig. 5. Normalised TSC and TL signal vs. fluence obtained by the integral of the TSC and TL signal as a function of the temperature, dividing by the heating rate and normalising to the value corresponding to the non-irradiated sample.

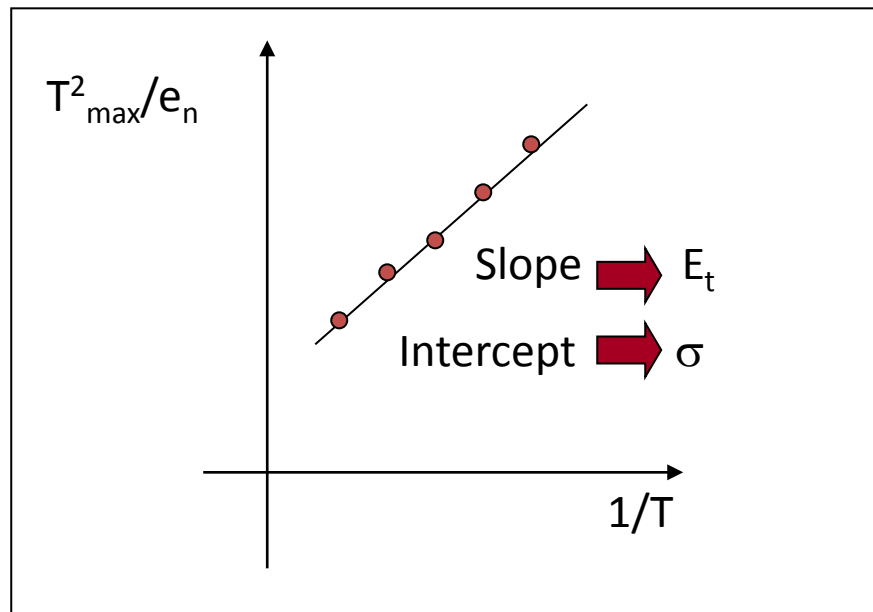
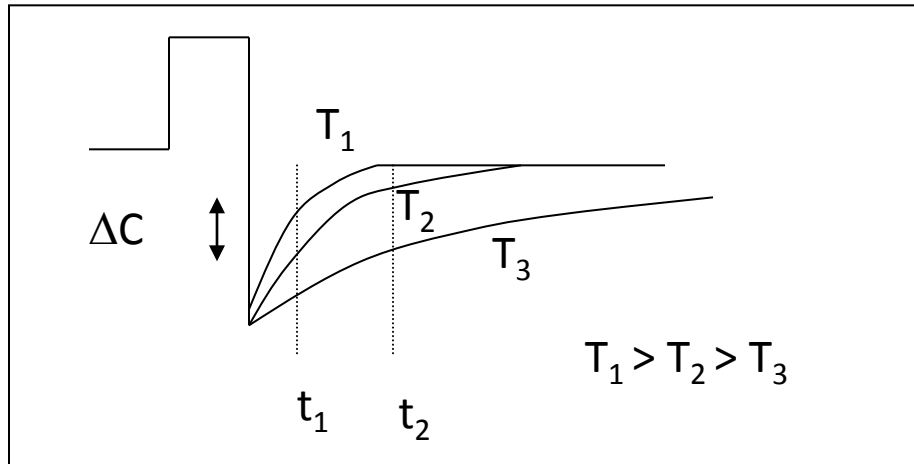
**1 MeV neutrons deactivate high temperature electrically active defects.**

# Deep Level Transient Spectroscopy DLTS

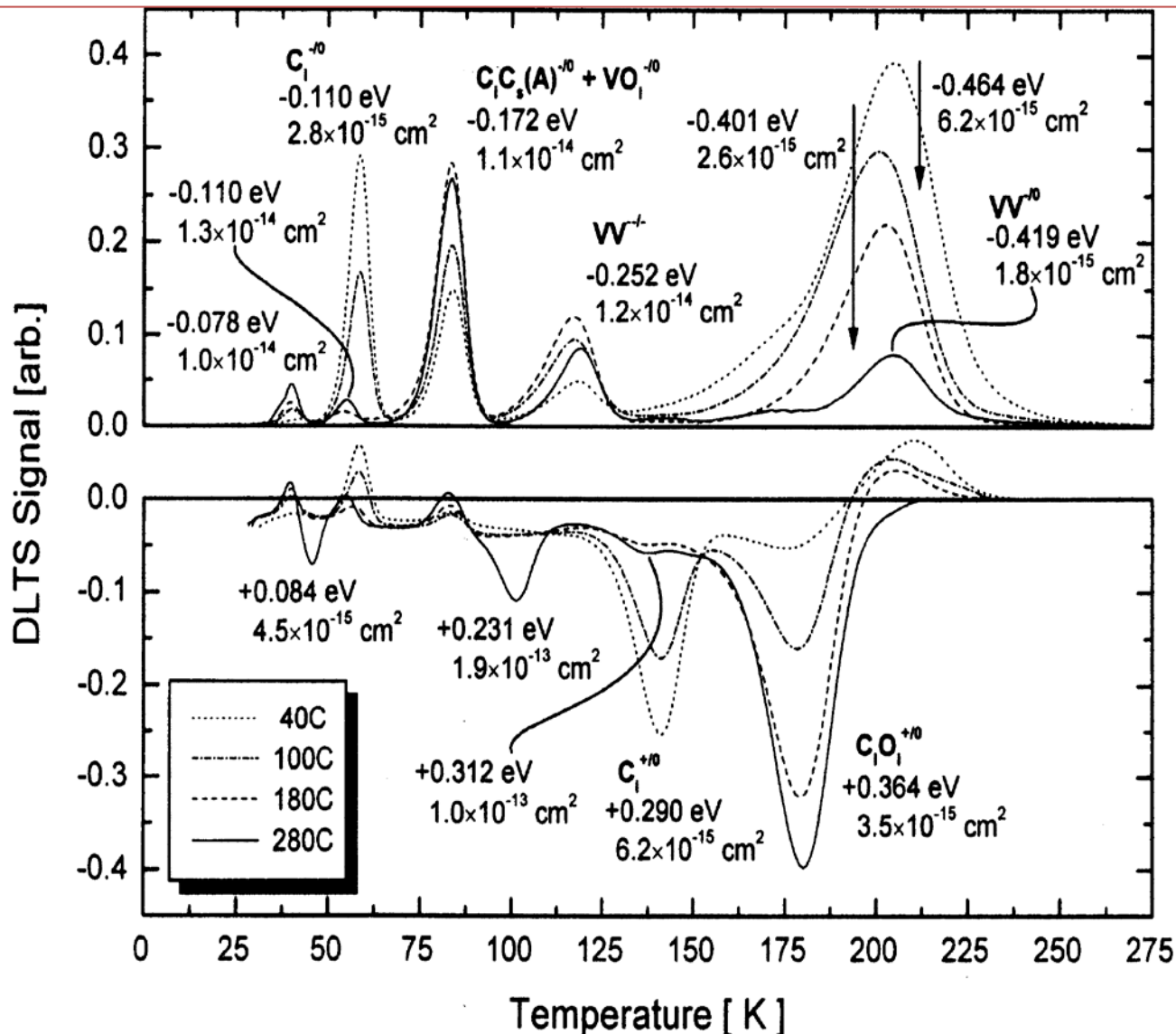


$$S = \Delta C_0 \left( e^{-e_n(T)t_1} - e^{-e_n(T)t_2} \right)$$

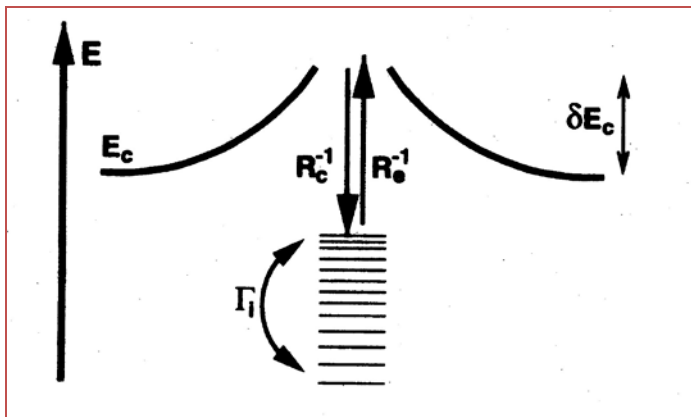
$$e_n(T_{\max}) = \frac{t_2 - t_1}{\ln(t_2/t_1)} \alpha T_{\max}^2 \cdot e^{-E_t/KT_{\max}}$$



Example: DLTS in Silicon  $f = 10^{11} \text{ cm}^{-2}$  5.3MeV neutrons  
ROSE Coll. NIM A 466 (2001) 308-326



## Clusters observed by DLTS in Silicon

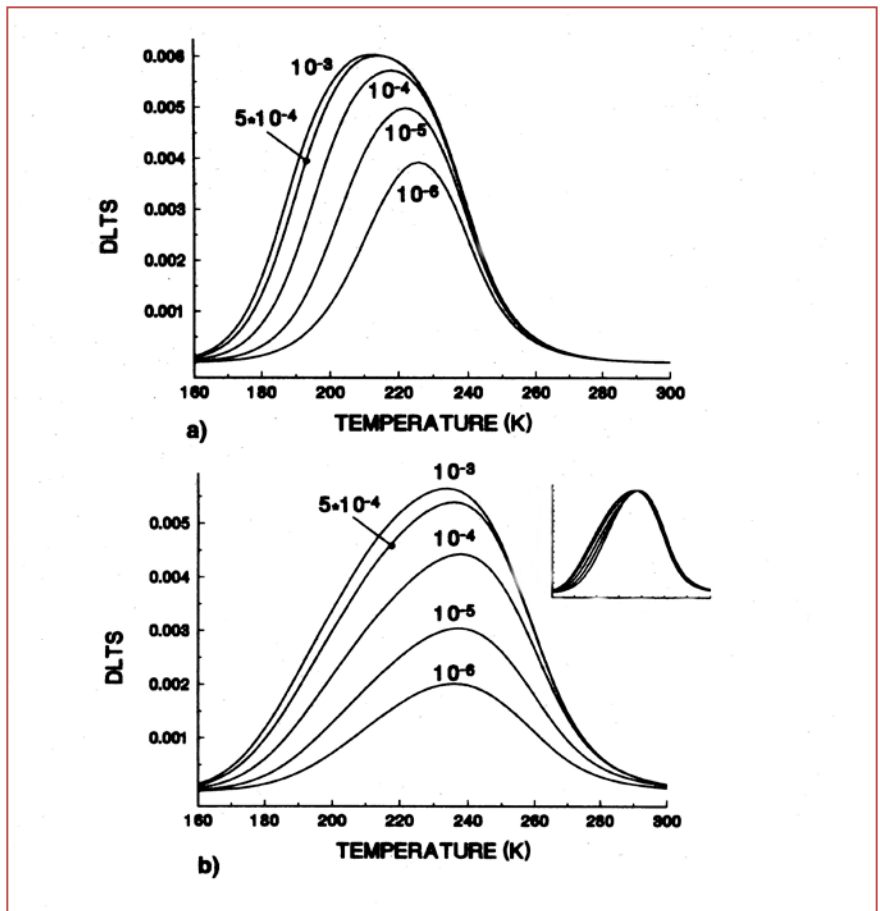


$$R_c(E, t) = \sigma_n v_{th} n [1 - f(E, t)] \exp\left[\frac{-\delta E_c}{kT}\right]$$

Main effect of clustering is a widening of the DLTS signal



A potential barrier is usually screening the extended defect



# Influence of deep levels on device properties

**Basic transport equations**

$$\frac{d^2 \psi_i}{dx^2} = -\frac{d\mathcal{E}}{dx} = -\frac{\rho}{\epsilon_s}$$

$$\frac{\partial n}{\partial t} = G_n - U_n + \frac{1}{q} \nabla \cdot \mathbf{J}_n,$$

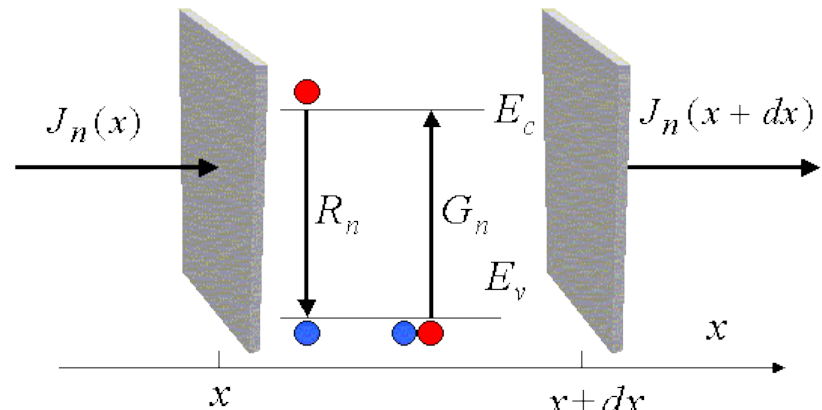
$$\frac{\partial p}{\partial t} = G_p - U_p - \frac{1}{q} \nabla \cdot \mathbf{J}_p$$

$$D_{n,p} = \mu_{n,p} \frac{KT}{e}$$

$$\mathbf{J}_n = q\mu_n n \mathcal{E} + qD_n \nabla n,$$

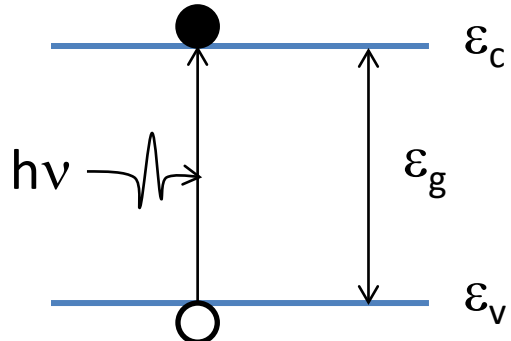
$$\mathbf{J}_p = q\mu_p p \mathcal{E} - qD_p \nabla p,$$

$$\mathbf{J}_{\text{cond}} = \mathbf{J}_n + \mathbf{J}_p,$$



Esempio: a 300K il valore di  $KT/e$  è pari a 25.9mV. Per una mobilità di  $1000\text{cm}^2/\text{Vs}$  abbiamo:  $D = 25.9\text{cm}^2/\text{s}$ .

## Generation of e/h pair s by ionizing radiation



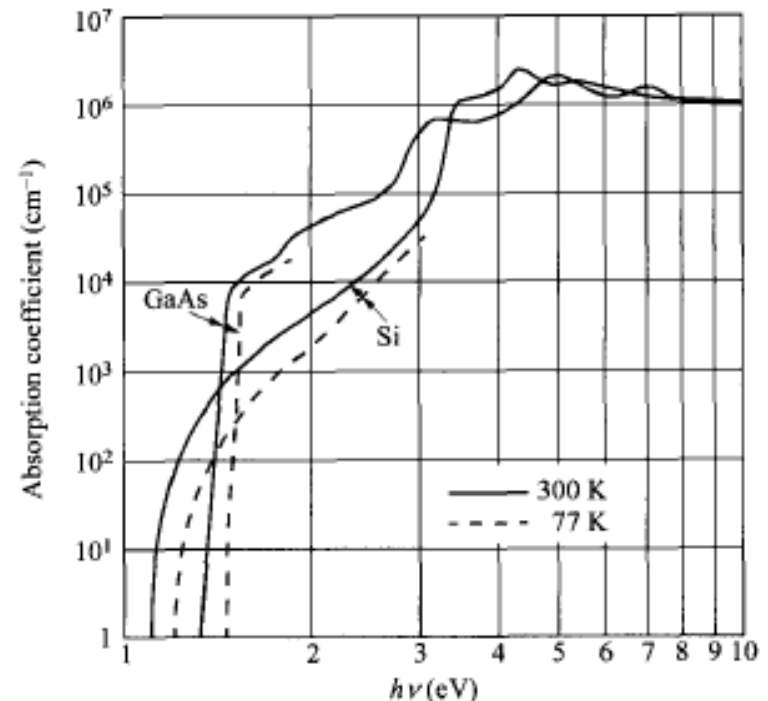
e/h pair generation  
coefficient

$$G_{e-h} = \frac{\alpha P_{opt}}{h\nu}$$

$\alpha$  = absorption coefficient ( $\text{cm}^{-1}$ )

$$\frac{dP_{opt}}{dx} = -\alpha P_{opt}$$

Nel grafico lo spostamento delle curve verso più alte energie al decrescere della temperatura è associato alla dipendenza dalla temperatura del gap proibito

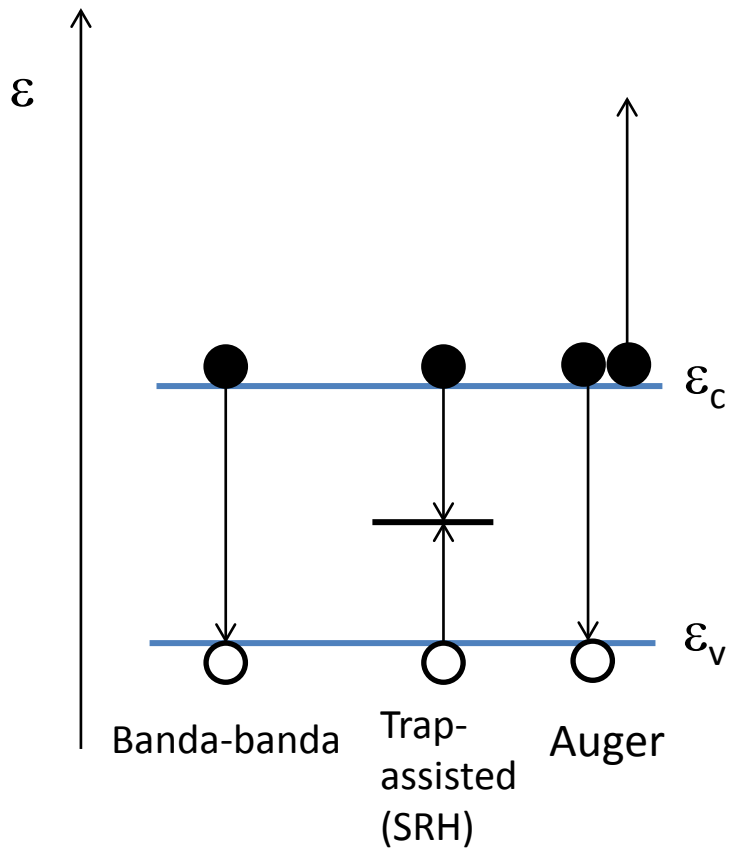


## Recombination processes

- **Ricombinazione banda-banda**: un elettrone in banda di conduzione si ricombina direttamente con una lacuna in banda di valenza. **Ricombinazione prevalente, generalmente anche radiativa, nei semiconduttori a gap diretto.**

- **Ricombinazione Auger** processo in cui un elettrone ed una lacuna ricombinano in una transizione banda-banda, ma l'energia risultante viene data ad un altro portatore, elettrone o lacuna.

- **Ricombinazione Shockley-Read-Hall (SRH)**: il processo è mediato da un livello intermedio nel gap dovuto ad un difetto reticolare. Esso cattura l'elettrone dalla banda di conduzione, successivamente l'elettrone nella trappola si ricombina con una lacuna in banda di valenza. **Processo di ricombinazione prevalente nei semiconduttori a gap indiretto.**



## Ricombinazione Banda-Banda

Questo meccanismo di ricombinazione dipende dalla concentrazione di elettroni e lacune libere, perciò, il tasso di ricombinazione banda-banda deve essere proporzionale al prodotto  $pn$ :

$$R_e = R_{ec} pn.$$

Con  $R_{ec}$  = coefficiente di ricombinazione All'equilibrio termico il tasso di ricombinazione deve essere uguale al tasso di generazione termica  $G_{th}$  poichè  $np = n_i^2$  possiamo scrivere  $G_{th} = R_{ec}n_i^2$ . In condizioni di non equilibrio il tasso netto di ricombinazione  $U$  è proporzionale a  $pn - n_i^2$ :

$$U = R_{ec} (pn - n_i^2) \quad ,$$

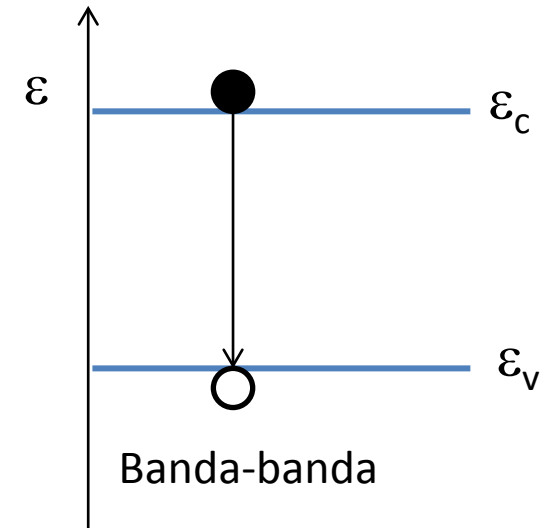
In condizioni di bassa iniezione, quando l'eccesso di portatori  $\Delta p = \Delta n$  è molto minore dei portatori maggioritari, in un semiconduttore tipo n abbiamo:

$$p_n = p_0 + \Delta p \text{ e } n_n \approx N_D \text{ quindi:}$$

$$U \approx R_{ec} \Delta p N_D = \frac{\Delta p}{\tau_p}.$$

Con  $\tau_p$  = vita media dei portatori minoritari:

$$\tau_p = \frac{1}{R_{ec} N_D}.$$



## Trap assisted recombination: the Shockley Read Hall Model

$$c_n = \sigma_n \langle v_n \rangle n$$

$$c_p = \sigma_p \langle v_p \rangle p$$

$$e_n = \sigma_n \langle v_n \rangle n_1$$

$$e_p = \sigma_p \langle v_p \rangle p_1$$

$$n = N_c \exp\left(\frac{E_F - E_C}{KT}\right)$$

$$p = N_v \exp\left(\frac{E_V - E_F}{KT}\right)$$

with:

$$n_1 = N_c \exp\left(\frac{E_t - \varepsilon_C}{KT}\right)$$

$$p_1 = N_v \exp\left(\frac{\varepsilon_V - E_t}{KT}\right)$$

$R_n$  net rate for exchanging electrons between conduction band and recombination center, is the difference between capture and emission rates:

$$R_c = c_n \frac{N_t - n_t}{N_t}$$



$$R_n = R_c - R_e = \sigma_n v_n \left[ n \frac{N_t - n_t}{N_t} - n_1 \frac{n_t}{N_t} \right]$$

$$R_e = e_n \frac{n_t}{N_t}$$

Similarly, for holes exchanged with the valence band:



$$R_p = \sigma_p v_p \left[ p \frac{n_t}{N_t} - p_1 \frac{N_t - n_t}{N_t} \right]$$

## RECOMBINATION OF ELECTRON – HOLE PAIR: $R_n = R_p$

$$\sigma_n v_n \left[ n \frac{N_t - n_t}{N_t} - n_1 \frac{n_t}{N_t} \right] = \sigma_p v_p \left[ p \frac{n_t}{N_t} - p_1 \frac{N_t - n_t}{N_t} \right]$$

From this we get the fraction of occupied traps:

$$\frac{n_t}{N_t} = \frac{\sigma_n v_n n + \sigma_p v_p p_1}{\sigma_n v_n (n + n_1) + \sigma_p v_p (p + p_1)}$$

Substituting in the expression of  $R_n$  we have:

$$R = \frac{\sigma_n \sigma_p v_n v_p (np - n_i^2)}{\sigma_n v_n (n + n_1) + \sigma_p v_p (p + p_1)}$$

defining  $U = R \cdot N_t$  and considering: most efficient traps at midgap,,  $v_n \approx v_p \approx v_{th}$ :

$$U = \frac{\sigma_n \sigma_p v_{th} N_t (np - n_i^2)}{\sigma_n (n + n_i) + \sigma_p (p + n_i)}$$

**Example: n-type semiconductor under low-injection :**  $U = \frac{\sigma_n \sigma_p v_{th} N_t (n(p_0 + \Delta p) - n_i^2)}{\sigma_n n}$



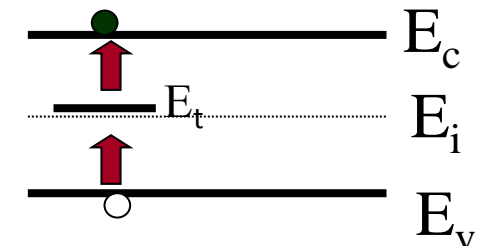
$$U \approx \sigma_p v_{th} N_t \Delta p = \frac{\Delta p}{\tau_p}$$

$\tau_p$  = minority carrier lifetime in the presence of  $N_t$  defects:  $\tau_p = \frac{1}{\sigma_p v_{th} N_t}$

## Leakage current in irradiated Si diodes: Thermal generation due to defects

When  $p n < n_i^2$  ( as in depleted junction ) the thermal generation mechanisms prevail over that of recombination. **The generation rate is :**

$$U \approx -\frac{\sigma_n \sigma_p v_{th} N_t n_i}{\sigma_n (1 + n/n_i) + \sigma_p (1 + p/n_i)} = -\frac{n_i}{\tau_g}$$



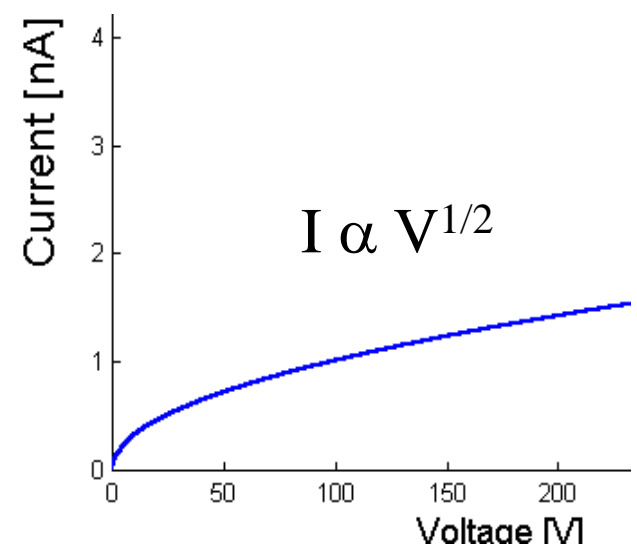
With:  $\tau_g = \frac{1+n/n_i}{\sigma_p v_{th} N_t} + \frac{1+p/n_i}{\sigma_n v_{th} N_t} = \left(1 + \frac{n}{n_i}\right) \tau_p + \left(1 + \frac{p}{n_i}\right) \tau_n$

Densità di corrente data dalla generazione:  $J_{gen} = \int_0^W q|U|dx = q|U|W = q \frac{n_i}{\tau_g} W$

$W$  = spessore della regione svuotata.

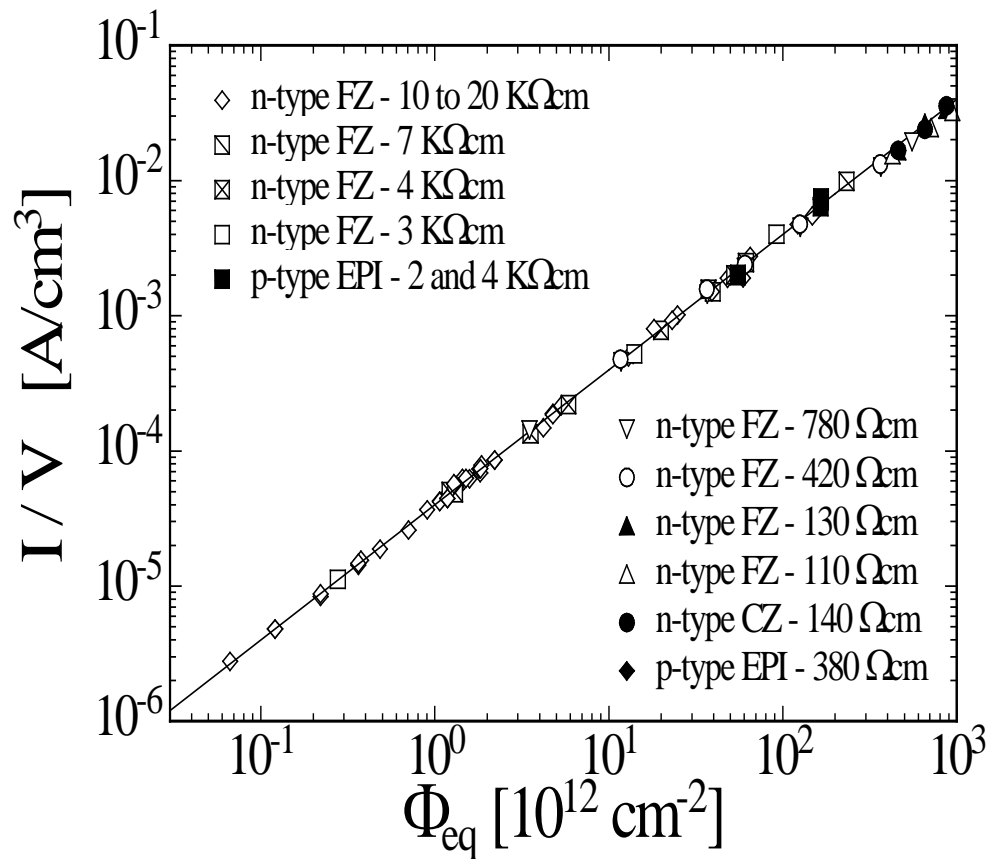
Poiché:  $W = \sqrt{\frac{2\varepsilon}{qN_B} (V_{bi} + |V_a|)}$

la corrente inversa risulta:  $J_R \propto \sqrt{(V_{bi} + |V_a|)}$



# Remind of macroscopic radiation damage

## 1. Leakage current increase with irradiation



$$\alpha = \frac{\Delta I}{V \cdot \Phi_{eq}}$$



Volumetric leakage current  
linearly dependent on fluence

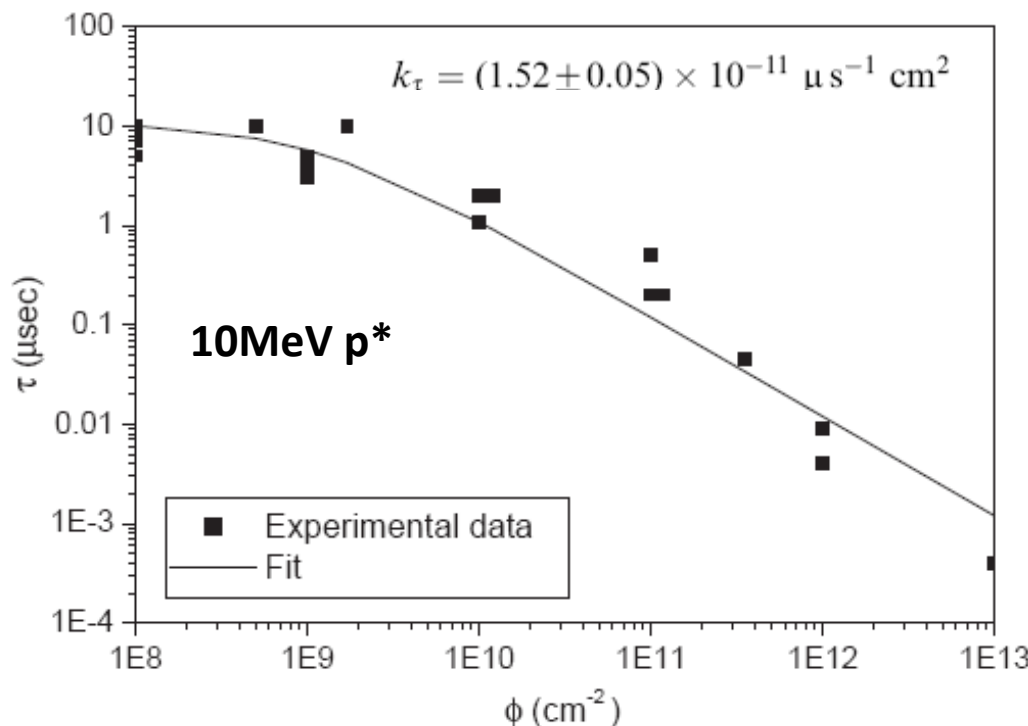
## A microscopic explanation of leakage current increase as due to the deterioration of the minority carrier lifetime with irradiation

$$\tau = \frac{1}{\sigma v_{th} N_t}$$

$N_t$  grows linearly with dose, thus:  $\frac{1}{\tau} = \frac{1}{\tau_0} + k_\tau \phi$

$$N_t \propto \Phi$$

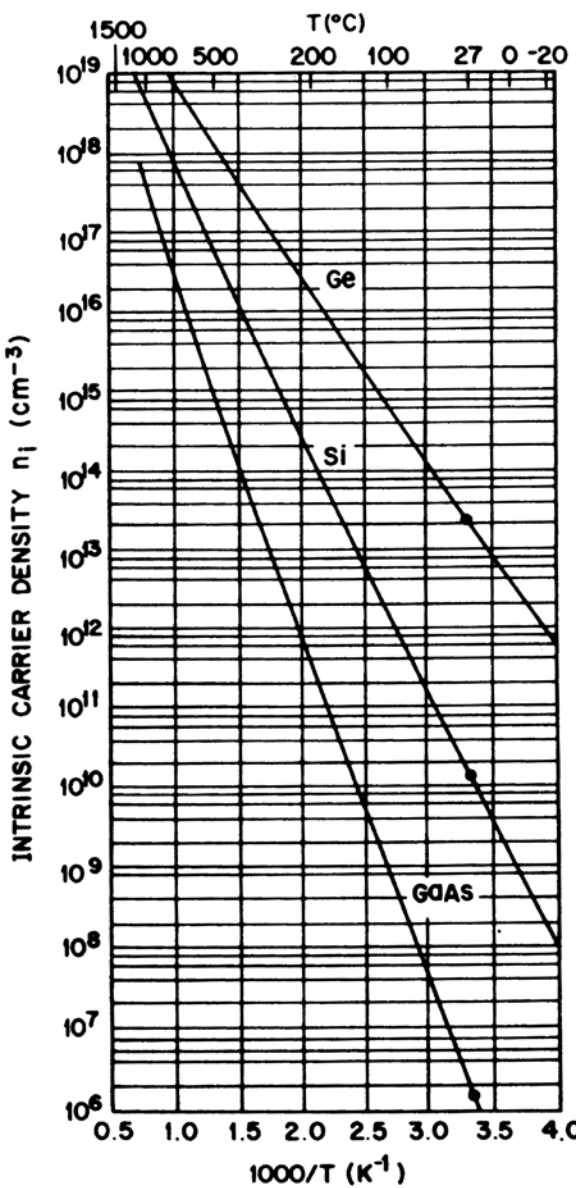
$$\text{as } I_{\text{leak}} \approx qAUW = qWn_i/\tau$$



Volumetric leakage current linearly dependent on fluence

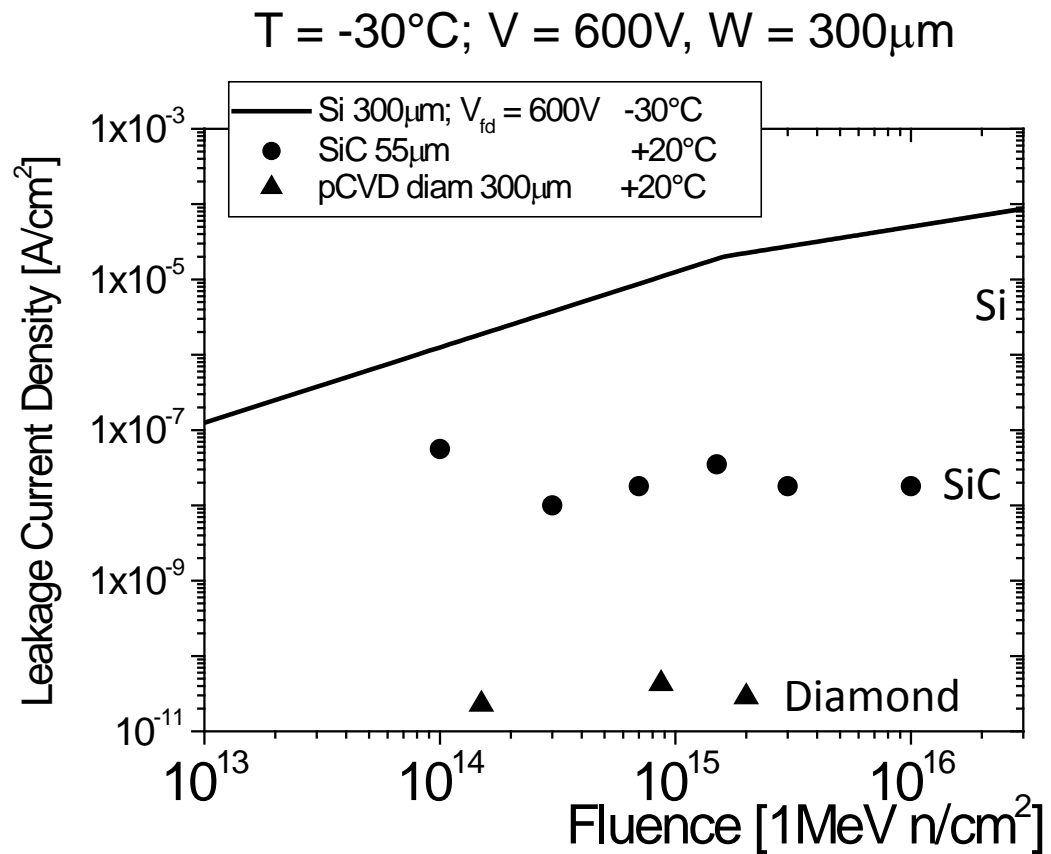
\*10 MeV protons produces a 3000 times larger equivalent damage compared to 1 MeV electrons

# High bandgap semiconductors: generation always negligible → intrinsically radiation hard



$$J_{gen} \propto \frac{n_i}{\tau_g} W$$

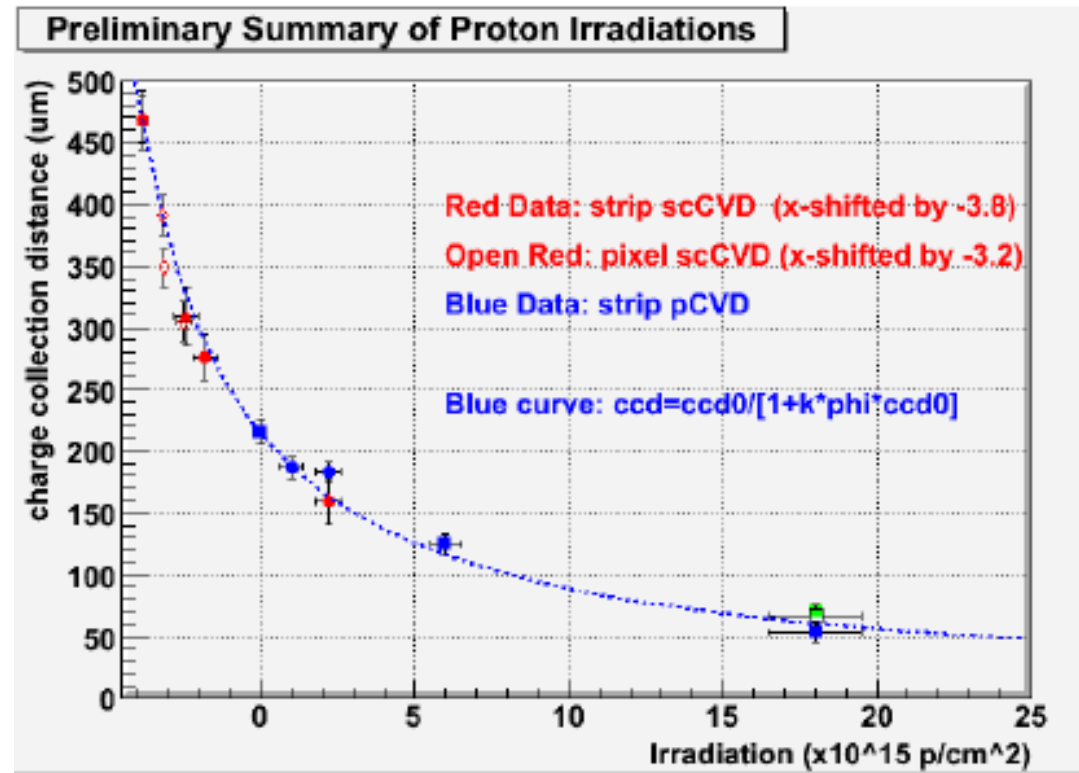
$$n_i \propto T^{\frac{3}{2}} e^{-\frac{\epsilon_{g,0}}{2K_B T}}$$



## 2. A microscopic explanation of Charge Collection Distance degradation in irradiated Diamond

*ccd = average distance h and e drift apart before recombination*

$$\frac{1}{CCD} = \frac{1}{CCD_0} + k \times \Phi$$



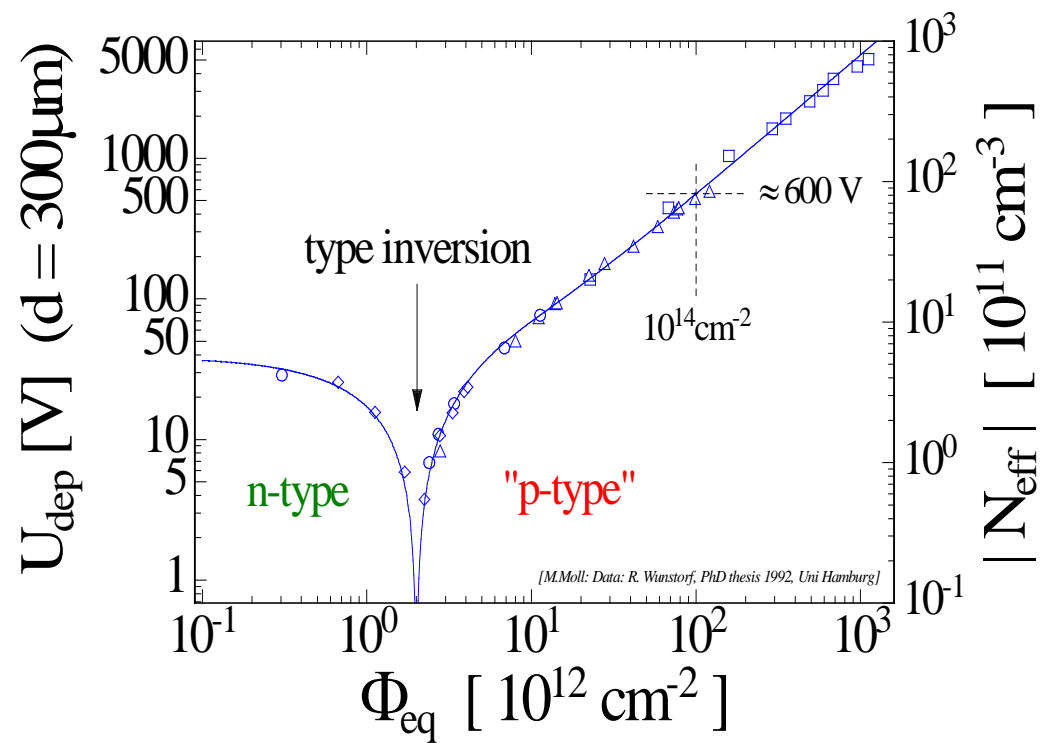
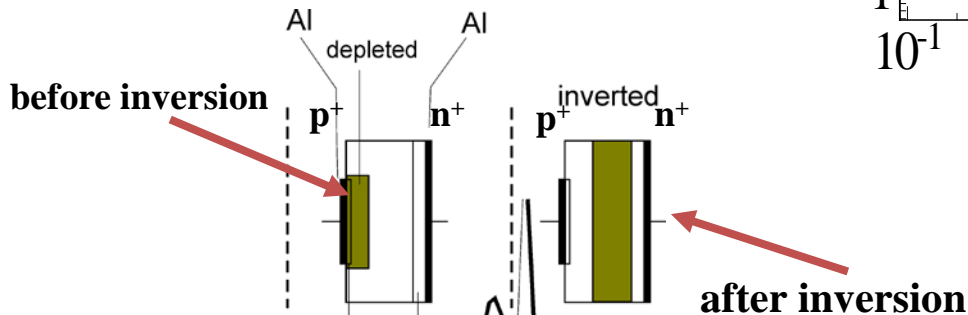
- $CCD_0$  initial traps in the material,  $k$  is the damage constant
- Single-crystal CVD and poly CVD fall along the same damage curve
- Larger  $CCD_0$  performs better at any fluence
- Proton damage well understood,  $k \sim 0.7 \times 10^{-18} \mu\text{m}^{-1}\text{cm}^{-2}$

# 3. Full depletion voltage

Radiation induced defects can contribute to the space charge density

$$\frac{d^2 \psi_i}{dx^2} = -\frac{d\mathcal{E}}{dx} = -\frac{\rho}{\epsilon_s}$$

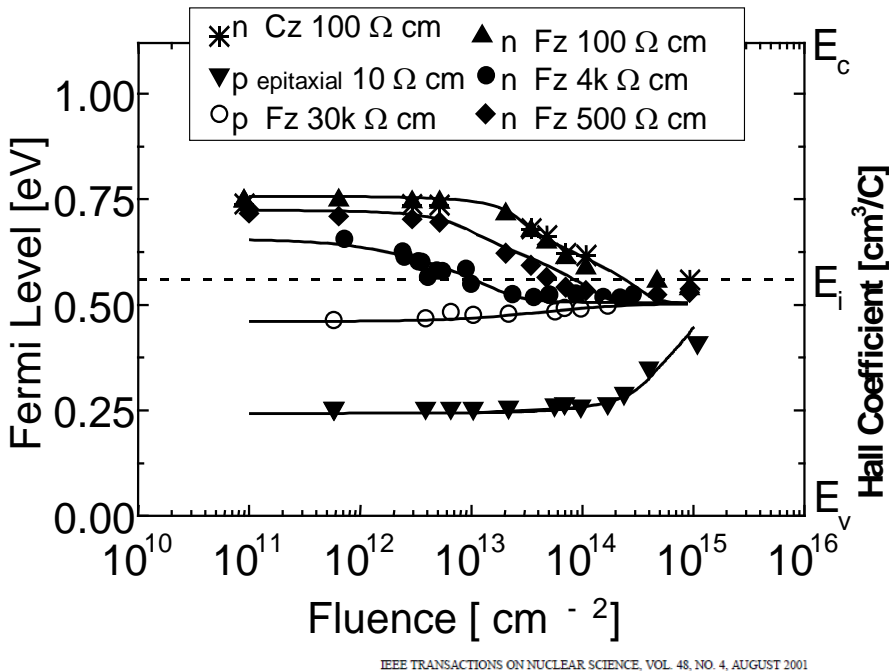
- “**Type inversion**”:  $N_{\text{eff}}$  changes from positive to negative (Space Charge Sign Inversion)



## 4. Radiation Damage of the Neutral bulk

Despite the high space charge at electrodes the neutral bulk, is almost intrinsic resistivity and slightly p-type conductivity ( measured through Hall coefficient).

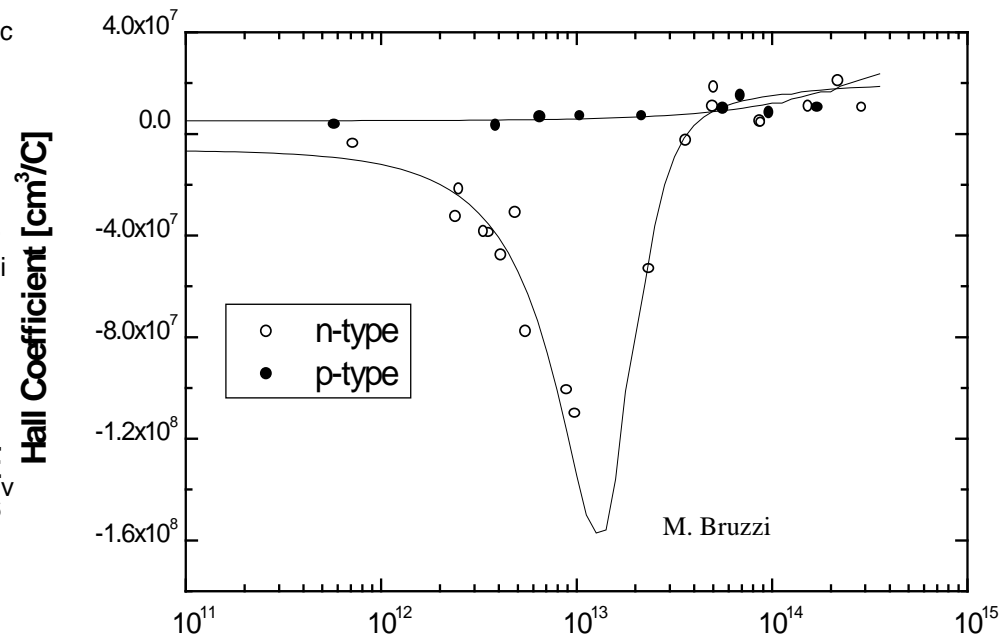
Irradiated Si (1MeV n-equivalent ) showing pinning of the Fermi level at  $E_v + 0.5$  eV in agreement with a quasi-intrinsic neutral bulk



IEEE TRANSACTIONS ON NUCLEAR SCIENCE, VOL. 48, NO. 4, AUGUST 2001

Radiation Damage in Silicon Detectors for  
High-Energy Physics Experiments

Mara Bruzzi



IEEE TRANSACTIONS ON NUCLEAR SCIENCE, VOL. 46, NO. 4, AUGUST 1999

| Effect Analysis in Irradiated Silicon Samples with Different Resistivities<sup>1</sup>

E. Borchi<sup>2</sup>, M. Bruzzi<sup>2</sup>, B. Dezillie<sup>3</sup>, S. Lazanu<sup>4</sup>, Z. Li<sup>3</sup> and S. Pirollo<sup>2</sup>

## Charge neutrality in semiconductor n-type prior to irradiation:

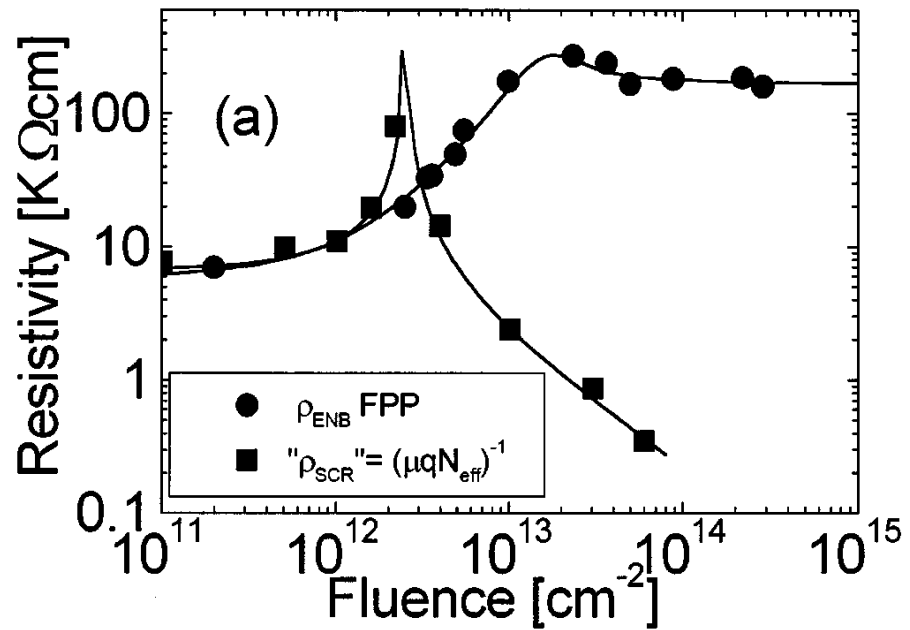
$n = N_D^+$  the free carrier concentration in neutral bulk is equal to the fixed positive charge in the depletion region due to shallow dopants.

## After irradiation:

$$n + N_{tA}^- = p + N_{tD}^+$$

Space charge dominated by the ionized traps,

Bulk neutral region almost intrinsic



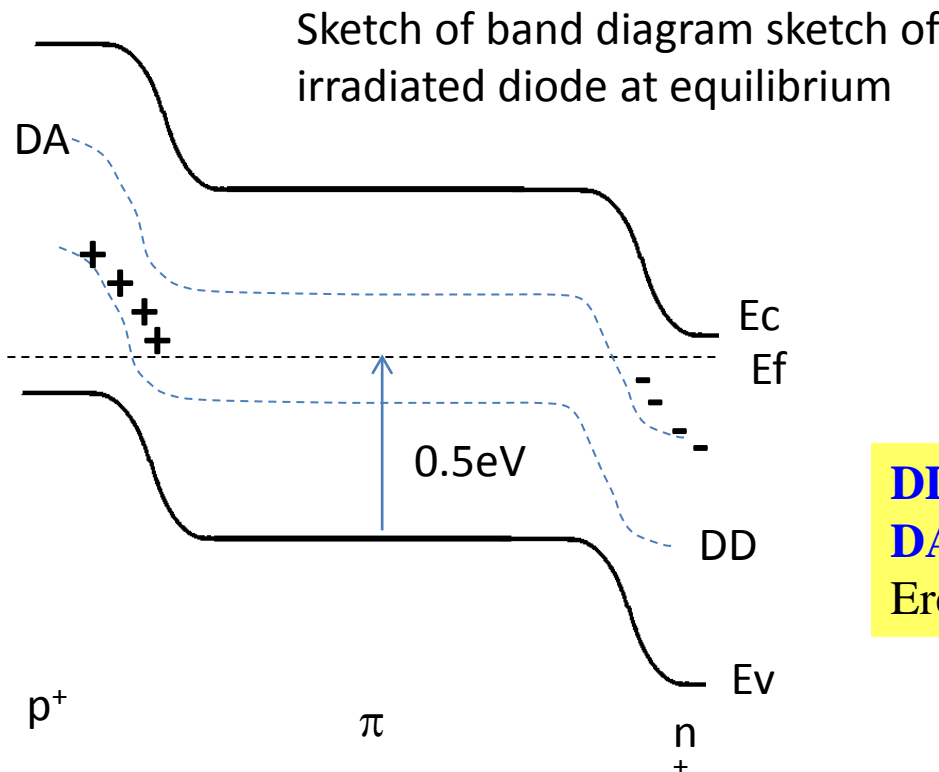
IEEE TRANSACTIONS ON NUCLEAR SCIENCE, VOL. 48, NO. 4, AUGUST 2001

Radiation Damage in Silicon Detectors for High-Energy Physics Experiments

Mara Bruzzi

# A microscopic explanation – the double level model

The discrepancy between high resistivity in bulk and high space charge in the depletion region is explained using a double level model with reversed behaviour : Deep Acceptor (DA) – Deep Donor (DD) DA in second half DD in first half of bandgap. They originate the double junction. Levels are neutral in bulk -> high resistivity, ionised close to contacts -> high space charge.



**DD:**  $E_v + 0.48 \text{ eV}$   
**DA:**  $E_c - 0.52 \text{ eV}$   
Eremin RESMDD2009

**Trap occupancy depends on free carrier concentration through  $c_n$ ,  $c_p$ .**

$$F = \frac{n_t}{N_t - n_t} = \frac{c_n + e_p}{c_p + e_n}$$

As:

$$n(x) = \frac{J_n(x)}{e v_{ndrift}}; \quad p(x) = \frac{J_p(x)}{e v_{pdift}}.$$

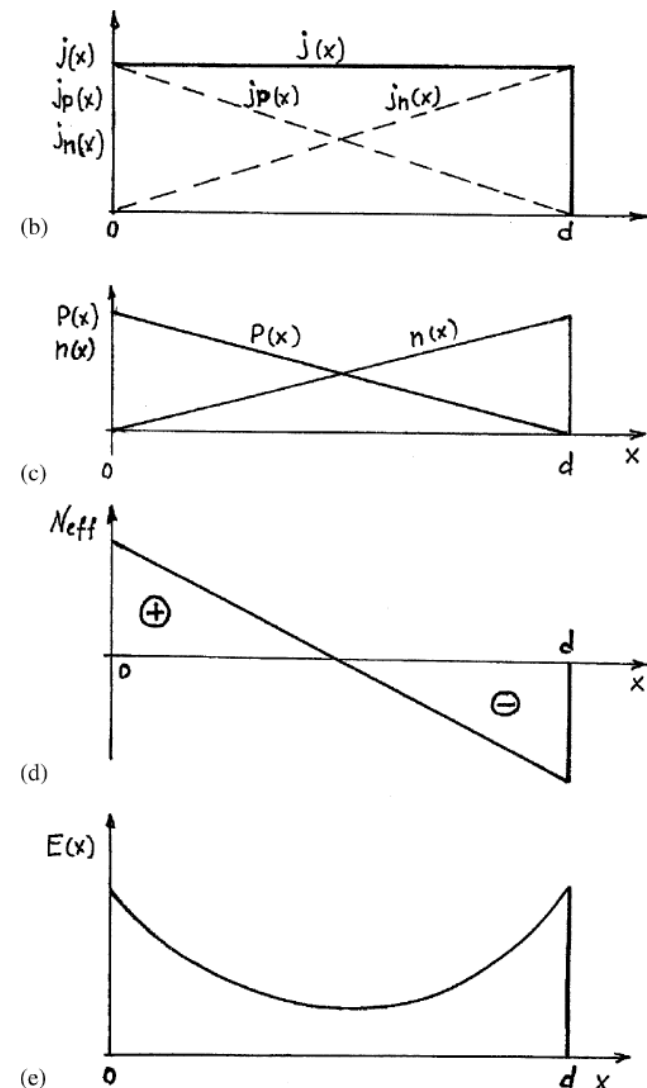
**charge state of deep traps is driven by the high current levels within the irradiated device**

e.g. in fully depleted detector, thermal generated current:

$J = Gd$  with d detector thickness, from continuity equation:

$$\nabla J_n = G \quad \text{with } J_n = 0 \text{ at } p^+ \text{ contact} \quad \nabla J_p = G \quad \text{with } J_p = 0 \text{ at } n^+ \text{ contact}$$

we get:  $J_n(x) = Gx$ ;  $J_p(x) = G(d - x)$ ; **high levels of defect in charge states +/- close to contacts → double junction, high Neff**



## 5. Charge Collection Efficiency (CCE) degradation due to trapping and charge multiplication

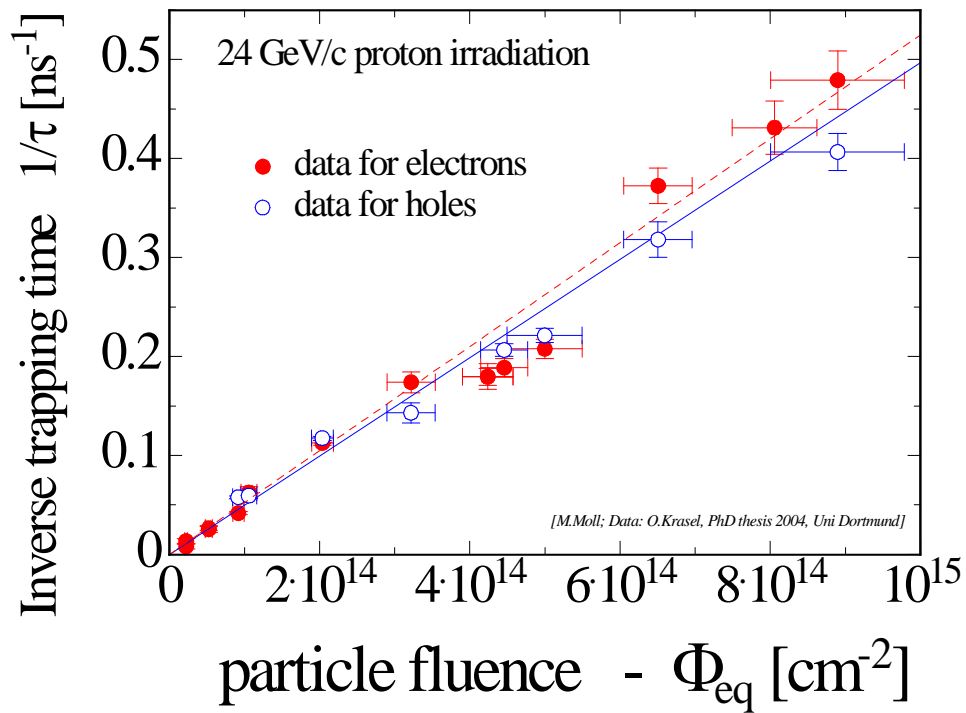
CCE degradation is mainly due to partial depletion and trapping.

Effective trapping time  $\tau_{\text{eff}}$  for electrons and holes:

$$Q_{e,h}(t) = Q_{0e,h} \exp\left(-\frac{1}{\tau_{\text{eff } e,h}} \cdot t\right)$$

where  $\frac{1}{\tau_{\text{eff } e,h}} \propto N_{\text{defects}}$

Increase of inverse  
trapping time ( $1/\tau$ )  
with fluence 



# Expected signal after charge trapping

## Effect of trapping on the Charge Collection Distance:

Expected collection distance at saturation velocity  $\lambda_{av}$ :

after  $1 \times 10^{15} n_{eq} \text{ cm}^{-2}$ :  $240 \mu\text{m}$   
expected charge  $\sim 19 \text{ ke}$ .

$\lambda_{av}$  after  $1 \times 10^{16} n_{eq} \text{ cm}^{-2}$ :  $25 \mu\text{m}$   
expected charge  $< 1.3 \text{ ke}$  : quite inefficient detector!

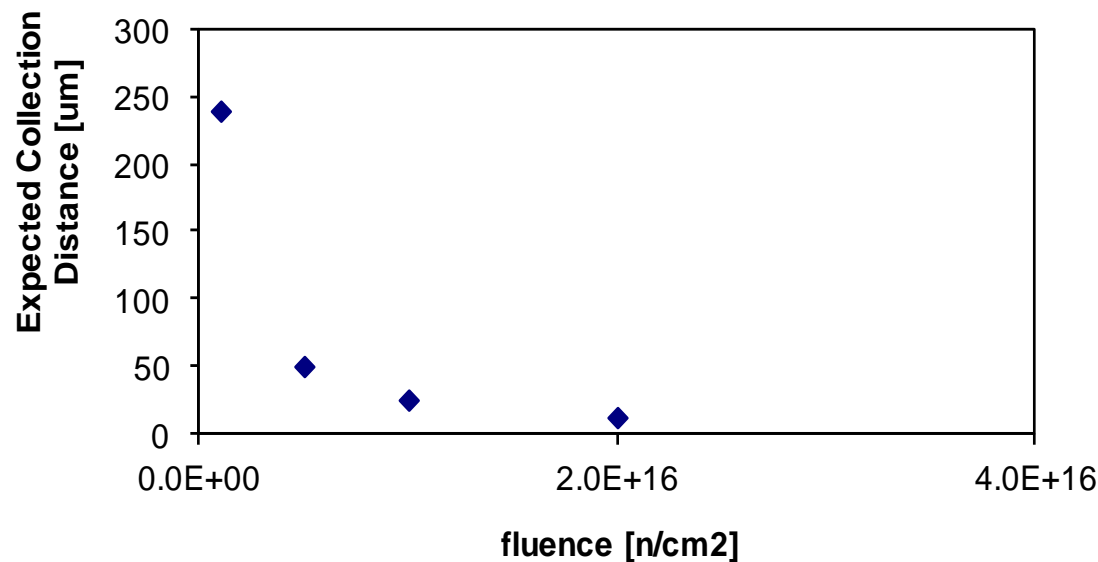
$$Q_{tc} \approx Q_0 \exp(-t_c/\tau_{tr}), \quad 1/\tau_{tr} = \beta \Phi.$$

$$v_{sat,e} \times \tau_{tr} = \lambda_{av}$$

$$\beta_e = 4.2 \times 10^{-16} \text{ cm}^{-2}/\text{ns}$$

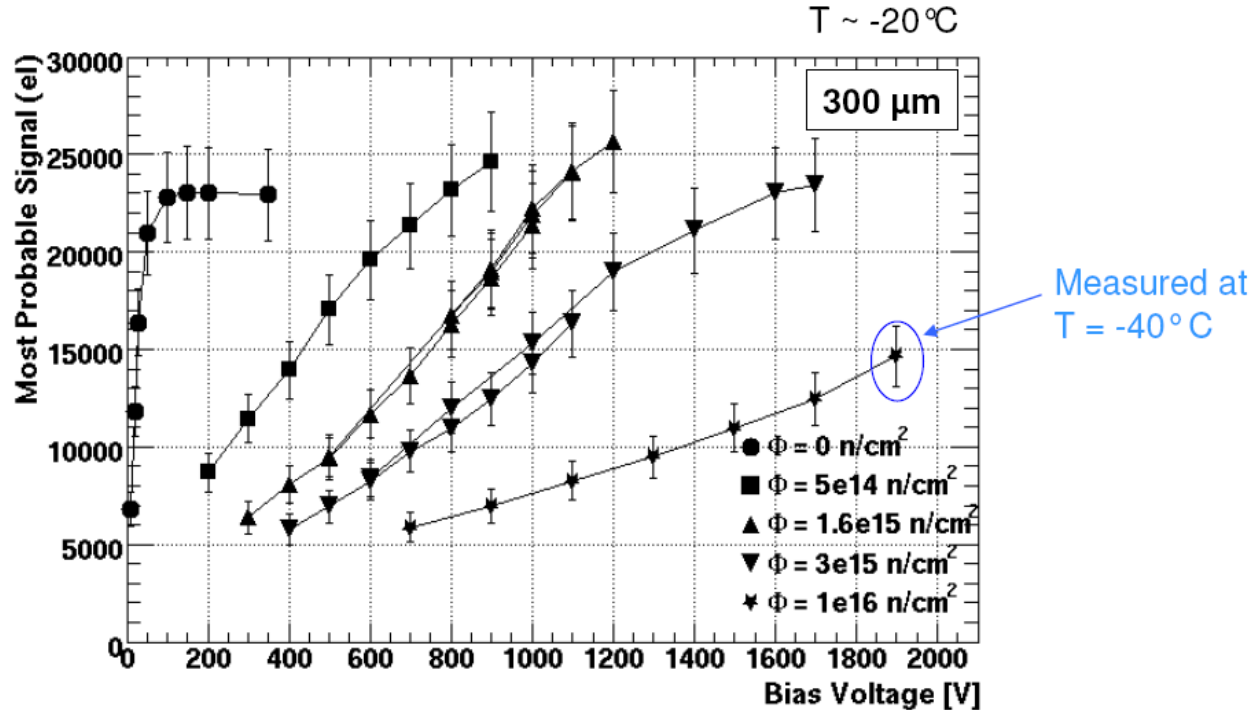
$$\beta_h = 6.1 \times 10^{-16} \text{ cm}^{-2}/\text{ns}$$

G. Kramberger et al.,  
NIMA 476(2002), 645-651.



# Charge Multiplication

CCE measured with p-type Si microstrip detectors at very high fluences shows evidence of a charge multiplication effect: 100% CCE seen after  $3 \times 10^{15} \text{ n/cm}^2$ , 15000 electrons after  $10^{16} \text{ n/cm}^2$



Increase of the electric field close to the strips causing impact ionization/carrier injection when high concentrations of effective acceptors are introduced at very high fluences.

# Avalanche multiplication

Quando il campo elettrico aumenta oltre un certo valore i portatori acquistano abbastanza energia da eccitare coppie e-h.

$\alpha$  = tasso di ionizzazione = n. di e-h generati da un portatore per unità di lunghezza percorsa

$$\alpha_n = \frac{1}{n} \frac{dn}{d(Iv_n)} = \frac{1}{nv_n} \frac{dn}{dt}$$

$\alpha$  fortemente dipendente dal campo applicato :

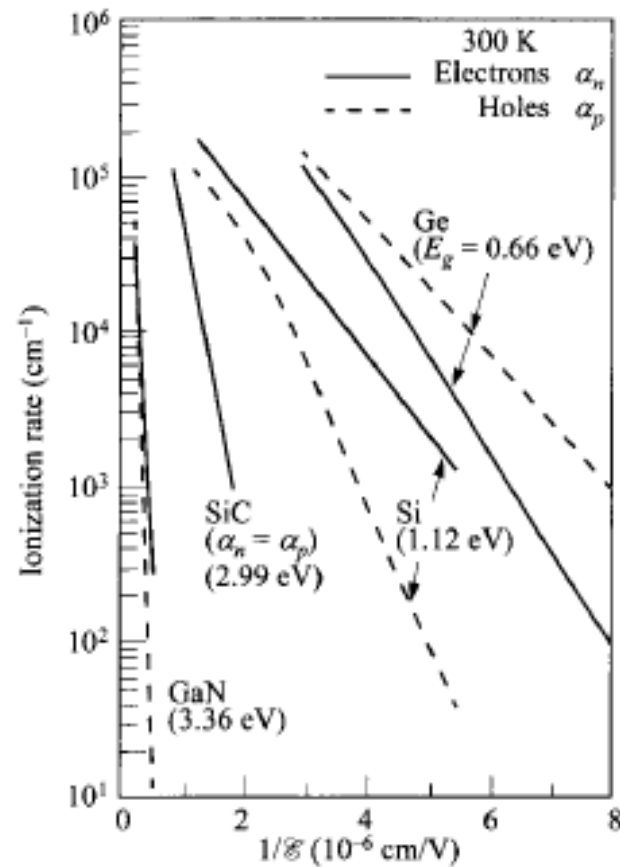
$$\alpha(\mathcal{E}) = \frac{q\mathcal{E}}{E_I} \exp \left\{ - \frac{\mathcal{E}_I}{\mathcal{E}[1 + (\mathcal{E}/\mathcal{E}_p)] + \mathcal{E}_T} \right\}$$

In Si :  $E_I = 3.6\text{eV}$  per elettroni,  $5.0\text{eV}$  per lacune.

$\mathcal{E}_T, \mathcal{E}_p, \mathcal{E}_I$ , soglie per il campo elettrico (thermal, optical-phonon and ionization scattering.)

Multiplication factor:

$$M = \int \alpha_{e,h} dx$$



# A microscopic explanation: Avalanche multiplication enhanced by defects in irradiated detectors

- formation of steady-state  $E(x)$  distribution due to generation of equilibrium carriers (bulk generation current) and carrier trapping to the deep levels of radiation induced defects;
- charge collection in the detector bulk with a calculated  $E(x)$  profile;
- avalanche multiplication of the carriers, which are transferred in the space charge region.

$$\text{div}E(x) = \frac{qN_{\text{eff}}(x)}{\epsilon\epsilon_0}$$

$$E = E(x)$$

$$Fe_n - (1-F)c_n n = 0$$

$$i(x) = Q(x)E^*(x)v_{dr}(x)$$

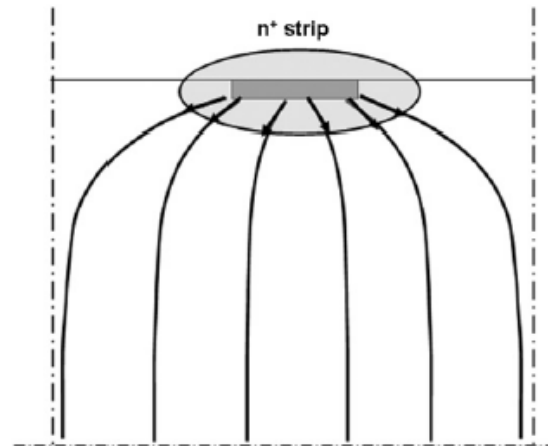
$$(1-F)e_p - Fc_p p = 0$$

$$Q(x) = Q_0 \exp\left(-\frac{t(x)}{\tau}\right)$$

$$\text{div}j_e = G_c$$

$$Q_c = \int_0^d i(x)dx$$

$$N_{\text{eff}} = N_{MGA}^+ - N_{MGA}^-$$



| Deep level | $\Delta E$ (eV) | $\sigma_e$ ( $\text{cm}^2$ ) | $\sigma_h$ ( $\text{cm}^2$ ) | $G$ ( $\text{cm}^{-1}$ ) |
|------------|-----------------|------------------------------|------------------------------|--------------------------|
| MGD        | $E_v + 0.48$    | $10^{-15}$                   | $10^{-15}$                   | 1                        |
| MGA        | $E_v + 0.595$   | $10^{-15}$                   | $10^{-15}$                   | 1                        |
| MGG        | $E_v + 0.65$    | $10^{-13}$                   | $10^{-13}$                   | 1                        |

## Results of simulation for avalanche multiplication enhanced by defects in irradiated detectors

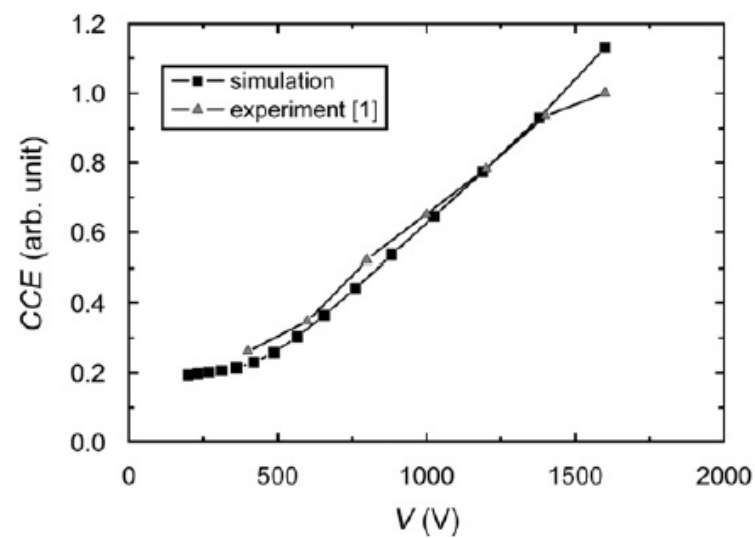
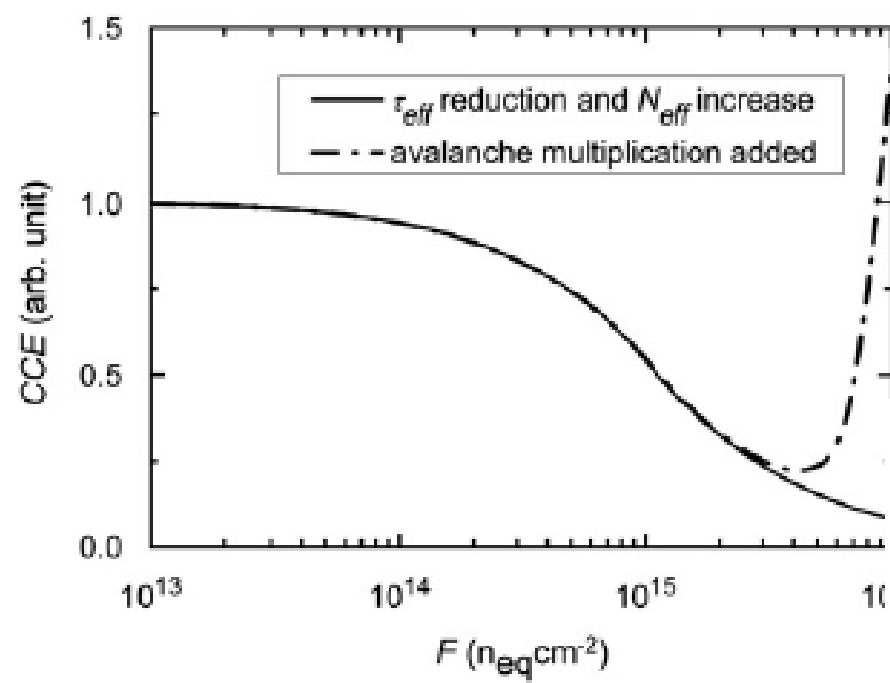


Fig. 7. Simulated dependence of CCE vs. bias voltage and experimental CCE on  $V$  data from Ref. [1] for detector irradiated to  $3 \times 10^{15} n_{eq}/cm^2$ .

# *Defect Engineering*

## Oxygen Enrichment for Radiation Hardening

RD48 (ROSE) CERN Collaboration

**Main Hypothesis: Oxygen sink of vacancies**

V-O<sub>i</sub> complex concentration increase → reduction of deeper levels  
mainly divacancy related

**1964 Significant radiation hardening for Co<sup>60</sup> γ-irradiation by increasing the oxygen concentration ( CZ Si )**

T.Nakano, Y.Inuishi, effects of dosage and impurities on radiation damage of carrier lifetime in silicon, J.Phys. Soc., 19, 851-858,(1964)

**1966 Neutron-induced degradation independent of the oxygen concentration ( CZ Si )**

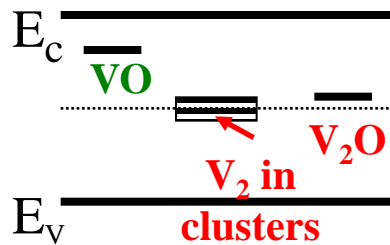
O.L.Curtis Jr., Effects of oxygen and dopant on lifetime in neutron-irradiated silicon, IEEE Trans. Nucl. Sci. NS-13, 6, 33-40 (1966).

# Oxygen Enrichment for Radiation Hardening

## RD48 (ROSE) and RD50 CERN Collaborations

**Main Hypothesis: Oxygen beneficial as sink of vacancies**

$V-O_i$  complex concentration increase  $\longrightarrow$  reduction of deeper levels  
mainly divacancy related



**Typical oxygen concentration in Si:**

-FZ [O<sub>i</sub>]  $10^{15} \text{ cm}^{-3}$

-Diffusion oxygenated FZ : DOFZ [O<sub>i</sub>]  $10^{16}\text{-}10^{17} \text{ cm}^{-3}$

-Czochralski Si: [O<sub>i</sub>] up to  $10^{18} \text{ cm}^{-3}$

**Note:** as VO is a point defect the beneficial effect of oxygen is expected especially when cluster formation by irradiation is less important than point defect formation.

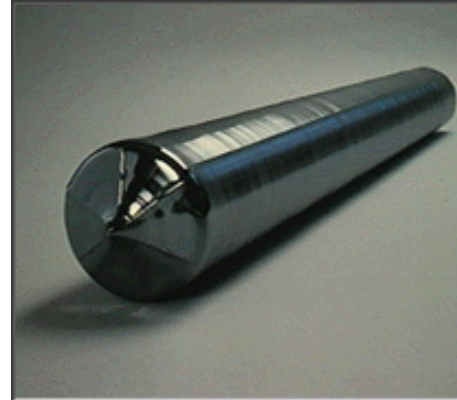
# Material: Float Zone Silicon (FZ)

## ■ Float Zone process

Using a single Si crystal seed, melt the vertically oriented rod onto the seed using RF power and “pull” the monocrystalline ingot

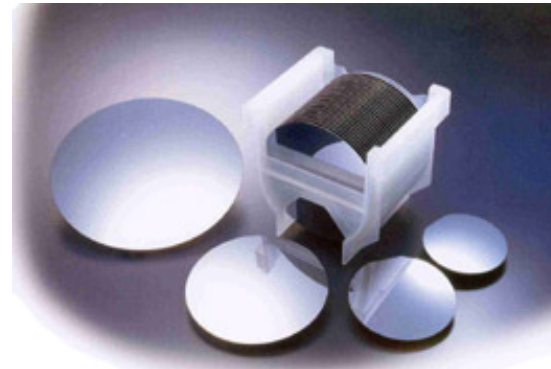


## ■ Mono-crystalline Ingot



## ■ Wafer production

- Slicing, lapping, etching, polishing

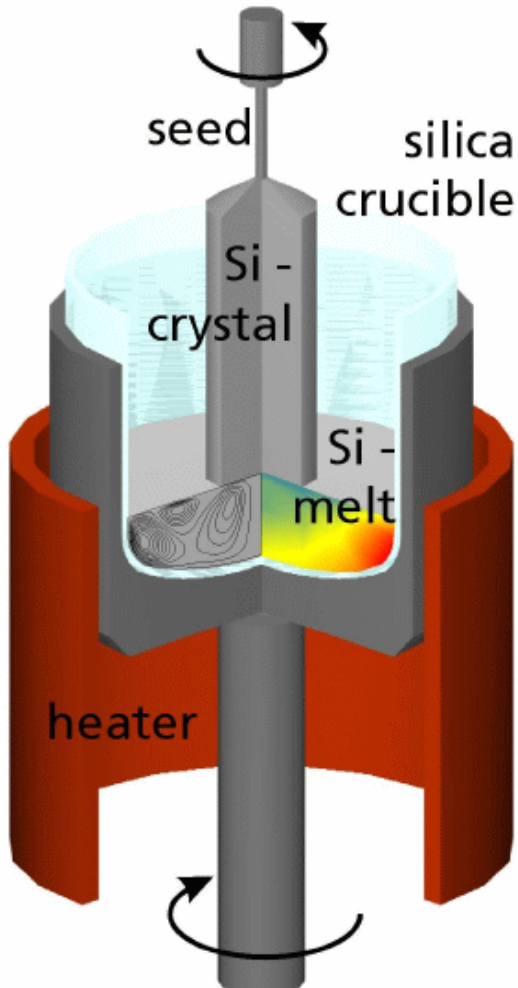


## ■ Highly pure crystal

- Low concentration of [O] and [C]  $10^{15} \text{cm}^{-3}$

# Czochralski silicon (Cz) & Epitaxial silicon (EPI)

### ■ Czochralski silicon



- Pull Si-crystal from a Si-melt contained in a silica crucible while rotating.
- Silica crucible is dissolving oxygen into the melt  $\Rightarrow$  high concentration of O in CZ
- Material used by IC industry (cheap)
- Recent developments (~5 years) made CZ available in sufficiently high purity (resistivity) to allow for use as particle detector.

### ■ Epitaxial silicon

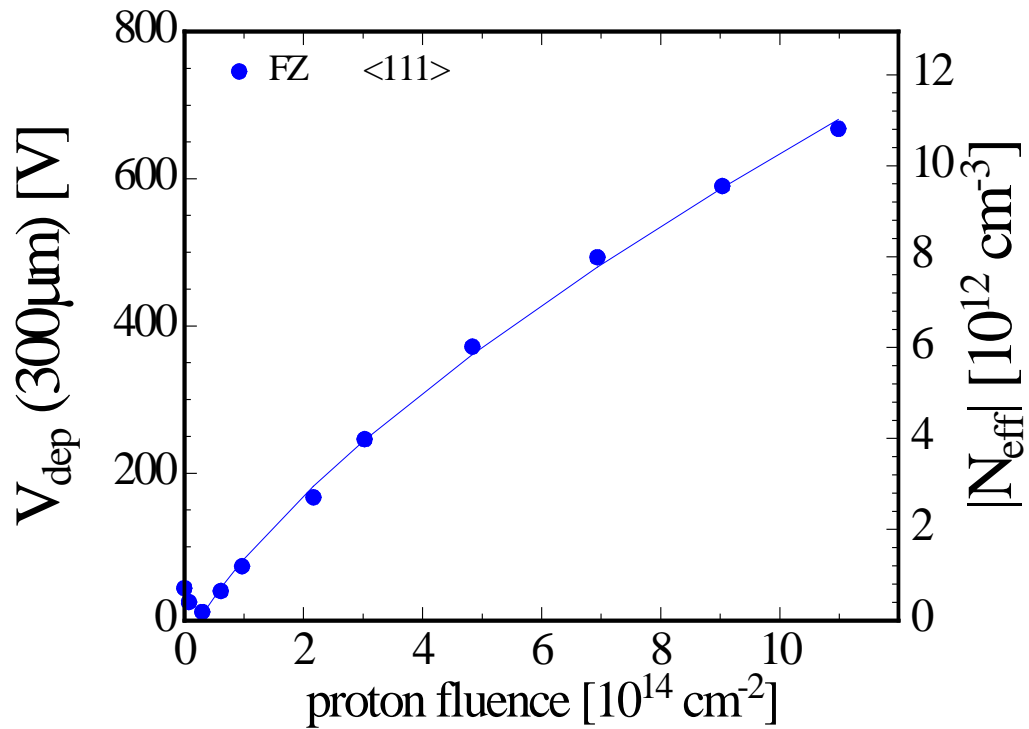
- Chemical-Vapor Deposition (CVD) of Silicon
- CZ silicon substrate used  $\Rightarrow$  in-diffusion of oxygen
- growth rate about  $1\mu\text{m}/\text{min}$
- excellent homogeneity of resistivity
- up to  $150\ \mu\text{m}$  thick layers produced (thicker is possible)
- price depending on thickness of epi-layer but not extending  $\sim 3 \times$  price of FZ wafer

# Standard FZ, DOFZ, MCz and Cz silicon

## 24 GeV/c proton irradiation

- **Standard FZ silicon**

- type inversion at  $\sim 2 \times 10^{13} \text{ p/cm}^2$
- strong  $N_{\text{eff}}$  increase at high fluence



# Standard FZ, DOFZ, MCz and Cz silicon

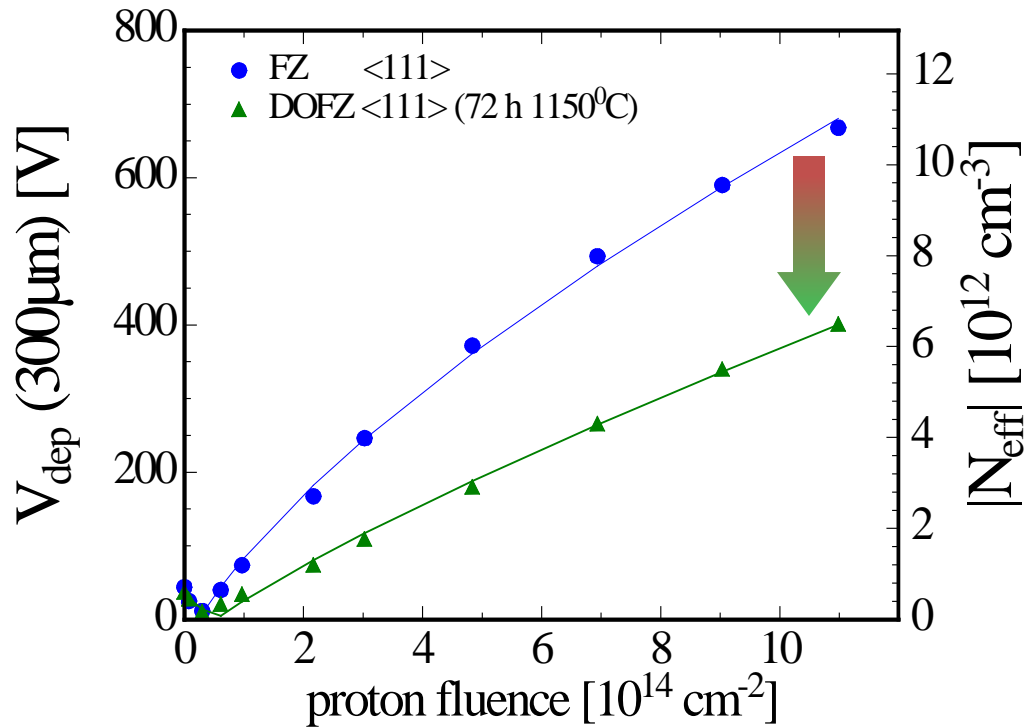
## 24 GeV/c proton irradiation

- **Standard FZ silicon**

- type inversion at  $\sim 2 \times 10^{13} \text{ p/cm}^2$
- strong  $N_{\text{eff}}$  increase at high fluence

- **Oxygenated FZ (DOFZ)**

- type inversion at  $\sim 2 \times 10^{13} \text{ p/cm}^2$
- reduced  $N_{\text{eff}}$  increase at high fluence



# Standard FZ, DOFZ, MCz and Cz silicon

## 24 GeV/c proton irradiation

- Standard FZ silicon

- type inversion at  $\sim 2 \times 10^{13} \text{ p/cm}^2$
- strong  $N_{\text{eff}}$  increase at high fluence

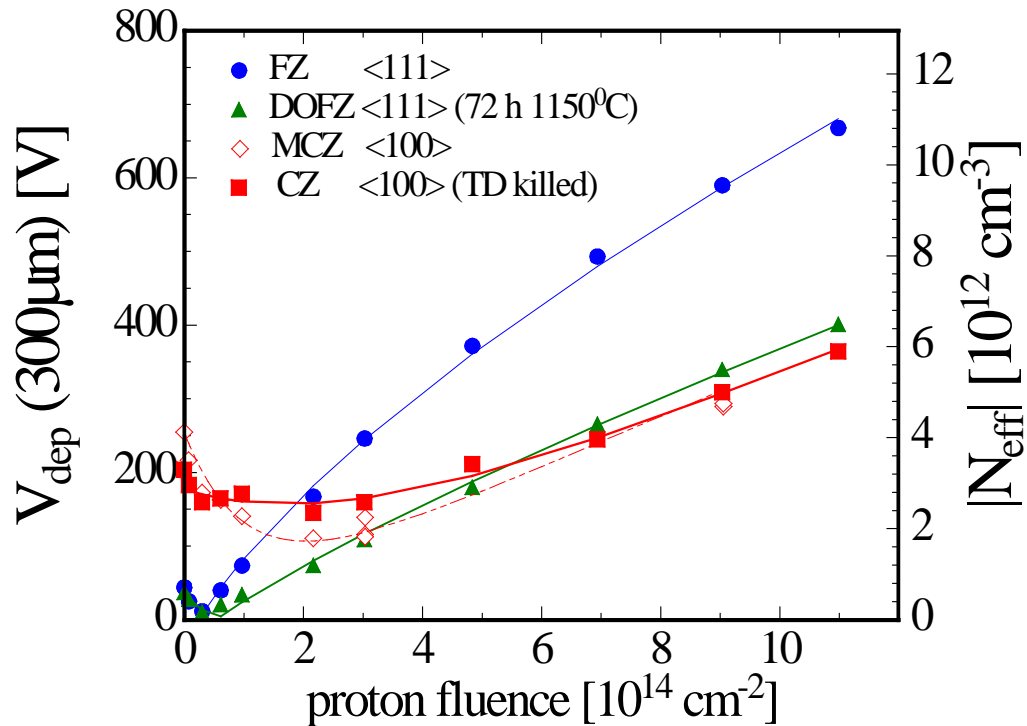
- Oxygenated FZ (DOFZ)

- type inversion at  $\sim 2 \times 10^{13} \text{ p/cm}^2$
- reduced  $N_{\text{eff}}$  increase at high fluence

- CZ silicon and MCZ silicon

- “no type inversion” in the overall fluence range

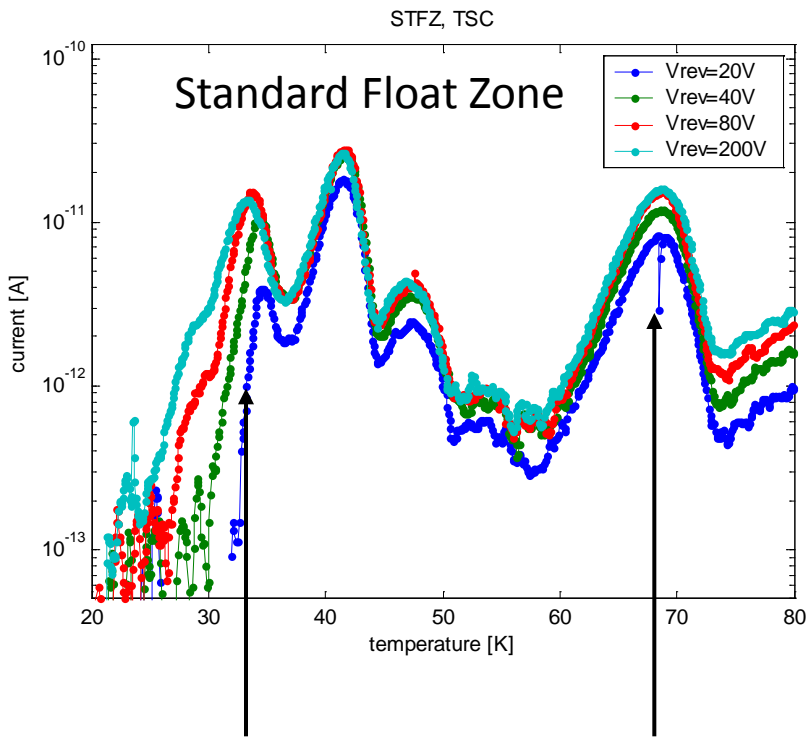
(for experts: there is no “real” type inversion, a more clear understanding of the observed effects is obtained by investigating directly the internal electric field; look for: TCT, MCZ, double junction)



- Common to all materials (after hadron irradiation, not after  $\gamma$  irradiation):
  - reverse current increase
  - increase of trapping (electrons and holes) within  $\sim 20\%$

# Rad-induced shallow donor created in MCz Silicon

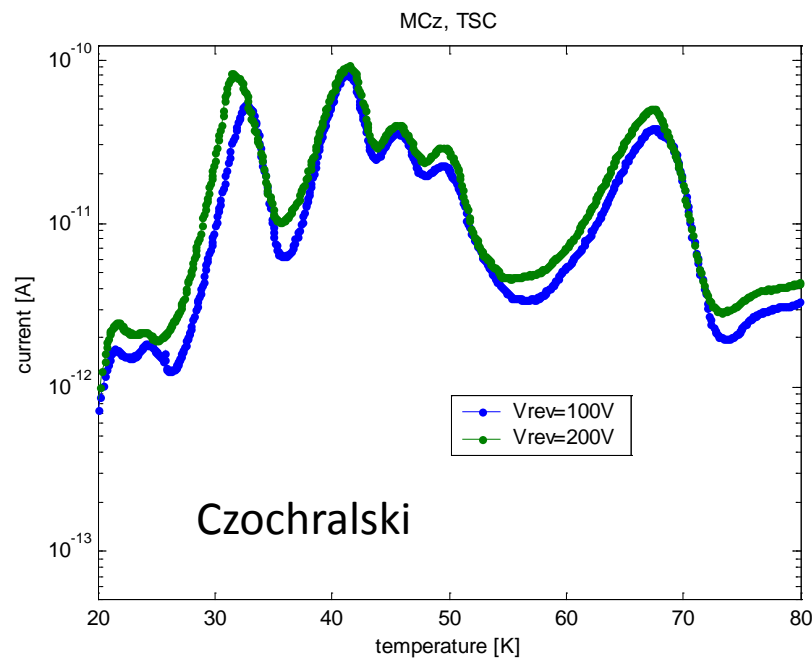
24 GeV p irradiated,  $\Phi=2\times10^{14}$  n/cm<sup>2</sup>



Shallow donor  
(SD) emission

VO emission

26 MeV p irradiated,  $\Phi=2.5\times10^{14}$  n/cm<sup>2</sup>



- Signal can be saturated for STFZ but not for MCz sample
- VO concentration is at least 3 times higher in MCz than in STFZ
- SD concentration is at least 5 times higher in MCz than in STFZ

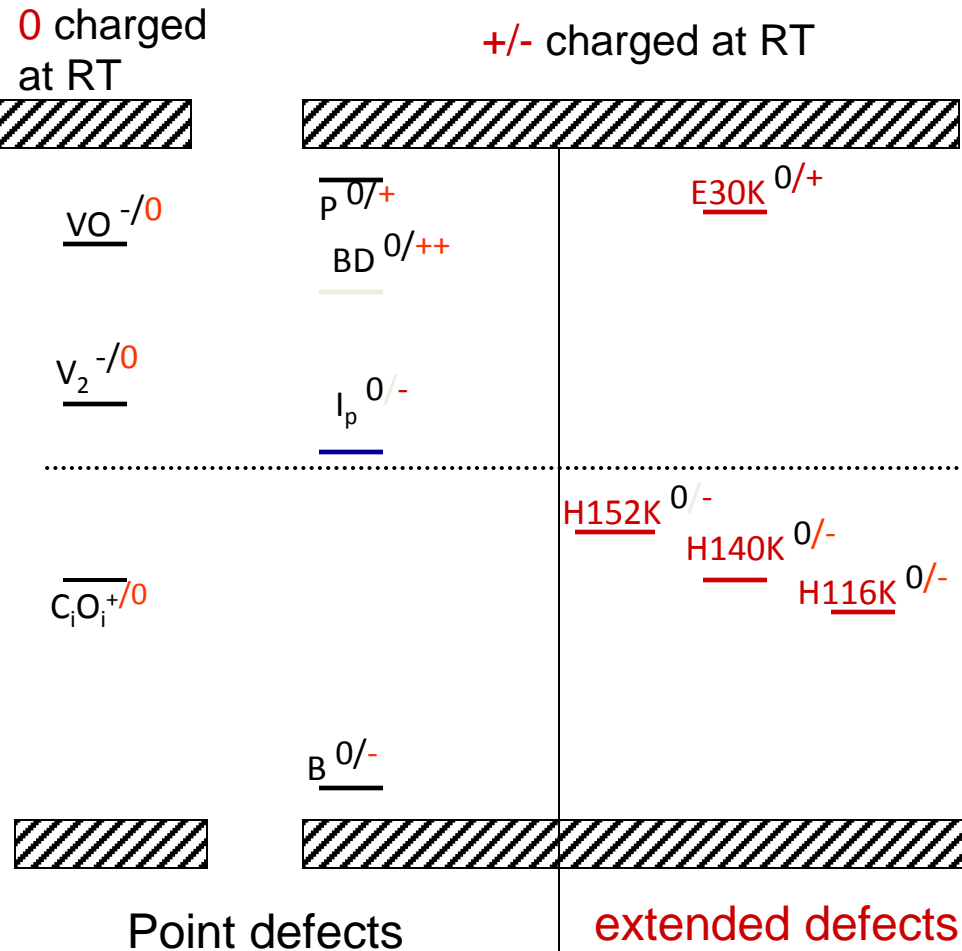
# Summary – defects with strong impact on the device properties

## Point defects

- $E_i^{BD} = E_c - 0.225 \text{ eV}$   
 $\sigma_n^{BD} = 2.3 \cdot 10^{-14} \text{ cm}^2$
- $E_i^I = E_c - 0.545 \text{ eV}$ 
  - $\sigma_n^I = 2.3 \cdot 10^{-14} \text{ cm}^2$
  - $\sigma p^I = 2.3 \cdot 10^{-14} \text{ cm}^2$

## Cluster related centers

- $E_i^{116K} = E_v + 0.33 \text{ eV}$
- $\sigma_p^{116K} = 4 \cdot 10^{-14} \text{ cm}^2$
- $E_i^{140K} = E_v + 0.36 \text{ eV}$
- $\sigma_p^{140K} = 2.5 \cdot 10^{-15} \text{ cm}^2$
- $E_i^{152K} = E_v + 0.42 \text{ eV}$
- $\sigma_p^{152K} = 2.3 \cdot 10^{-14} \text{ cm}^2$
- $E_i^{30K} = E_c - 0.1 \text{ eV}$
- $\sigma_n^{30K} = 2.3 \cdot 10^{-14} \text{ cm}^2$



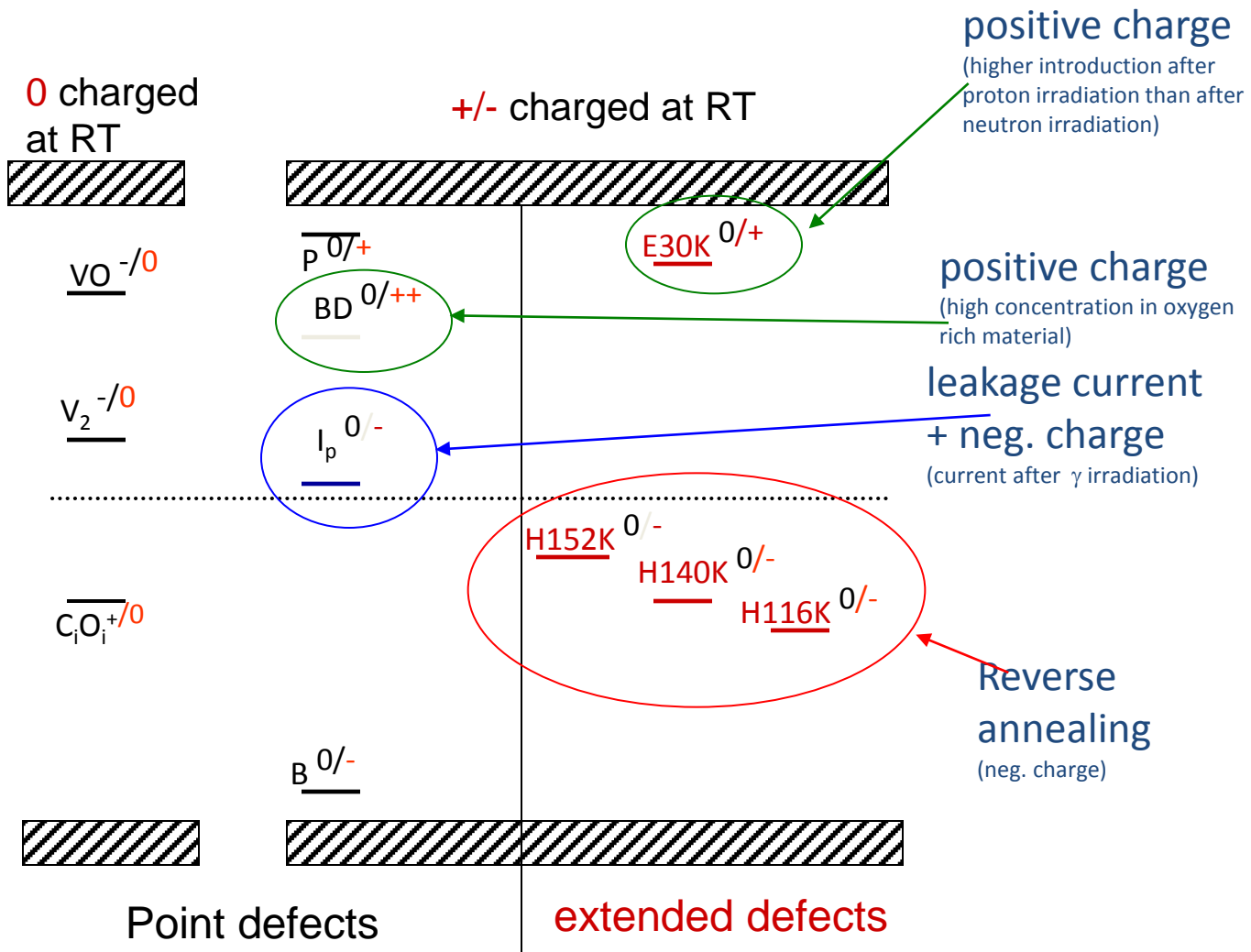
# Summary – defects with strong impact on the device properties at operating temperature

## Point defects

- $E_i^{BD} = E_c - 0.225 \text{ eV}$
- $\sigma_n^{BD} = 2.3 \cdot 10^{-14} \text{ cm}^2$
- $E_i^I = E_c - 0.545 \text{ eV}$ 
  - $\sigma_n^I = 2.3 \cdot 10^{-14} \text{ cm}^2$
  - $\sigma p^I = 2.3 \cdot 10^{-14} \text{ cm}^2$

## Cluster related centers

- $E_i^{116K} = E_v + 0.33 \text{ eV}$
- $\sigma_p^{116K} = 4 \cdot 10^{-14} \text{ cm}^2$
- $E_i^{140K} = E_v + 0.36 \text{ eV}$
- $\sigma_p^{140K} = 2.5 \cdot 10^{-15} \text{ cm}^2$
- $E_i^{152K} = E_v + 0.42 \text{ eV}$
- $\sigma_p^{152K} = 2.3 \cdot 10^{-14} \text{ cm}^2$
- $E_i^{30K} = E_c - 0.1 \text{ eV}$
- $\sigma_n^{30K} = 2.3 \cdot 10^{-14} \text{ cm}^2$



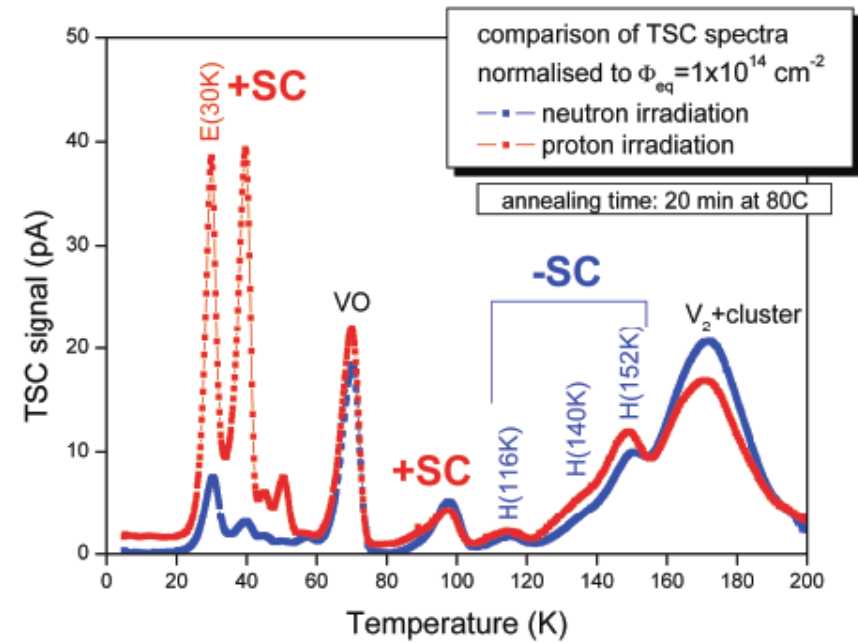
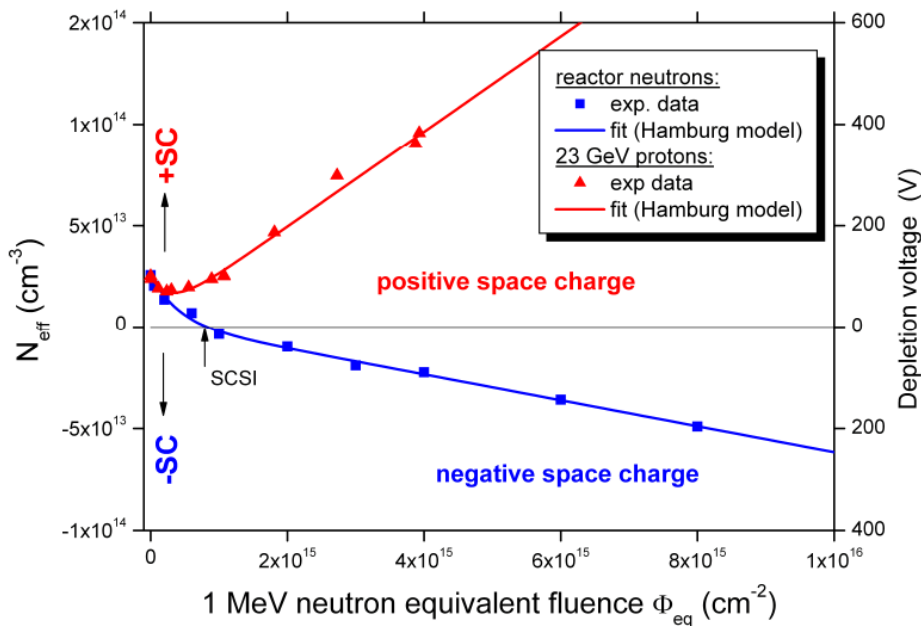
I.Pintilie, NSS, 21 October 2008, Dresden

Mara Bruzzi, Danno da radiazione in semiconduttori

Scuola Nazionale rivelatori ed elettronica per fisica delle alte energie , astrofisica 12 Aprile 2011,  
Legnaro, Italy

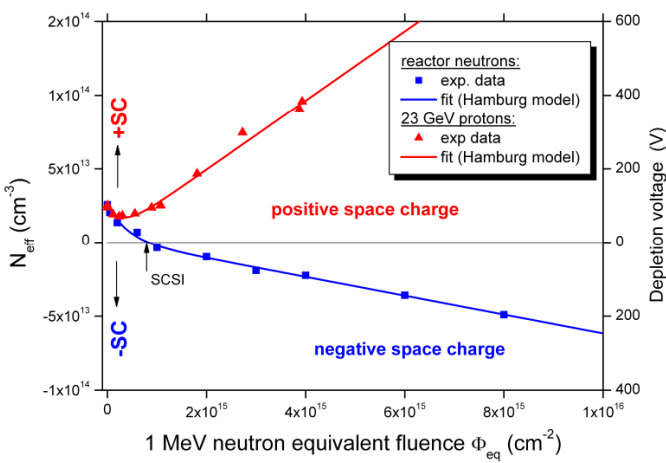
SCSI "Type Inversion" after neutrons but not after  
protons due to  
donor generation enhanced after proton irradiation

Epi-Si irradiated with 23 GeV protons and reactor neutrons

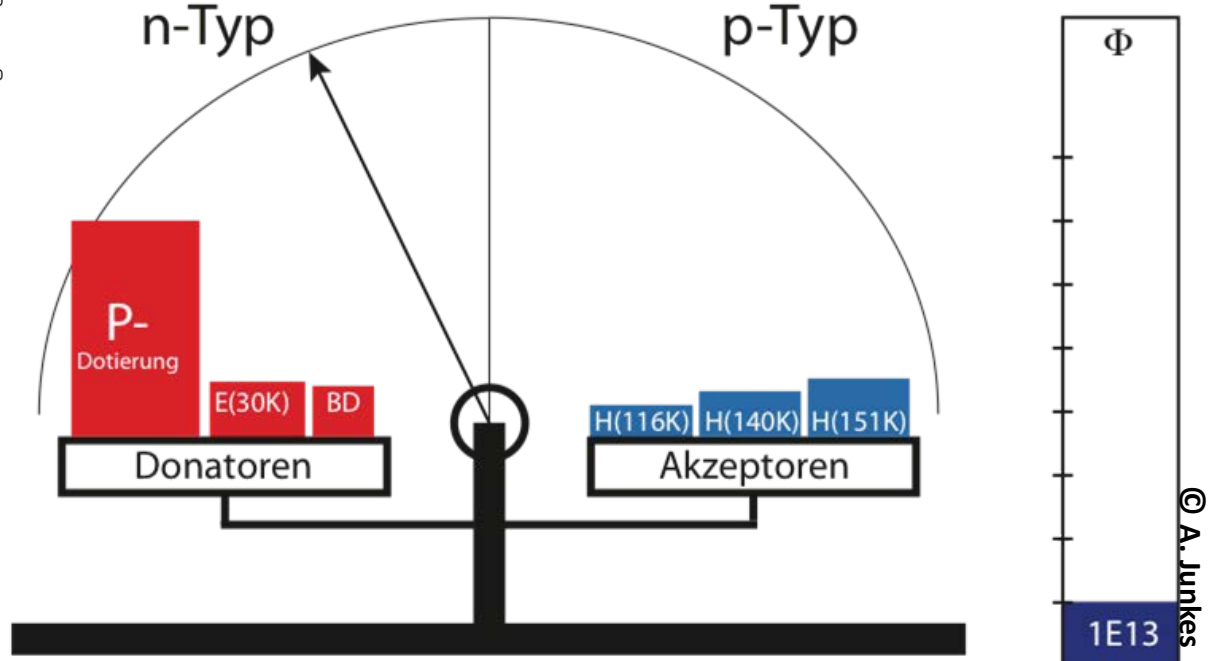
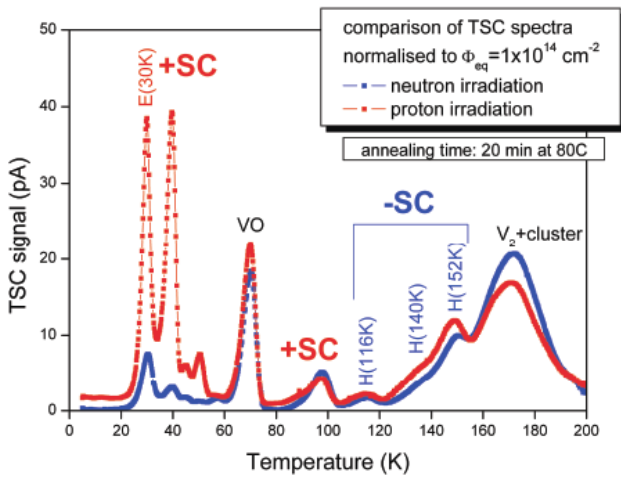


[Pintilie, Lindstroem, Junkes, Fretwurst, NIM A 611 (2009) 52–68]

# $N_{\text{eff}}$ : Neutron irradiation

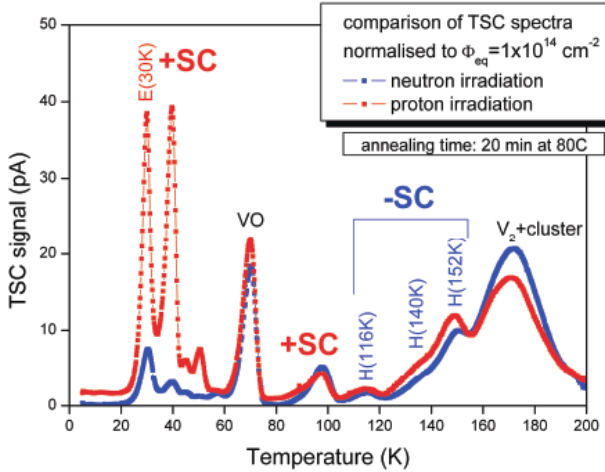
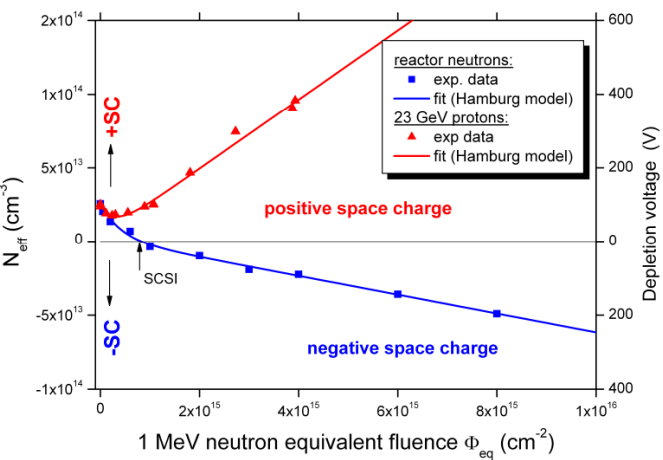


Epitaxial silicon (*EPI-DO, 72 μm, 170 Ωcm, diodes*) irradiated with reactor neutrons



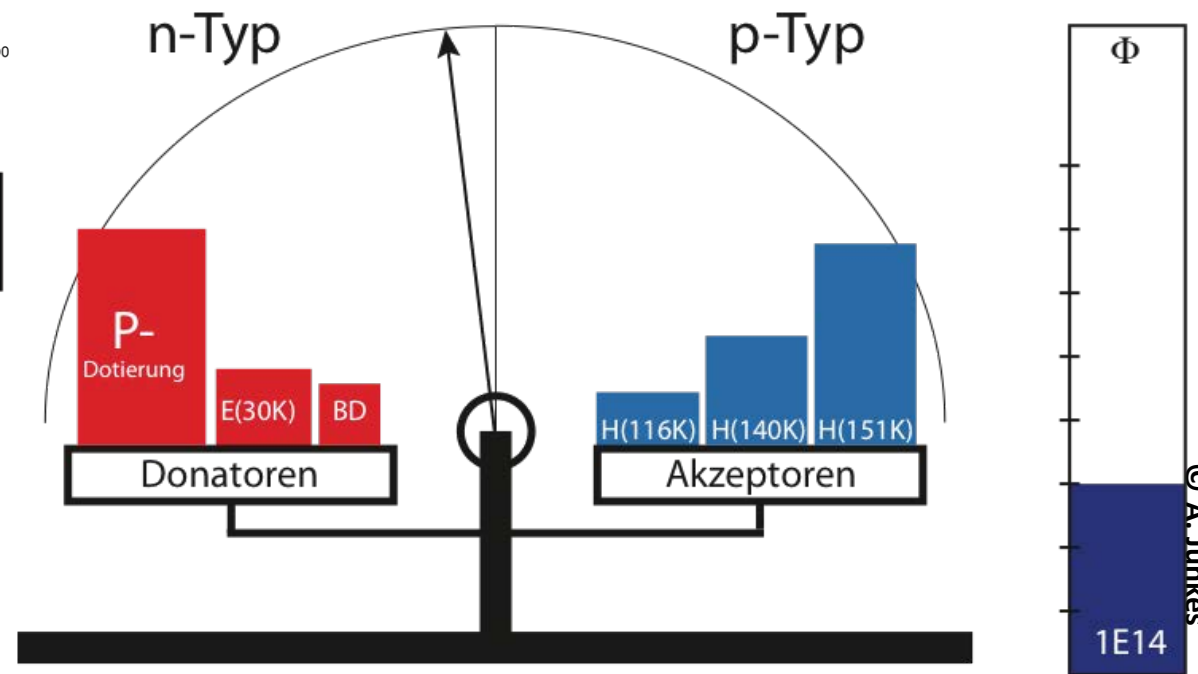
By A. Junkes, presented by U. Parzefal on behalf of the RD50 Collaboration, RESMDD10 , Oct. 2010, Florence

# $N_{\text{eff}}$ : Neutron irradiation

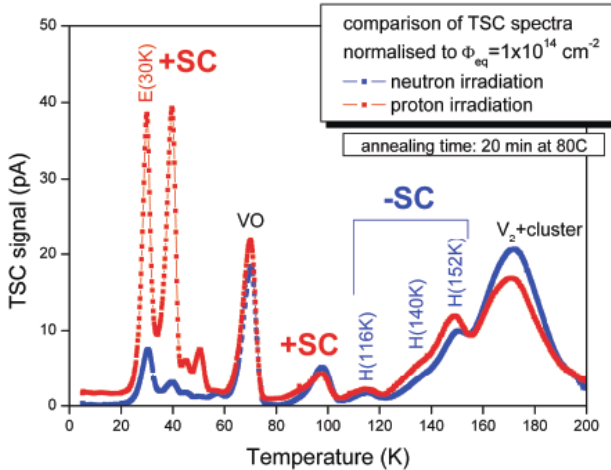
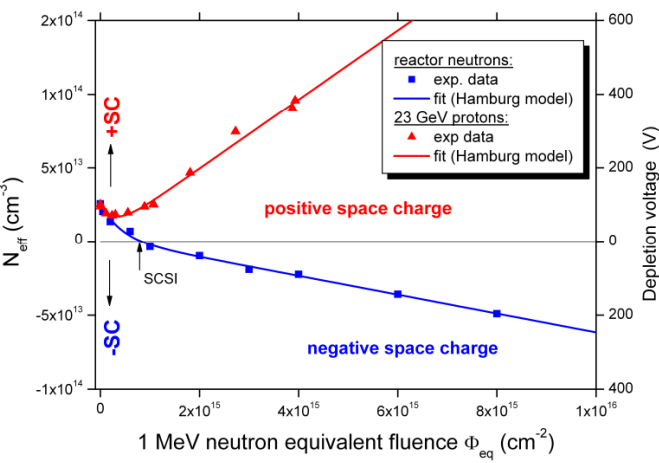


By A. Junkes, presented by U. Parzefal on behalf of the RD50 Collaboration, RESMDD10 , Oct. 2010, Florence

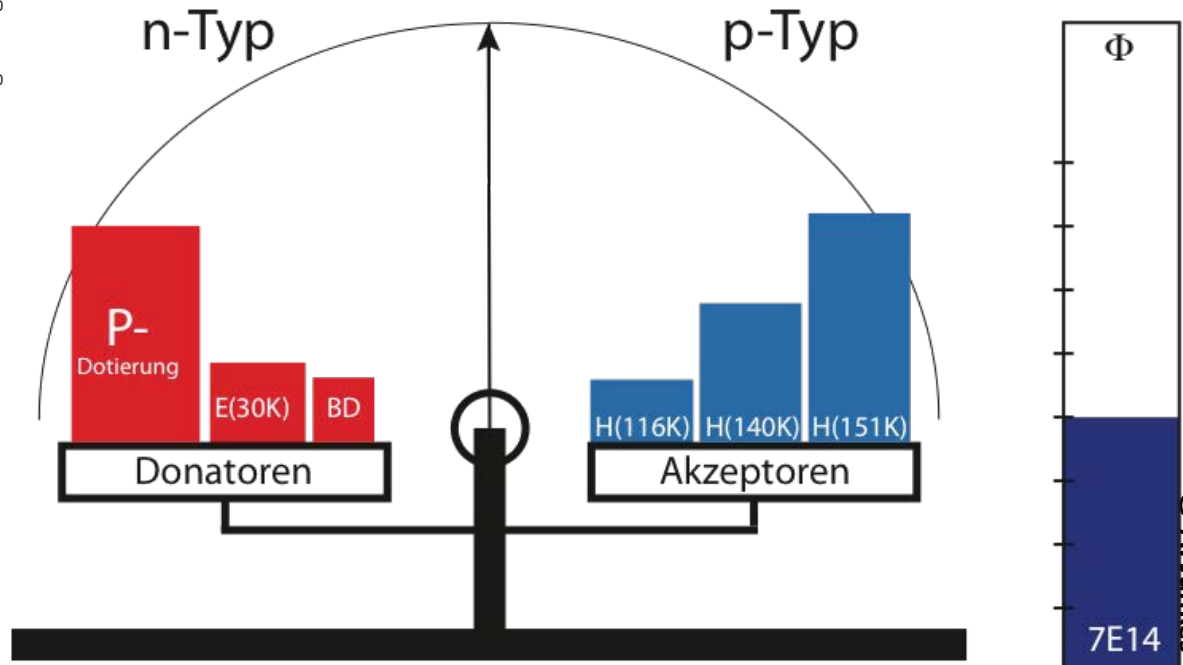
Epitaxial silicon (*EPI-DO, 72 μm, 170 Ωcm, diodes*) irradiated with reactor neutrons



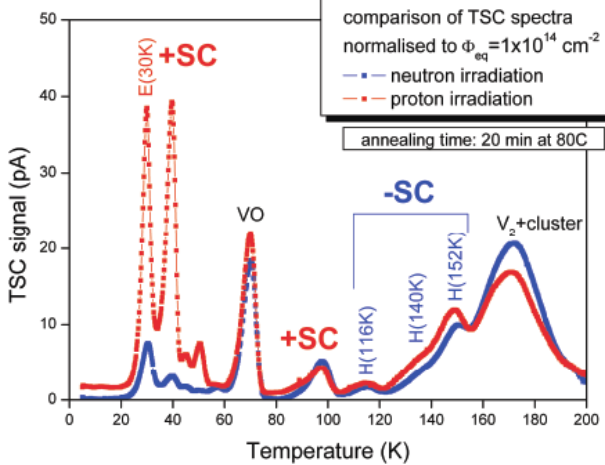
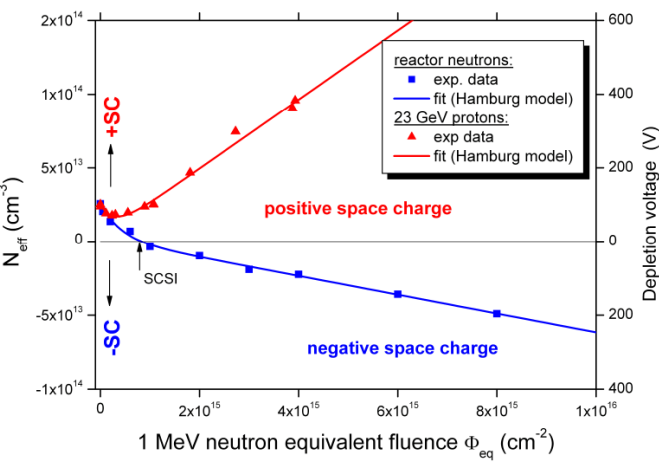
# $N_{\text{eff}}$ : Neutron irradiation



Epitaxial silicon (*EPI-DO, 72 μm, 170 Ωcm, diodes*) irradiated with reactor neutrons

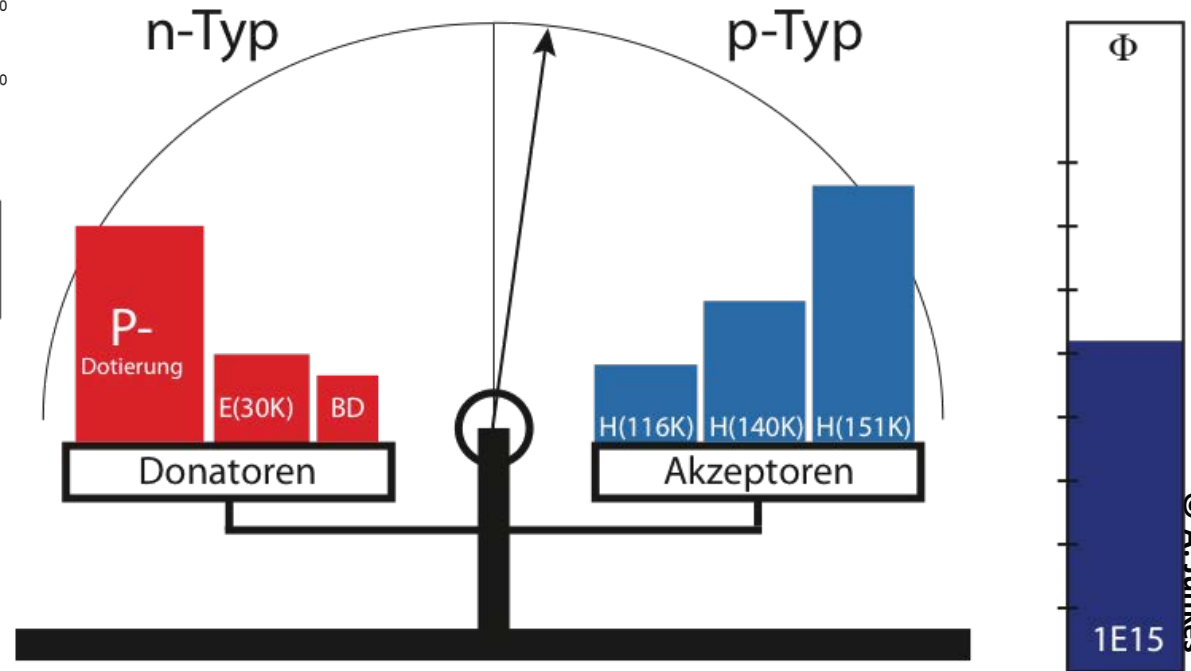


# $N_{\text{eff}}$ : Neutron irradiation

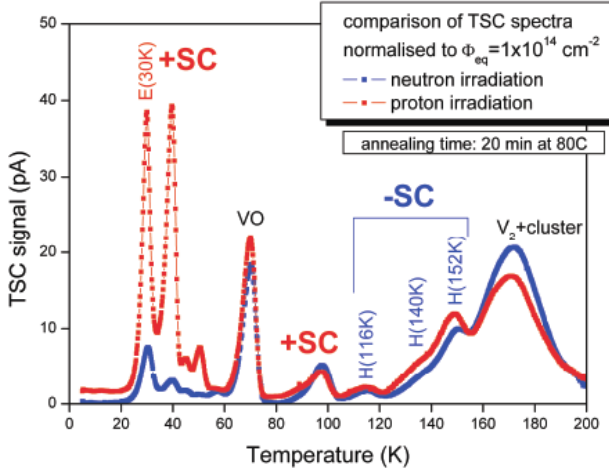
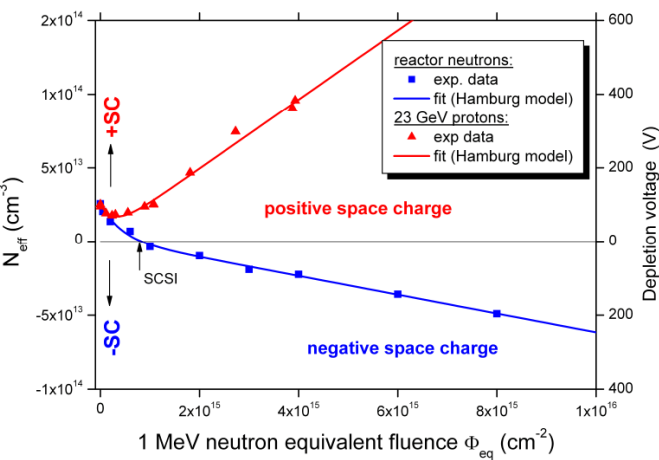


By A. Junkes, presented by U. Parzefal on behalf of the RD50 Collaboration, RESMDD10 , Oct. 2010, Florence

Epitaxial silicon (*EPI-DO, 72 μm, 170 Ωcm, diodes*) irradiated with reactor neutrons

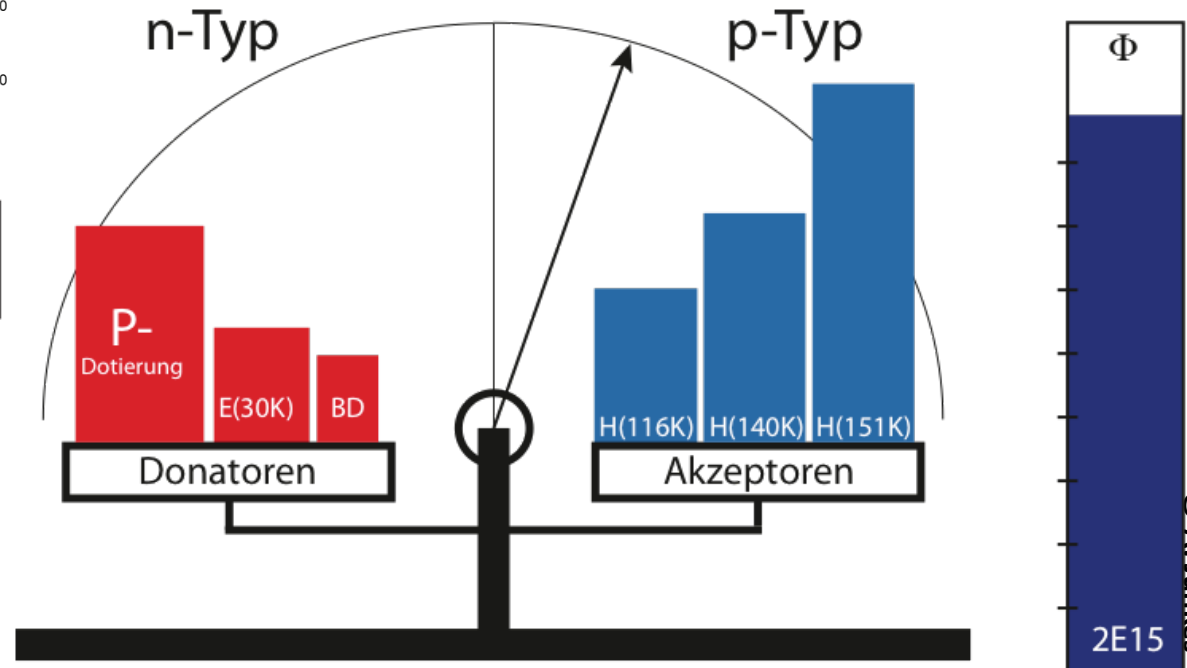


# $N_{\text{eff}}$ : Neutron irradiation

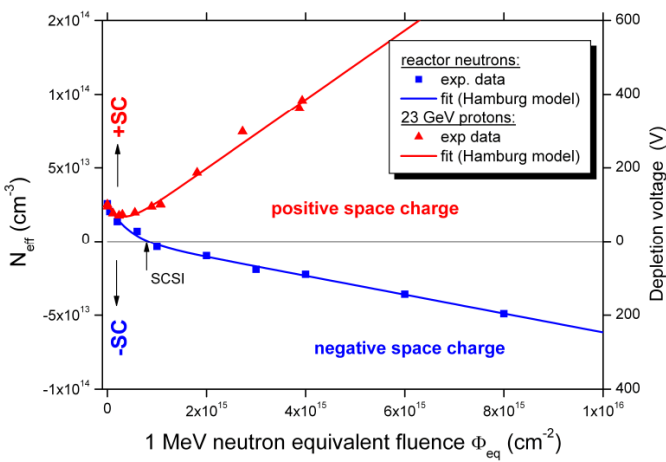


By A. Junkes, presented by U. Parzefal on behalf of the RD50 Collaboration, RESMDD10 , Oct. 2010, Florence

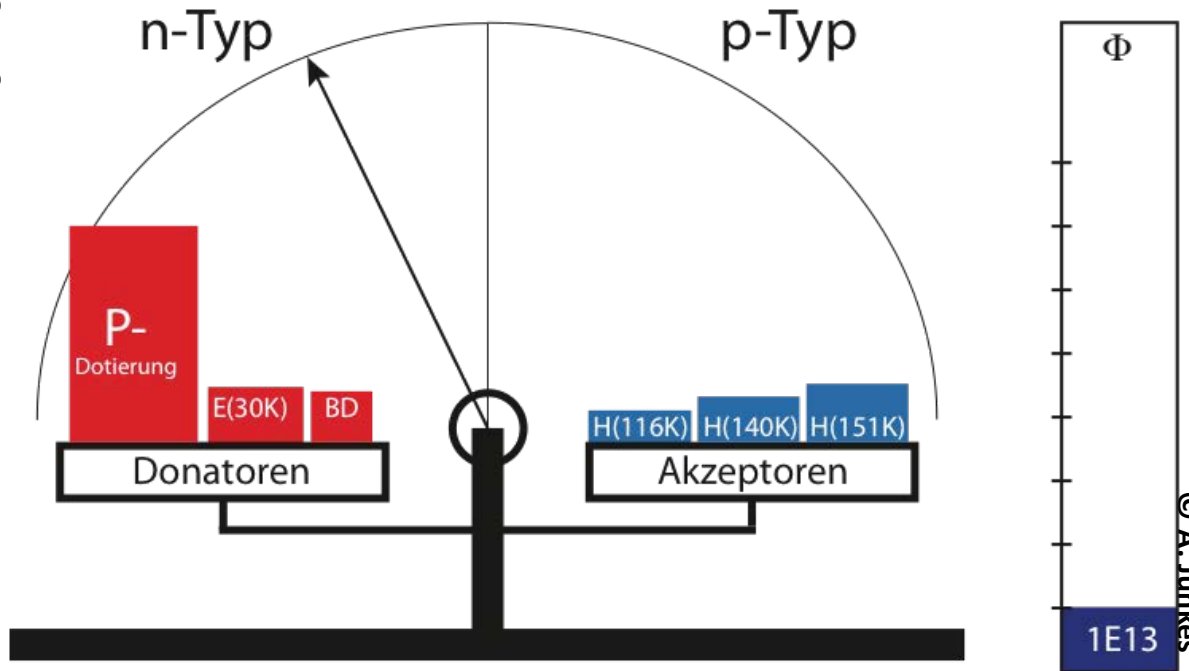
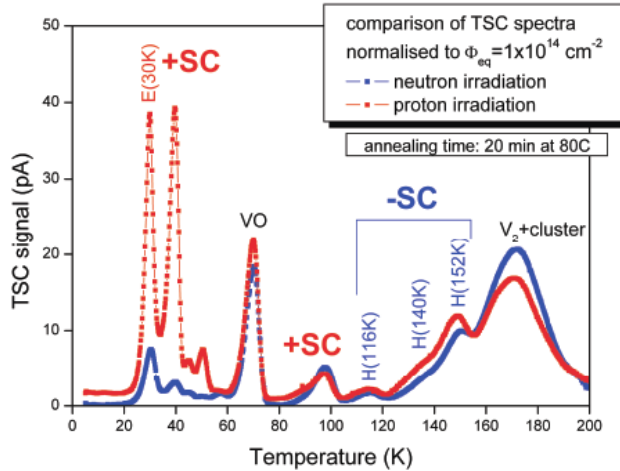
Epitaxial silicon (*EPI-DO, 72 μm, 170 Ωcm, diodes*) irradiated with reactor neutrons



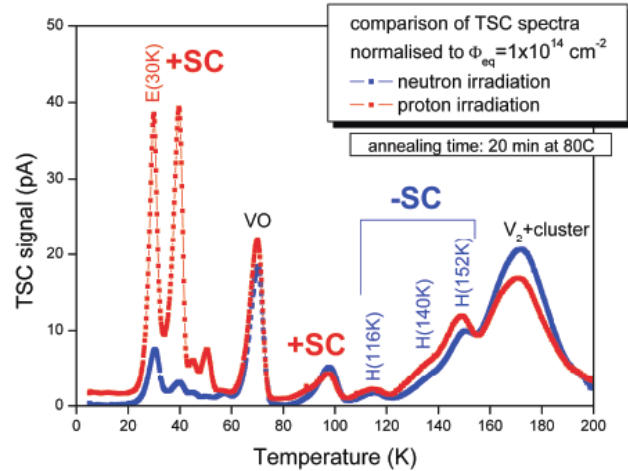
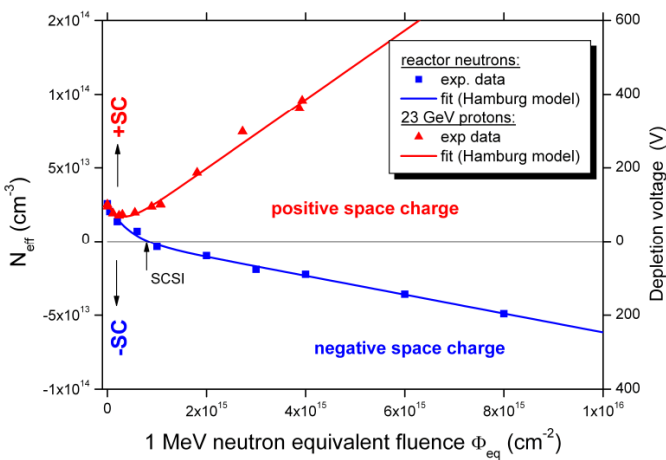
# $N_{\text{eff}}$ : Proton irradiation



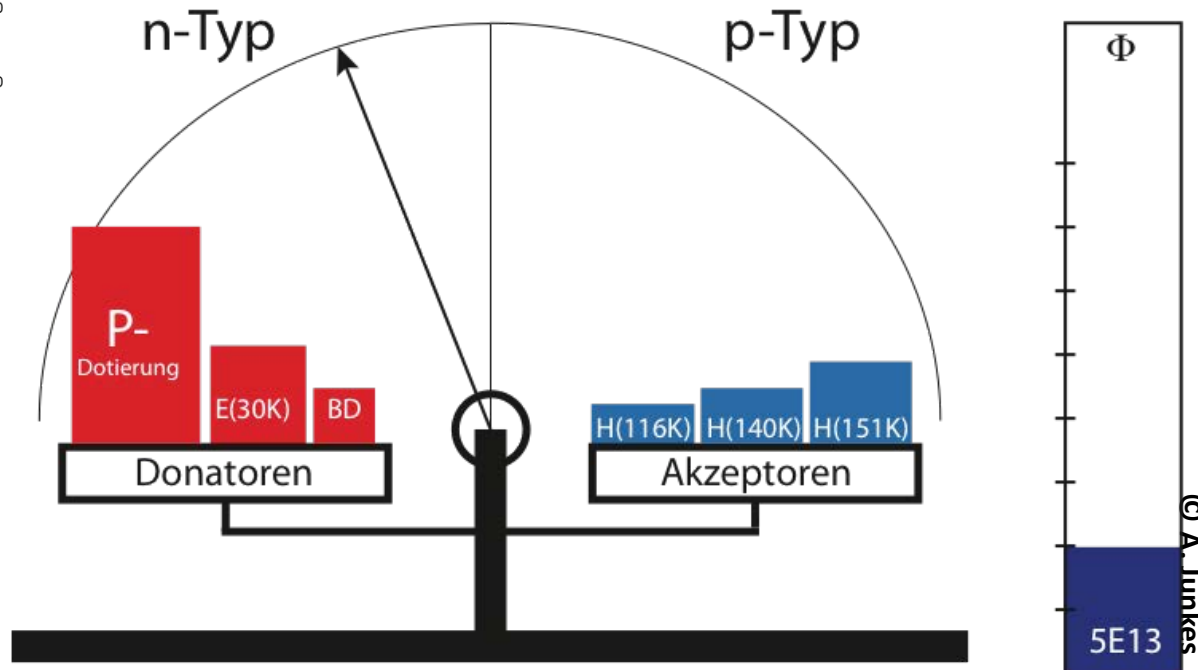
Epitaxial silicon (*EPI-DO, 72 μm, 170 Ωcm, diodes*) irradiated with 23 GeV Protons



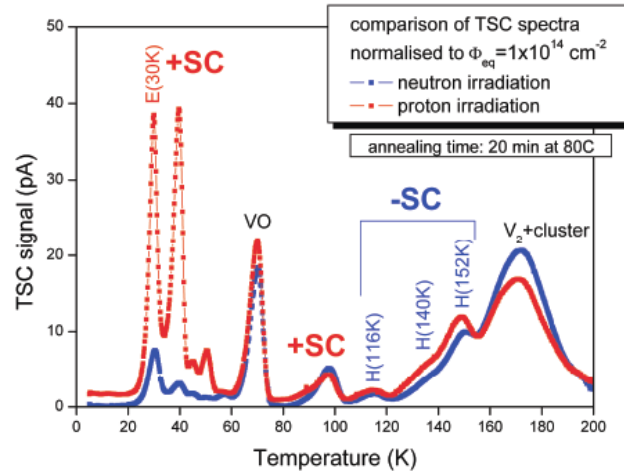
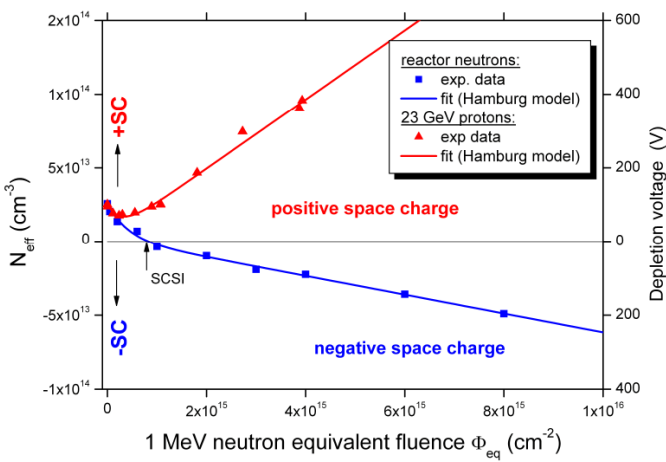
# $N_{\text{eff}}$ : Proton irradiation



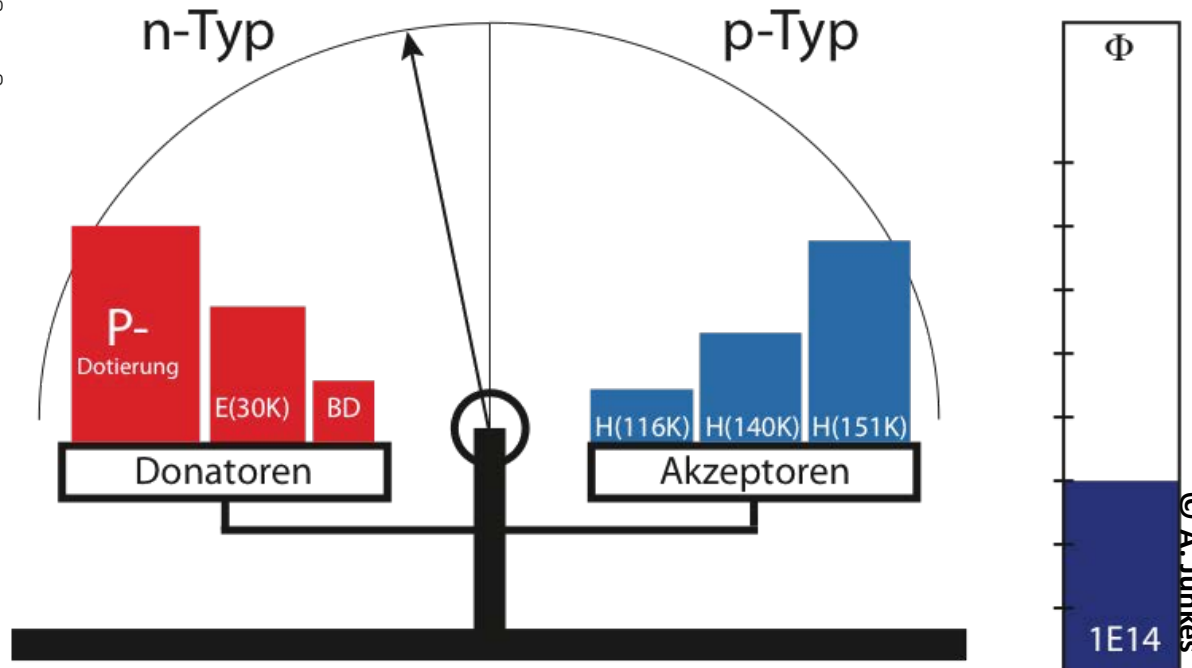
Epitaxial silicon (*EPI-DO, 72 μm, 170 Ωcm, diodes*) irradiated with 23 GeV Protons



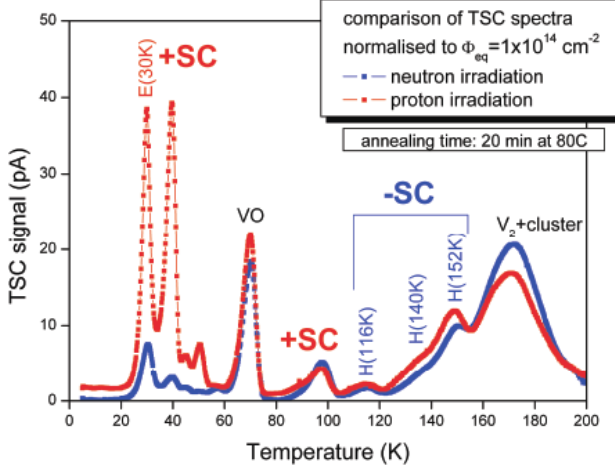
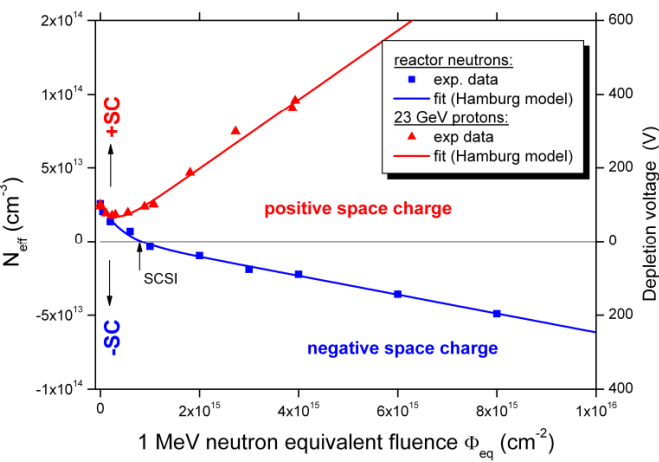
# $N_{\text{eff}}$ : Proton irradiation



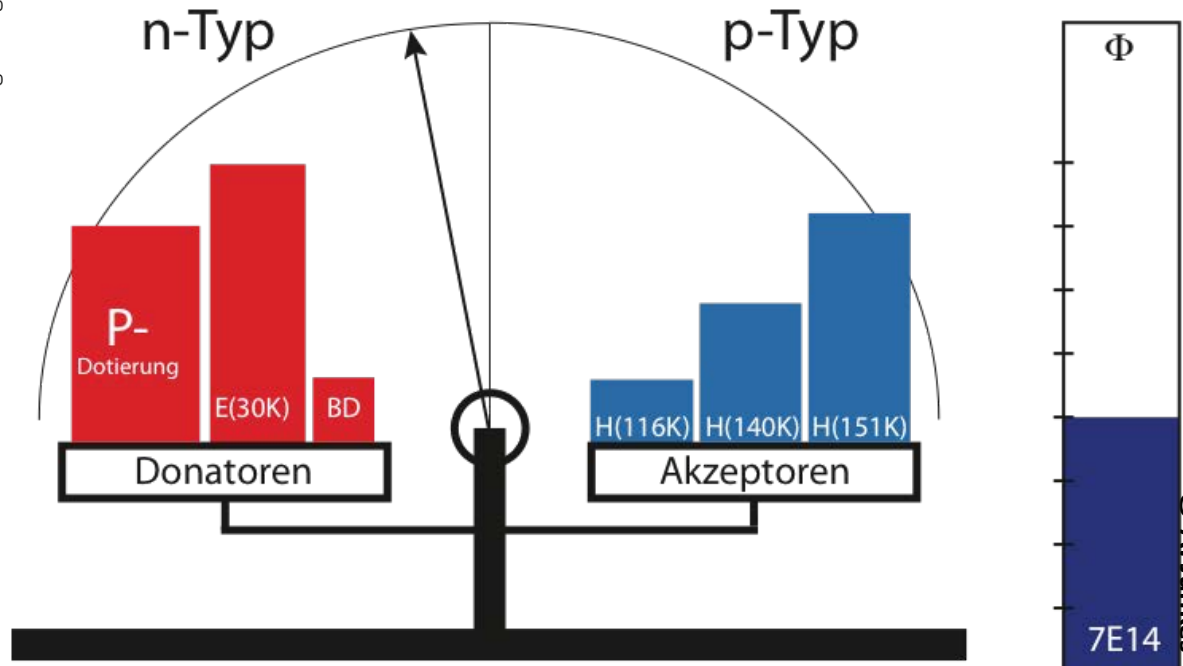
Epitaxial silicon (*EPI-DO, 72 μm, 170 Ωcm, diodes*) irradiated with 23 GeV Protons



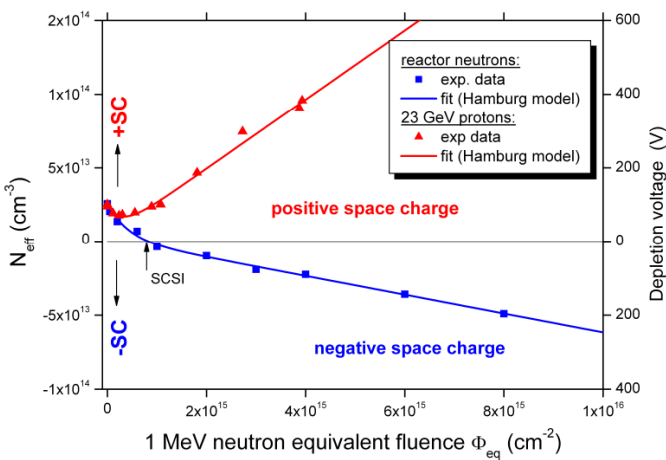
# $N_{\text{eff}}$ : Proton irradiation



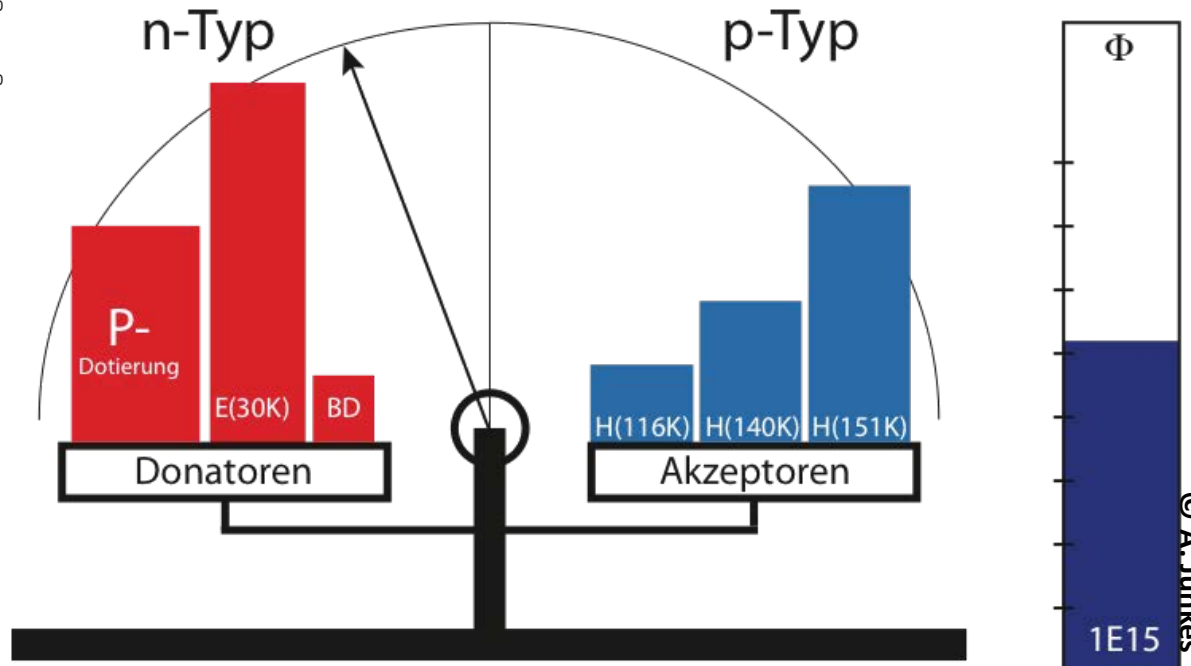
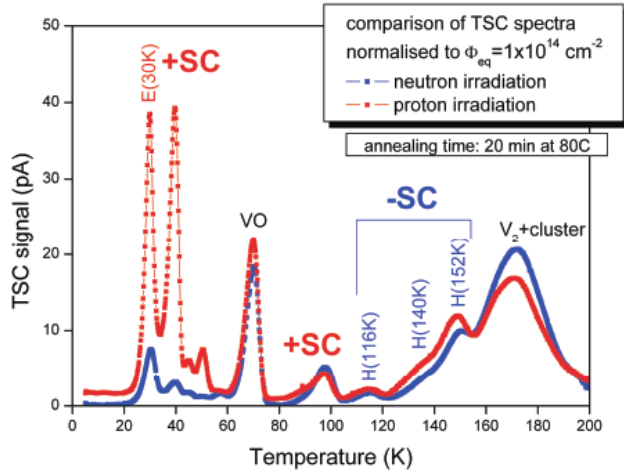
Epitaxial silicon (*EPI-DO, 72 μm, 170 Ωcm, diodes*) irradiated with 23 GeV Protons



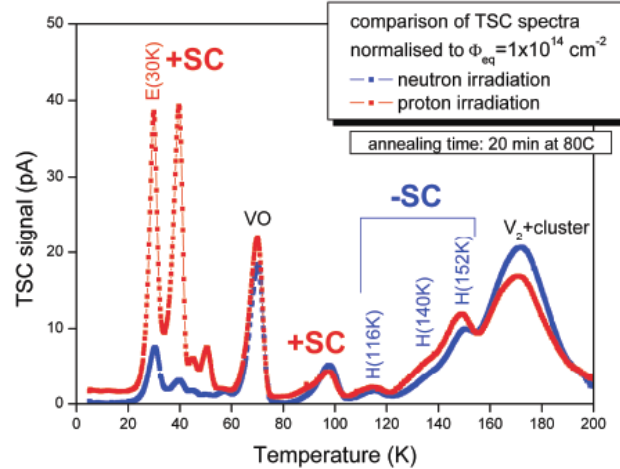
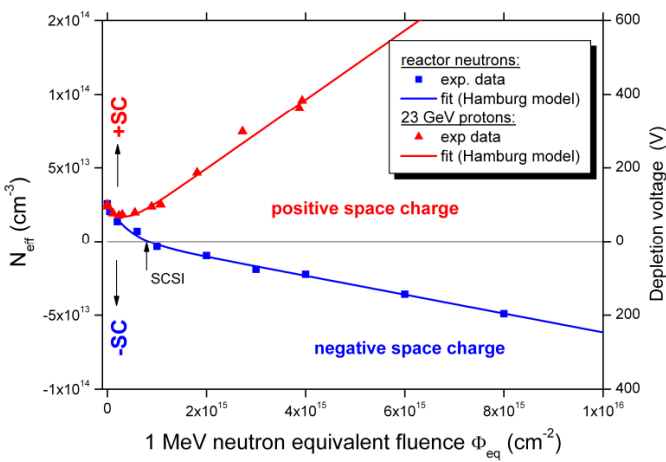
# $N_{\text{eff}}$ : Proton irradiation



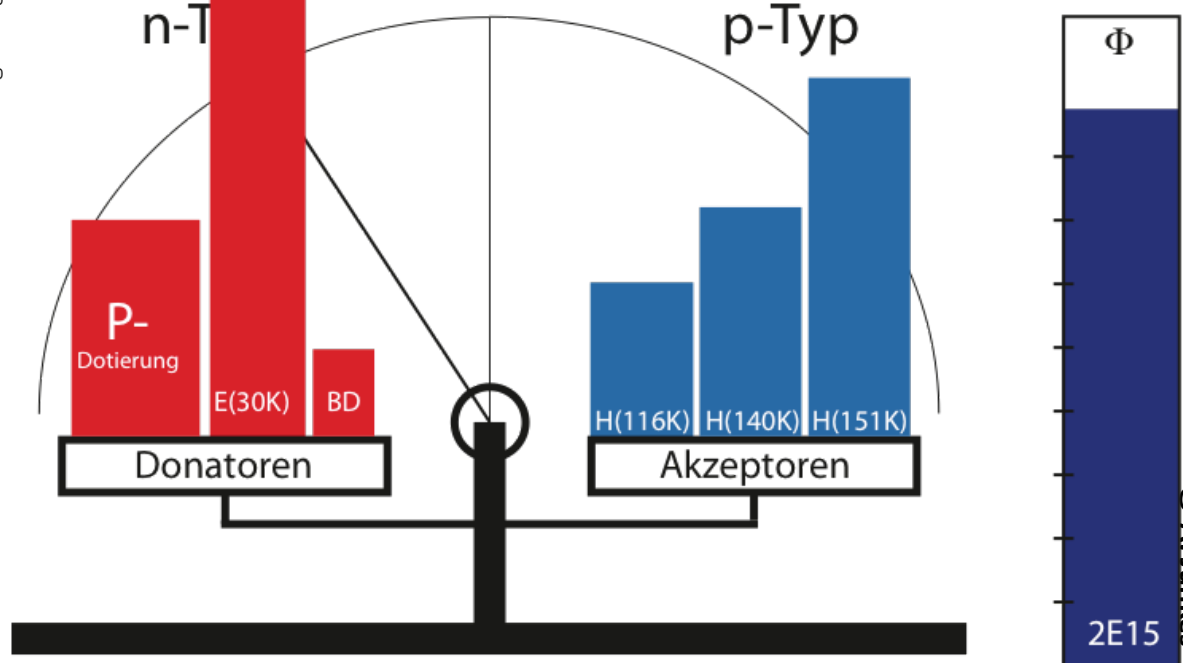
Epitaxial silicon (*EPI-DO,  $72\mu\text{m}$ ,  $170\Omega\text{cm}$ , diodes*) irradiated with 23 GeV Protons



# $N_{\text{eff}}$ : Proton irradiation



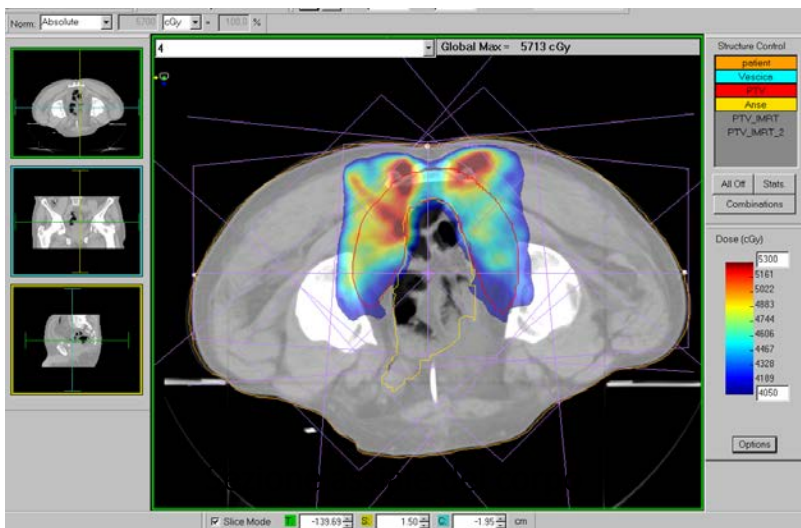
Epitaxial silicon (*EPI-DO, 72 μm, 170 Ωcm, diodes*) irradiated with 23 GeV Protons



# Radiation damage in dosimeters for clinical radiotherapy

Con la radioterapia conformazionale si utilizzano tecniche di imaging CT per identificare con adeguata precisione sia il bersaglio del trattamento che gli organi a rischio prossimali. La pianificazione del trattamento viene eseguita utilizzando sistemi computerizzati (Treatment Planning System TPS) che effettuano sia il calcolo della dose, che la procedura di pianificazione del trattamento.

TPS IMRT per prostata



POSIZIONAMENTO DEL PAZIENTE

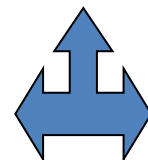


Per non vanificare le potenzialità offerte da queste tecniche, l'accuratezza deve essere elevata in ogni fase del processo radioterapico

GTV = gross target volume

CTV = clinical target volume = gTV + margini

PTV planning target volume = cTV + margini

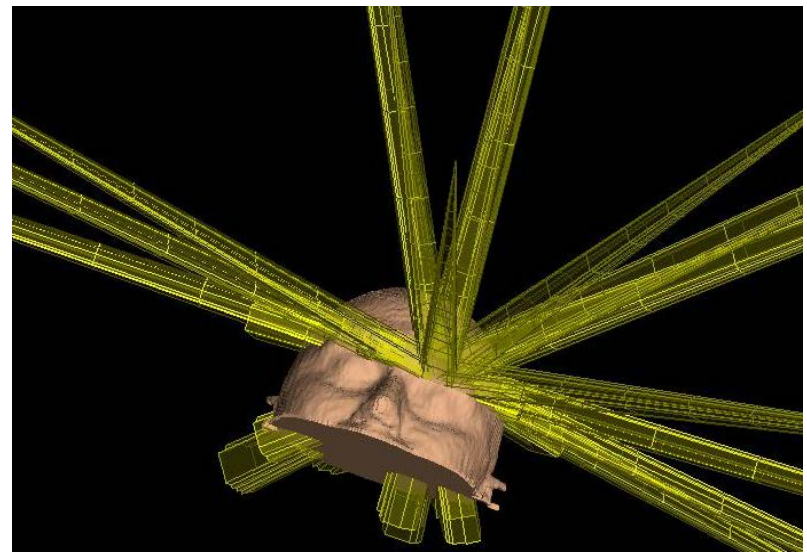
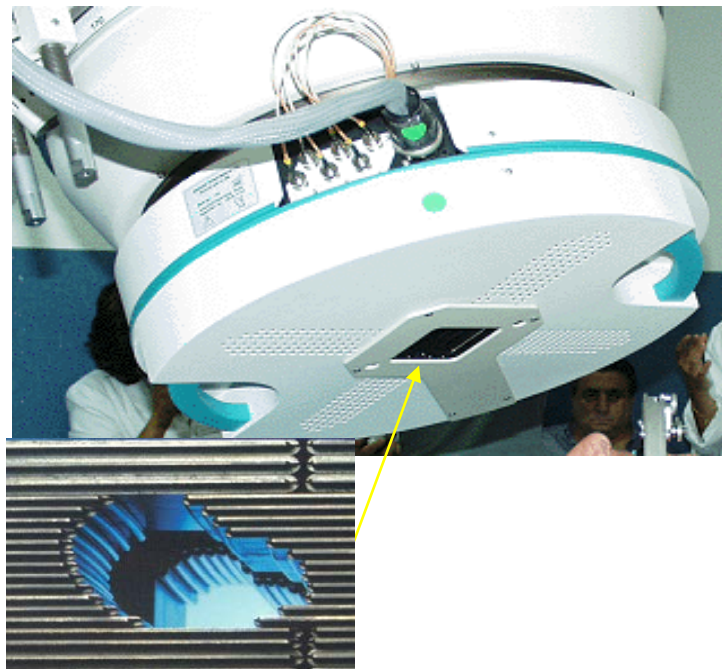


CALCOLO DELLA  
DISTRIBUZIONE  
DI DOSE

Nel caso dei fasci di fotoni la conformazione della distribuzione di dose ai volumi da irradiare si può ottenere con tecniche quali **Stereotassi** e **IMRT** (Intensity Modulated Radiation Therapy).

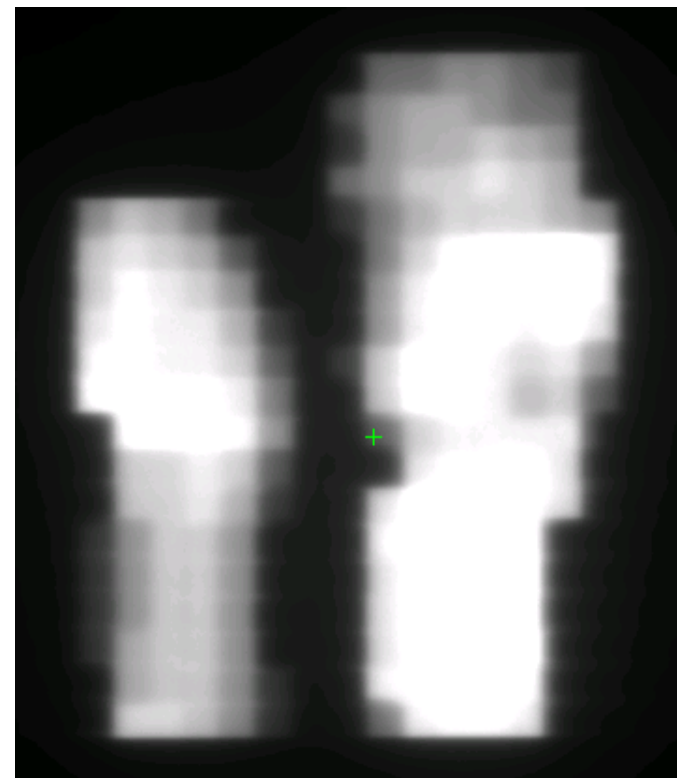
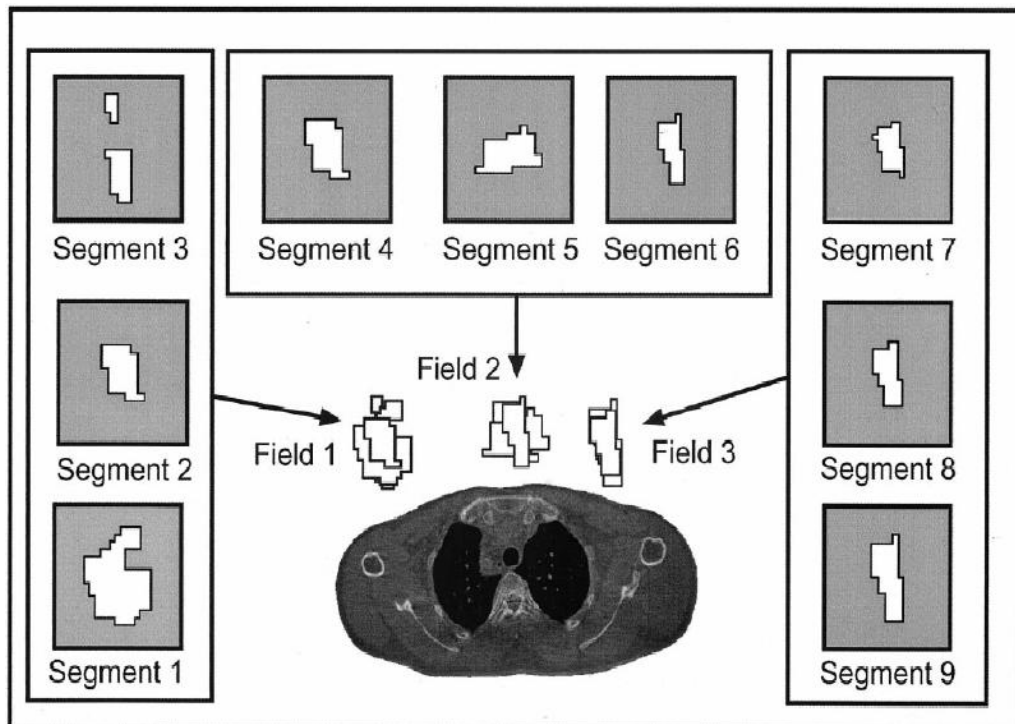
Tipicamente: fasci di fotoni da linac:

6MV testa - 10MV polmoni - 6.25MV prostata

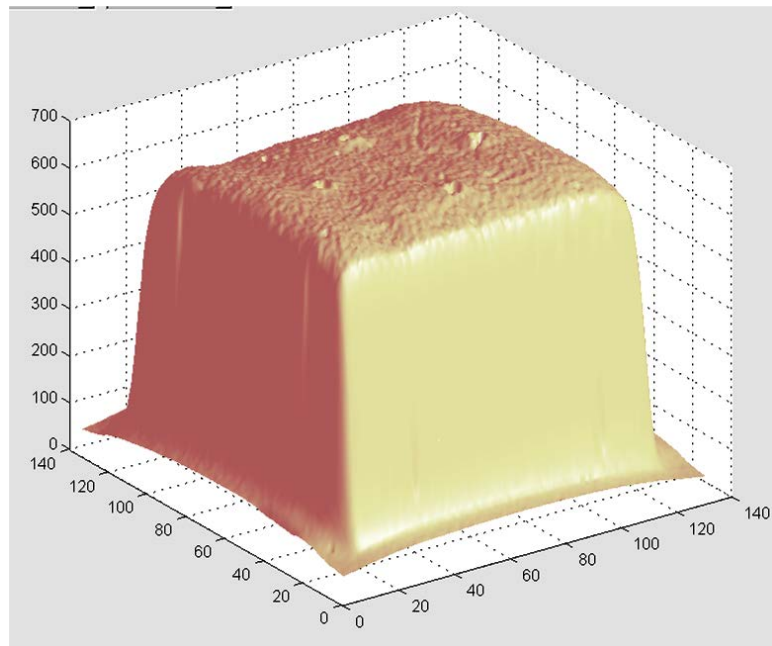


# IMRT: Step and shoot modality

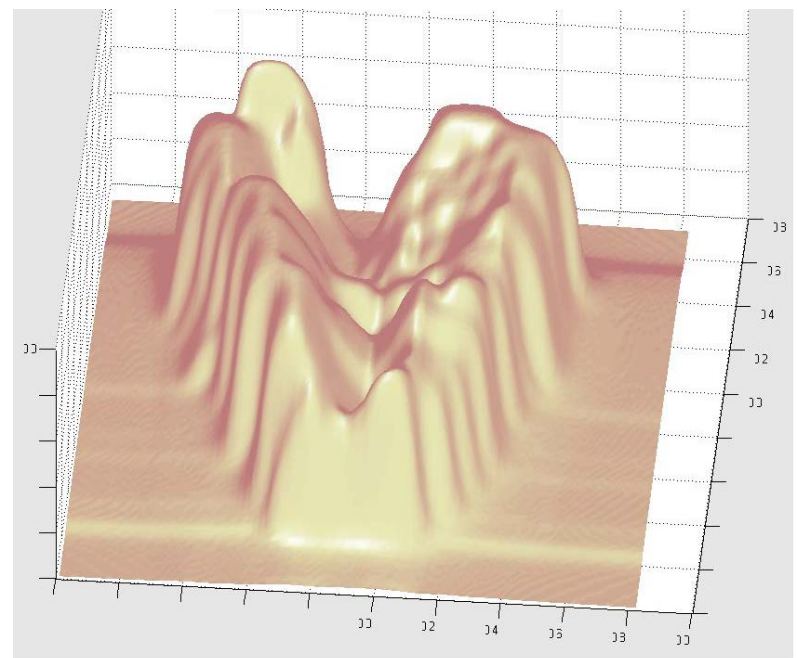
The desired non uniform fluence distribution is obtained for each beam by a sequence of numerous static irradiations (segments) each characterized by a different MLC configuration; the beam is switched off during the MLC rearrangement.



# Confronto distribuzione di dose convenzionale e conformata

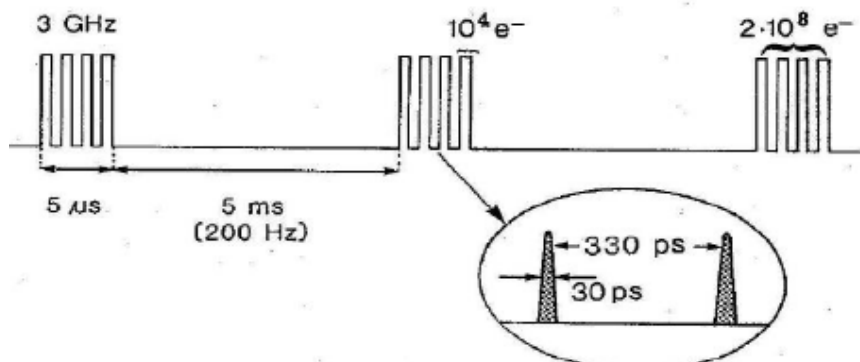


Distribuzione di dose convenzionale



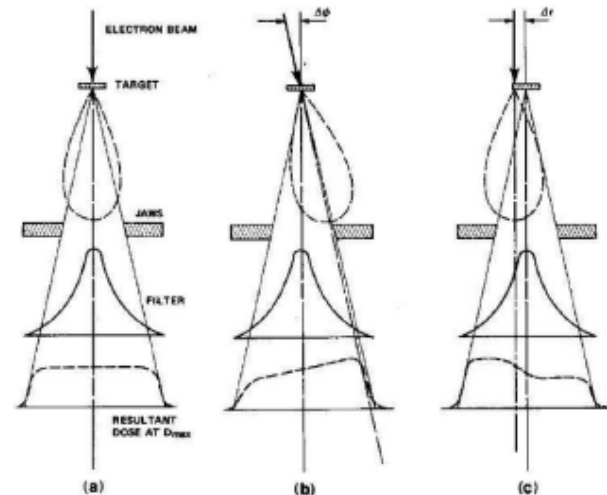
Distribuzione di dose IMRT

# Struttura del fascio LINAC



Typical beam parameter:

Radiation: electrons or Bremsstrahlung photons



(Macro) pulse duration:

$\approx 5 \mu$ s.

PRF:

$\sim 200$ Hz (i.e. 5ms period).

(Micro) pulse frequency:

$\sim 3$ GHz (i.e. 330ps period).

(Micro) pulse duration:

$\sim 30$ ps.

Beam quality:

6-18MV (photons).

6-18MeV (electrons).

Dose rate:

3-6Gy/min (flattened).

10-50Gy/min (unflattened).

Dose:

0.3-0.5mGy/pulse (flattened)

0.8-4mGy/pulse (unflattened)

# Dosimetri a Giunzione (Si)



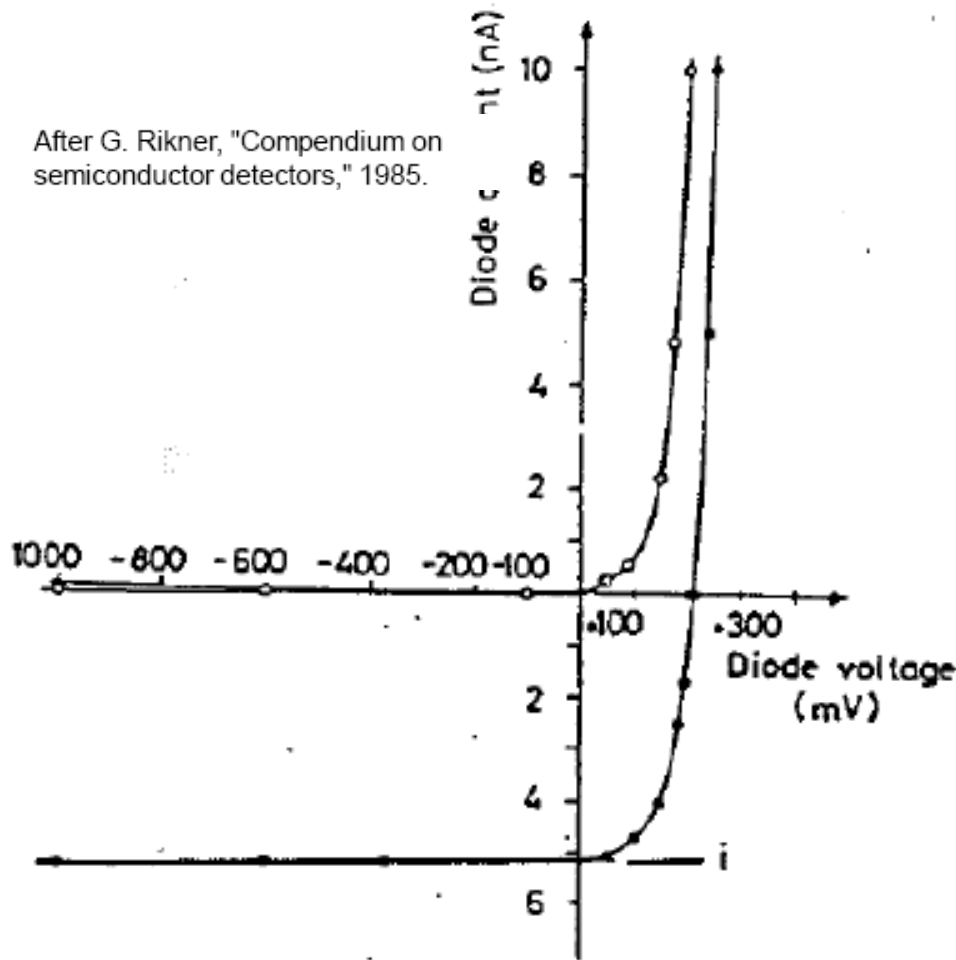
elevato rapporto segnale rumore  
risposta veloce  
volume attivo molto ridotto  
operante anche a tensione nulla



non tessuto equivalente (  $Z = 14$  )  
Risposta dipendente dall'energia  
bassa resistenza all'irraggiamento  
➔ segnale dipendente da dose accumulata  
➔ necessaria una frequente ricalibrazione

## Caratteristica I-V di un dosimetro a Si al buio ed esposto a radiazione pari a 1.5Gy/min

After G. Rikner, "Compendium on semiconductor detectors," 1985.



### Caratteristiche Operative:

- Tensione applicata nulla per minimizzare la corrente di buio
- tempo di campionamento intorno a  $T \geq 10\text{ms}$
- Misura carica integrata

sensibilità

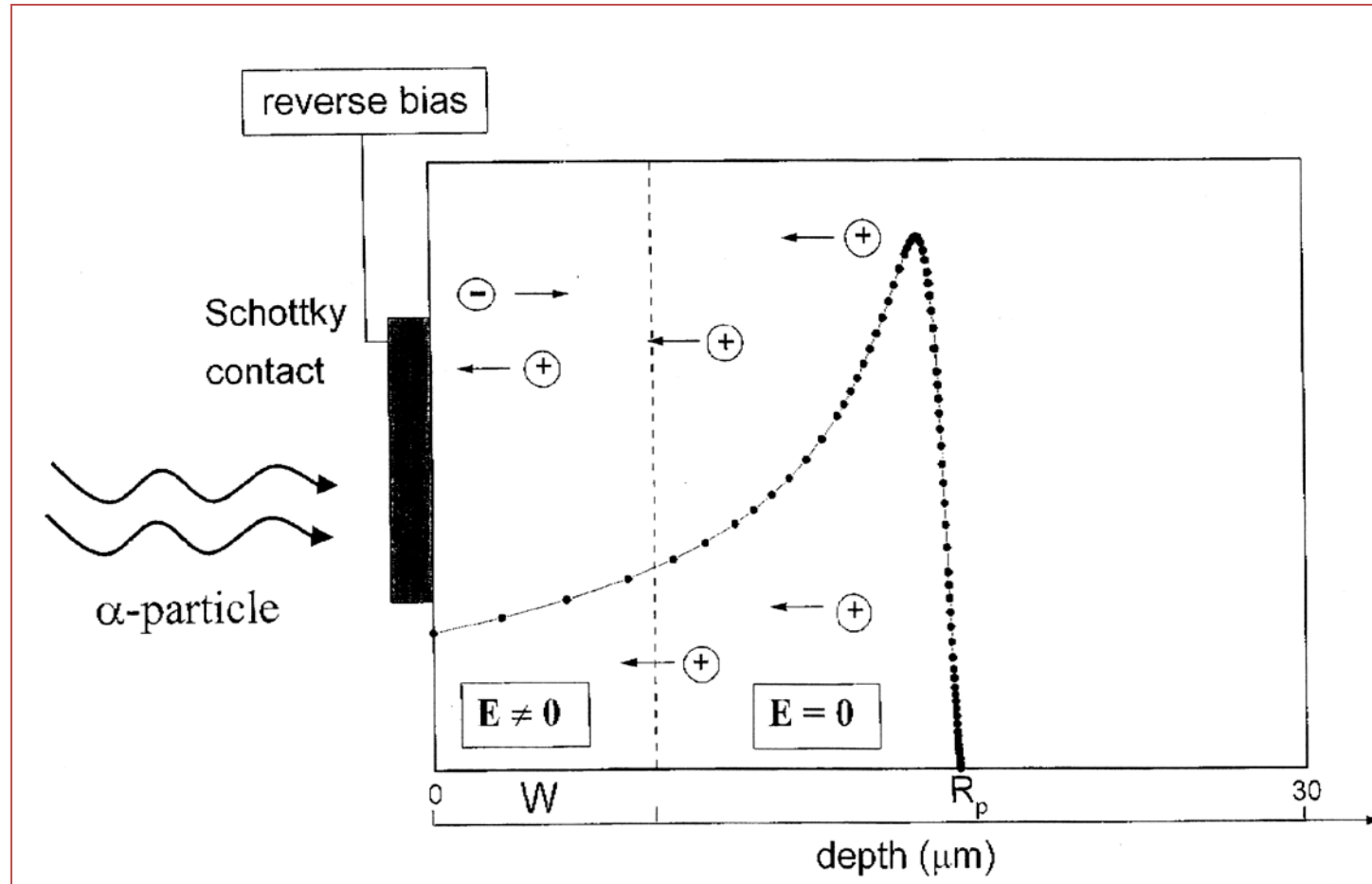
$$\rightarrow S = \frac{dI}{dD}$$

# Regione attiva del rivelatore

$W$  = larghezza di svuotamento

$R_p$  = range delle particelle

$L$  = lunghezza di diffusione



Si puo' avere contributo al segnale per la diffusione dei portatori minoritari che vengono creati in  $R_p$  all'interno della regione neutra

## Regione attiva in un rivelatore/dosimetro con tensione applicata nulla

$$W_D = W_0 + L = \sqrt{\left( \frac{2 \epsilon \cdot V_{bi}}{q \cdot N_{eff}} \right)} + \sqrt{D_h \cdot \tau_h}$$

Lunghezza di diffusione per i portatori minoritari

$$D_h = \mu_h K \cdot T/e$$

$\tau_h$  = tempo di vita media del portatore minoritario

La sensibilità del rivelatore/dosimetro è direttamente proporzionale alla larghezza della regione attiva:

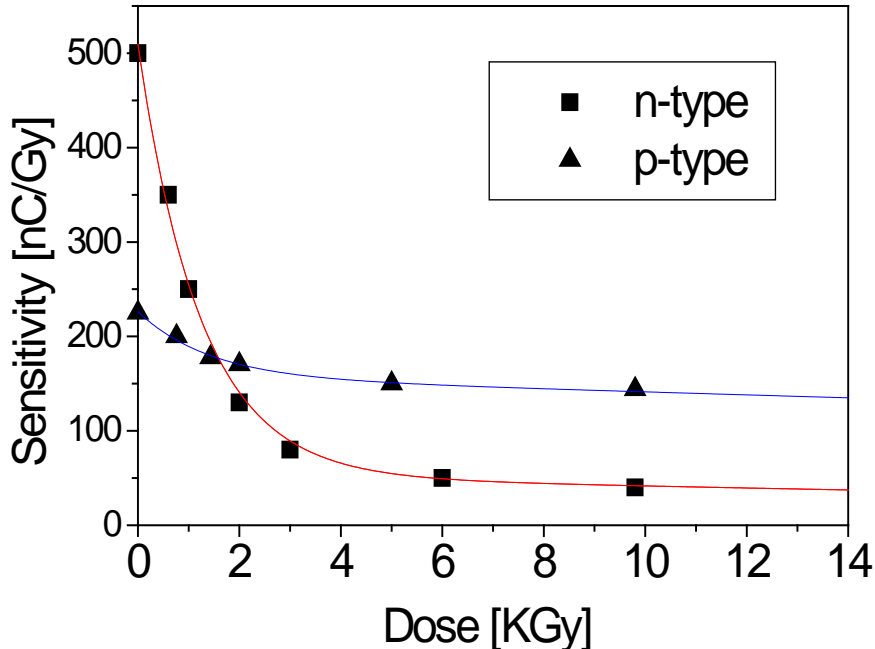
$$s \propto W_D$$

## Standard Si dosimeters: thickness 300um

Signal degrades with accumulated dose as:

$$1/\tau = 1/\tau_0 + K \phi$$

$\phi$  accumulated dose, with  $\tau_0$  minority carrier lifetime at zero dose.



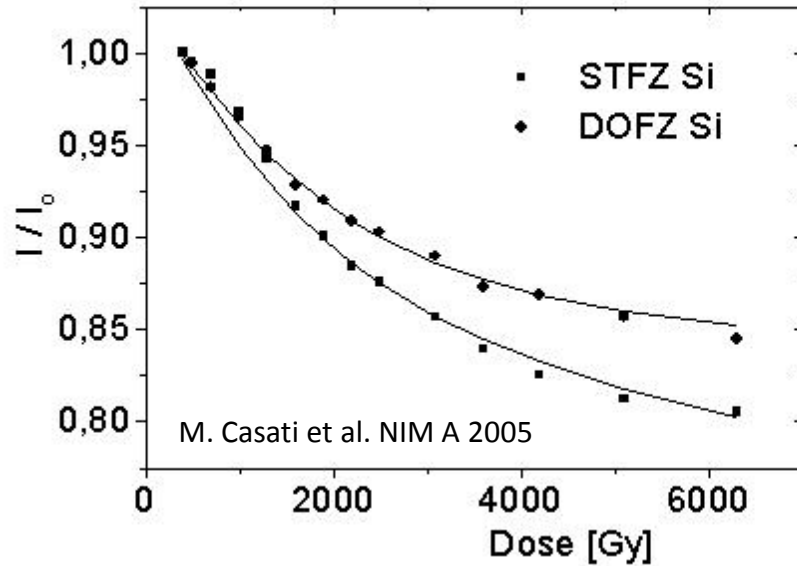
G.Rikner et al.Phys. Med. Biol. 28, 1983, 1261-1267

$$S = \frac{q\rho_{Si}}{E_i} \sqrt{\frac{D_e}{\sigma_e v_e N_t}} \propto N_t^{-1/2}$$

$S \propto N_t^{-1/2}$  il pre-irraggiamento diminuisce la pendenza della curva sensibilità vs dose. Per questo i dosimetri a Si vengono di solito pre-irraggiati ( $\approx 10\text{kGy}$ )

## Material engineering concepts have been applied also to Silicon dosimeters for radiotherapy

### Improved radiation hardness of DOFZ Si



Decrease in sensitivity with the accumulated dose due to the generation of a dominant trap acting as lifetime killer.

$$1/\tau - 1/\tau_0 = \sigma v_{th} N_t, \quad N_t = a \phi; \quad a = \text{trap generation rate}$$

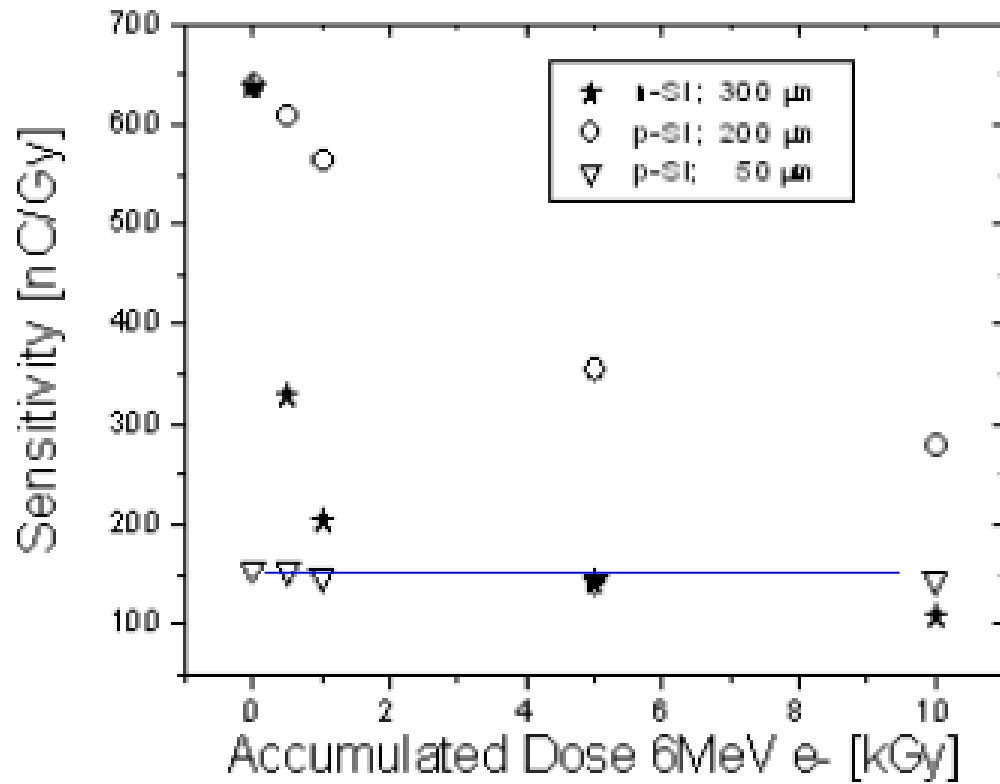
$\sigma$  capture cross section ;  $v_{th}$  carrier thermal velocity.  $N_t$  trap concentration.

$a_{DOFZ} < a_{SFZ} \Rightarrow$  increased radiation hardness of the device to radiotherapeutic beams.

$$a_{DOFZ} = 5.0 \times 10^7 \text{ cm}^{-3}\text{Gy}^{-1}, \quad a_{SFZ} = 8.1 \times 10^7 \text{ cm}^{-3}\text{Gy}^{-1}$$

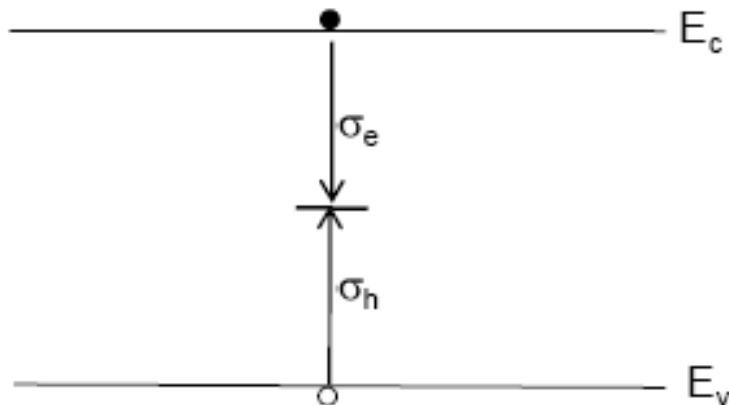
## Our recipe: epitaxial p-type Si on MCz substrates to limit active thickness

Active region is limited in any direction to a value shorter than  $L_n$  at the highest dose of interest. Epitaxial Layer is used to limit active depth, guard-ring to limit active area.



M. Bruzzi et al., "Epitaxial silicon devices for dosimetry applications," Appl. Phys. Lett., vol. 90 (2007) 172109 1-3.

## p-type as radiation harder material ( dosimetry )



In fact, dominant center produced by electron irradiation has cross sections:

$$\sigma_e = 1.62 \times 10^{-16} \text{ cm}^2,$$
$$\sigma_h = 8.66 \times 10^{-16} \text{ cm}^2.$$

see Shi J., Simon W. E., 2003, Med. Phys. 30, 2509-19  
and cited refs.

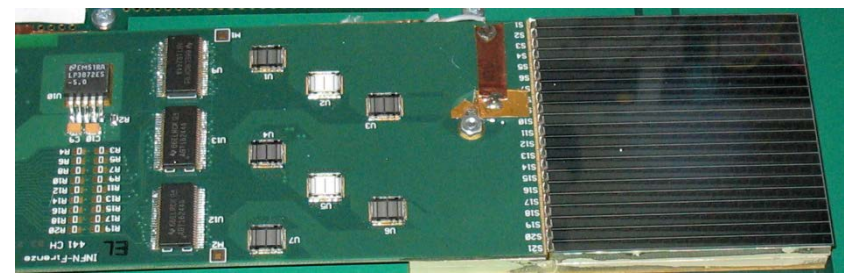
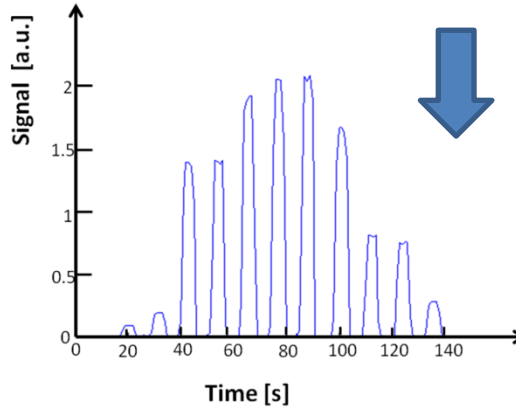
This means that for this center it is easier to capture holes. As diffusion is ruled out by minority carriers, to get a transport less influenced by irradiation, minority carriers must be electrons, thus material has to be p-type.

# Si bidimensional dosimeter

In the framework of the MAESTRO EU Integrated project the Florence group designed and manufactured a high performance cost-effective device based on epitaxial p-type silicon (radiation-hard, no dependence on the accumulated dose), designed to get a high resolution matrix of macropixels ( $2 \times 2 \text{mm}^2$ ). Module:  $6.3 \times 6.3 \text{cm}^2$ , 441ch.

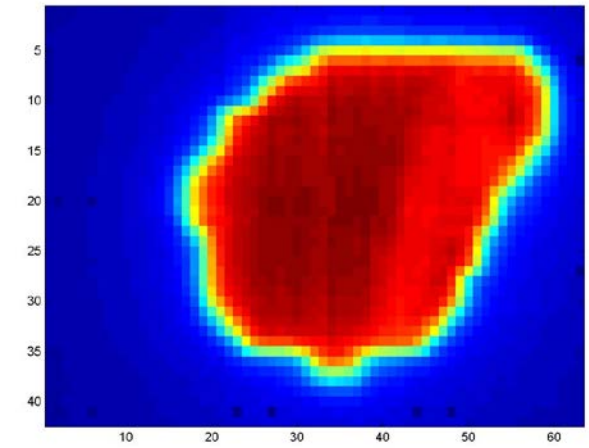
C.Talamonti, M.Bruzzi et al. 2011 Nucl. Instr. Meth A, vol. 658, p. 84-89.

Measured time structure of dose segments



Large area IMRT covered by mosaic composition and/or shifting modules along x-y axes.

Dose map of an IMRT field for prostate cancer as measured by the Epi-Si 2D silicon dosimeter.



# Beyond Silicon: Diamond Dosimeters

- **it is almost water equivalent**



- it doesn't perturb the radiation field → small fields

- the energy is absorbed as in the water → no correction factors

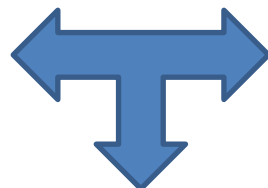
- **high radiation hardness** → long term stability

- **high density** → **high sensitivity** → small dimensions

- **non toxic**

- Natural diamond**

- **very high production costs, difficult to select stones with proper dosimetric response**



- Polycrystalline CVD diamond**

- ability to produce large area wafers of 3-5"

- Single crystal CVD (Chemically Vapour Deposited) diamond**

- **persistent currents due to trapping** → slow dynamics

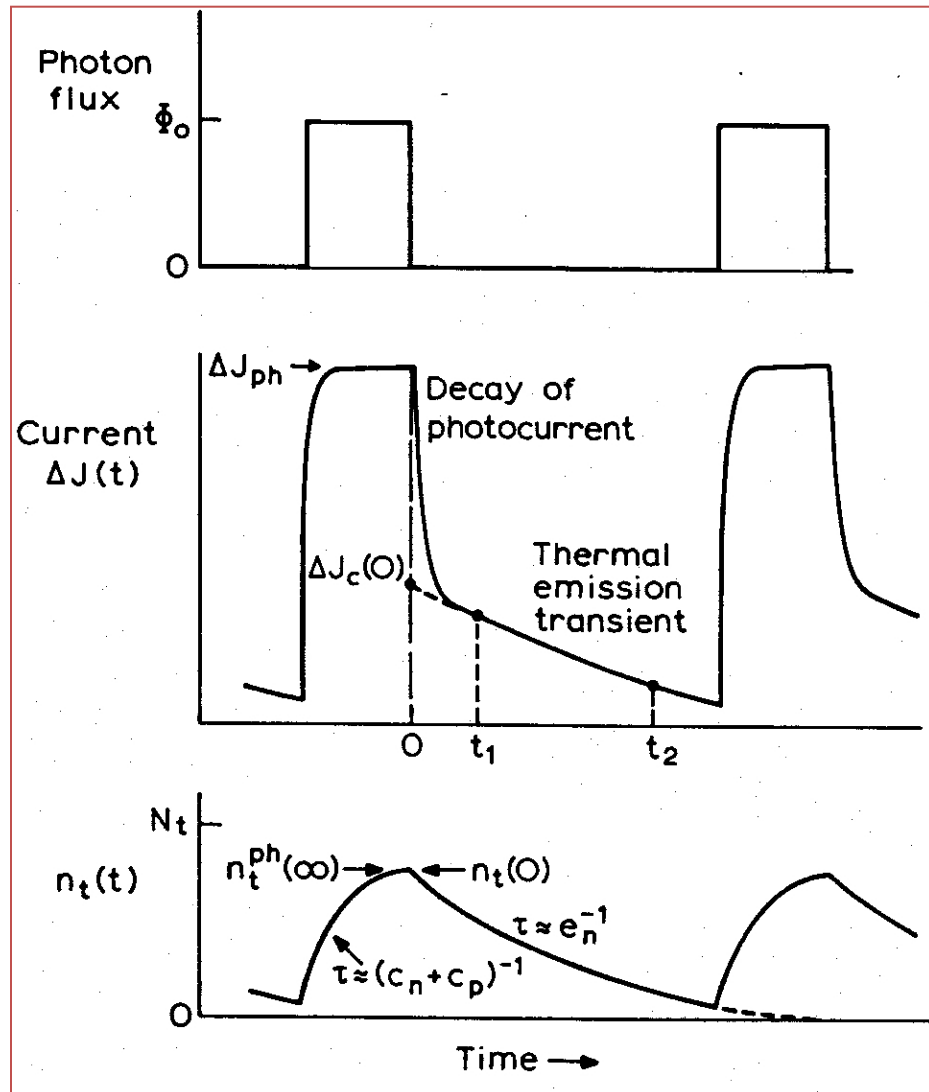
- grown on HPHT diamond, not available in large areas



# Transient Photoconductivity

Carriers trapped and released by defects also contribute to the transient photoconductivity with time constants depending on capture and emission coefficient.

→ Defects and recombination centres affects the dynamic response of the device



Neutron irradiation in pCVD diamond beneficial as removes dominant defect and increase recombination centres, bringing to faster dynamics

Measurements of pCVD diamond photoresponse under different cycles of X-ray irradiations

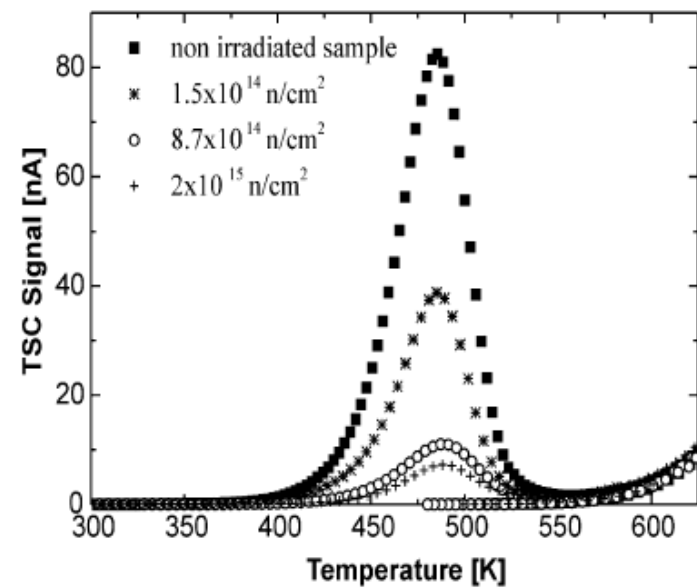
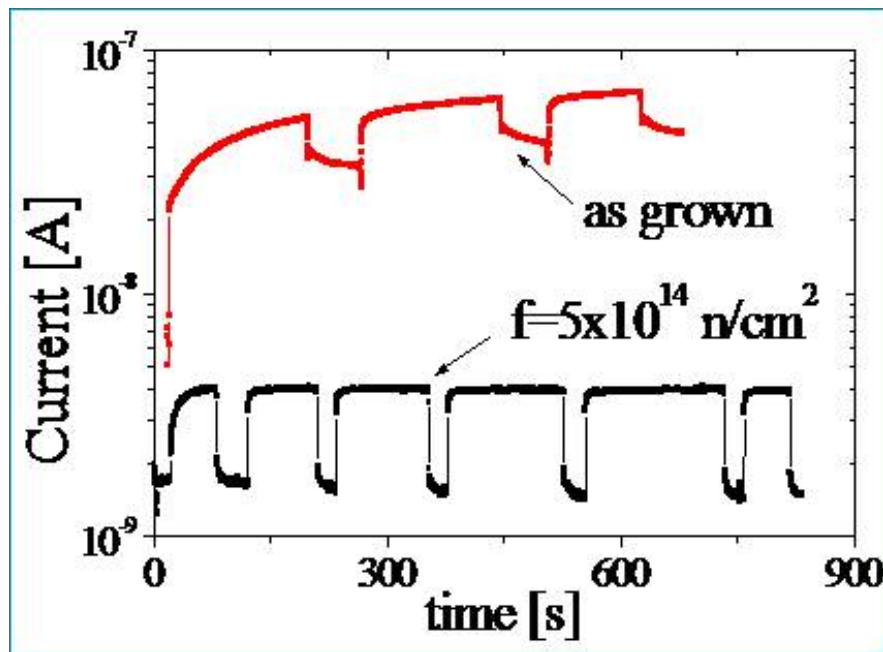
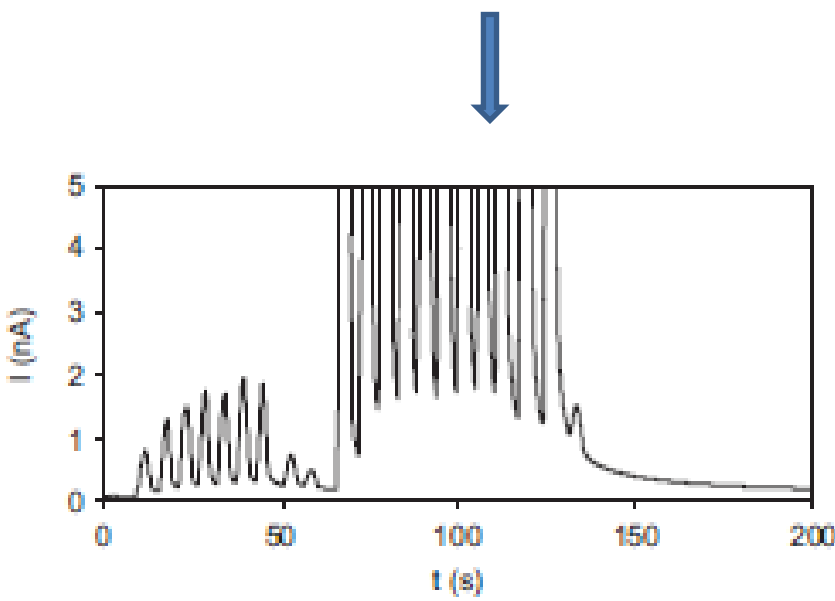


Fig. 1. TSC signal vs. temperature for non-irradiated and irradiated samples, after filling with UV xenon lamp for 20 min. The samples are biased with 100 V. The heating rate is 0.15 K/s. The neutron fluences are indicated in the legend.

M. Bruzzi et al., Appl. Phys. Lett, (2002)

**Priming and instability effects due to trapping and polarization in pCVD are dominant at high voltage with ohmic contacts and high electric field applied.**

Slow dynamics due to persistent currents in pCVD in conventional beam and in IMRT modality



C. De Angelis et al. / Nuclear Instruments and Methods in Physics Research A 583 (2007) 195–203

**Polarization is negligible at low/zero bias operation when using Schottky contacts.**

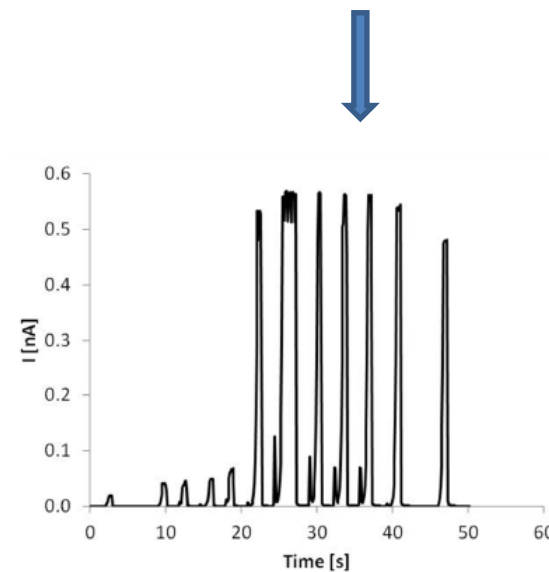
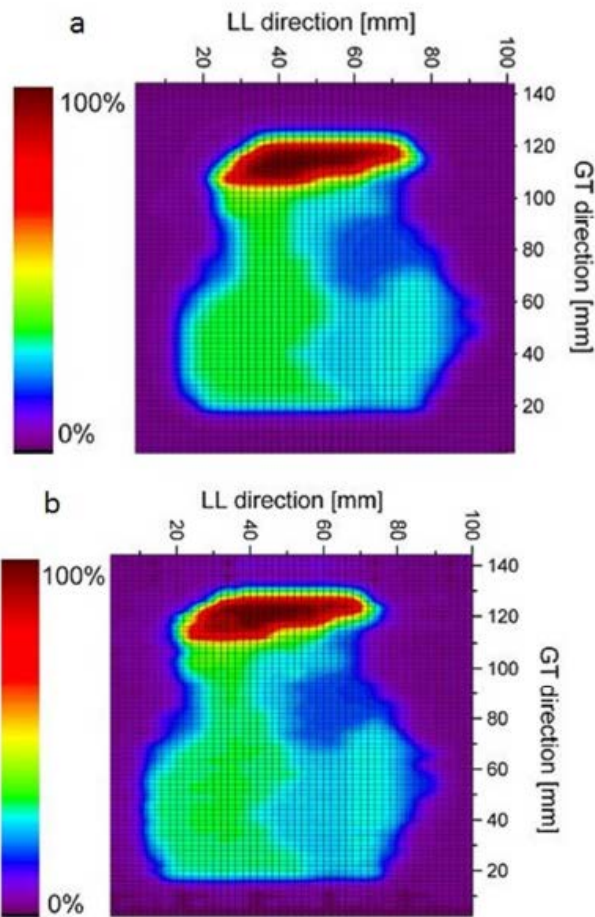
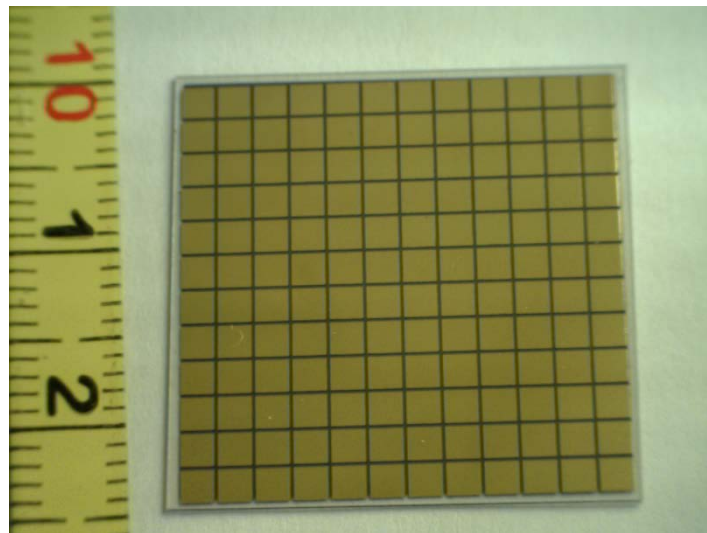


Fig.5 Time structure of the IMRT segments as measured by one of the pCVD diamond pixels under an IMRT prostate cancer treatment.

M. Scaringella et al. / Nuclear Instruments and Methods in Physics Research A in press

# First dose-map measured with a polycrystalline diamond 2D dosimeter under an intensity modulated radiotherapy beam

M. Scaringella<sup>a,\*</sup>, M. Zani<sup>b,c</sup>, A. Baldi<sup>d</sup>, M. Bucciolini<sup>b,c</sup>, E. Pace<sup>b,e</sup>, A. de Sio<sup>b,e</sup>, C. Talamonti<sup>b,c</sup> and M. Bruzzi<sup>b,e</sup>



M. Scaringella et al. / Nuclear Instruments  
and Methods in Physics Research A in press

Fig.6 (a) IMRT breast cancer map as measured by the pCVD Diamond bidimensional dosimeter (GT = gantry target direction; LL = lateral-lateral direction); (b) IMRT breast cancer map as calculated by the TPS. Grid spacing is 3 mm.

# Conclusions

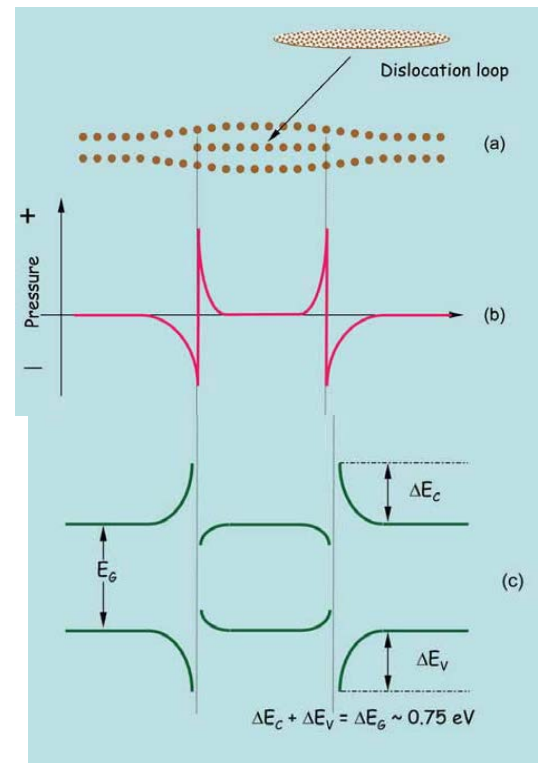
- Microscopic view of radiation damage is a useful tool to quantitatively explain macroscopic radiation damage in semiconductor devices. RD50 forum for development of Ultra Radiation Hard Semiconductor Detectors
- Defect Engineering approach successful in many different fields
- Best to work on the subject interdisciplinarily

# Other examples of Defect Engineering

- Dislocation Engineered LEDs

Semiconductor market dominated by silicon but due to indirect band gap fundamentally unsuited as optical emitter. Non-radiative recombination routes operate in parallel with the radiative route: point defects in the bulk and recombination at the surface.

Controlled introduction of an array of intrinsic extended defects – dislocation loops, to prevent electrically injected carriers from reaching the bulk defects and surface centers. When this loop is inserted into the Si lattice, the Si atoms outside the loop are pushed apart, introducing negative hydrostatic pressure. The potential in the conduction band energy is increased.



In a conventional device, carriers injected across the junction under forward bias diffuse into the bulk of the Si where they can reach bulk defects and the surface and recombine non-radiatively.

In the dislocation-engineered device we have spatially localized the carriers in a small region free of defects where we can efficiently inject carriers. That will recombine radiatively.

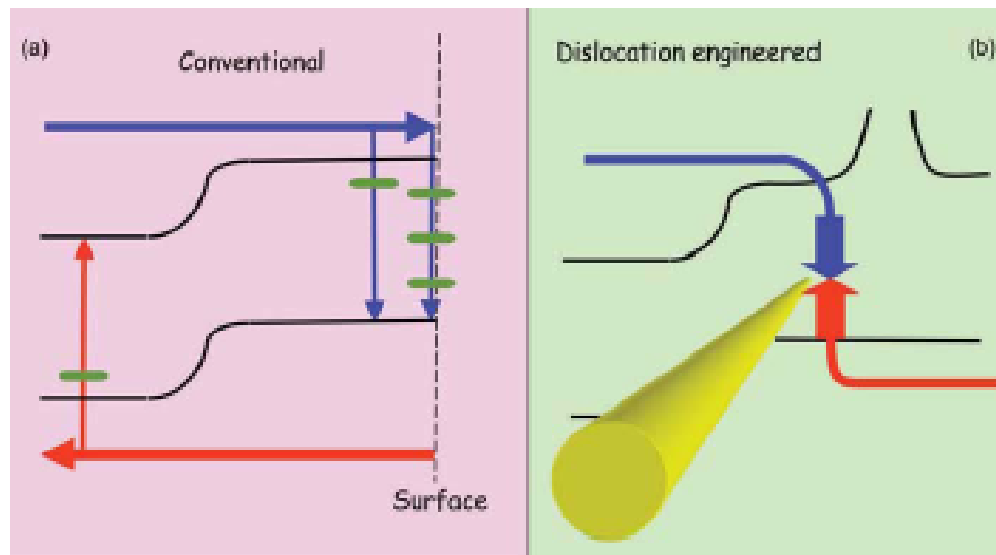


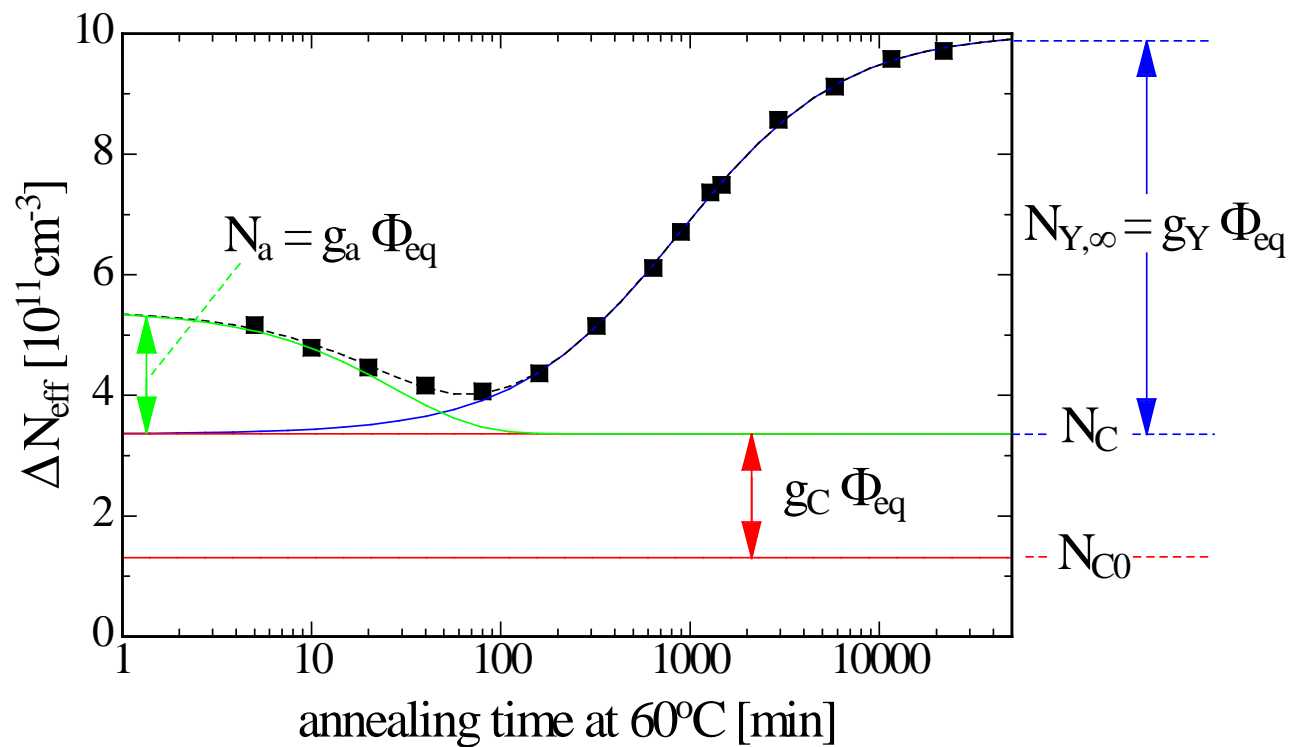
Fig. 6 Band diagrams illustrating (a) a conventional and (b) a dislocation-engineered diode. In (a), injected carriers diffuse to defects in the bulk and surface where they recombine nonradiatively. In (b), onward electron transport to the bulk and surface is prevented by spatial localization because of the loop-induced potential barrier. The carriers are only able to recombine radiatively.

# Annealing behaviour

Shallow removal      beneficial annealing      Reverse annealing

$$\Delta N_{\text{eff}} = N_{C0}(1 - e^{-c \cdot f}) + [g_c + g_a e^{-\frac{t}{\tau_a(T)}} + g_y(1 - e^{-\frac{t}{\tau_y(T)}})]f$$

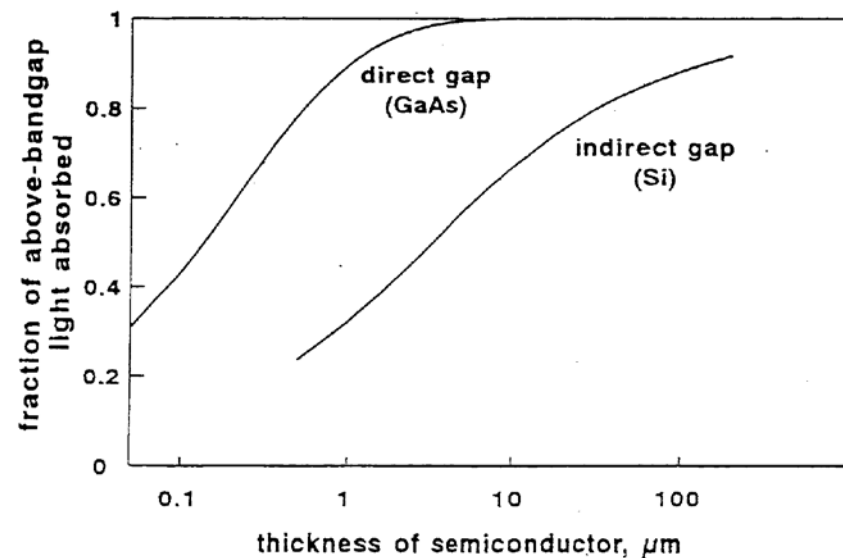
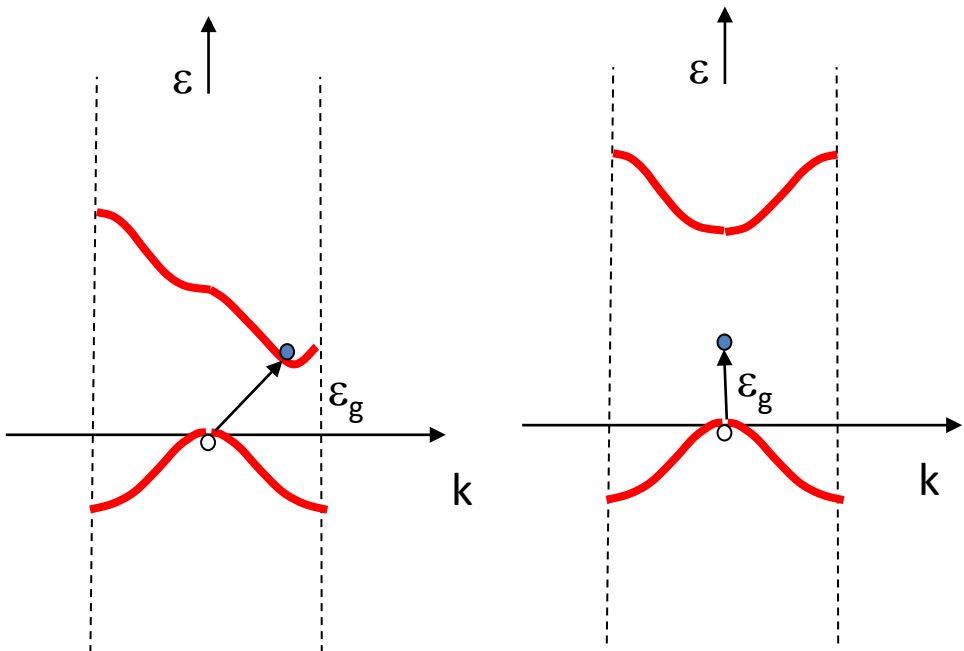
Stable damage



1. Shallow removal
2. Increase of acceptor-like defect
3. Presence of acceptor/donor pair to explain double junction
4. Changes in trap distribution with time/temperature

## 2. Gap indiretto

In un semiconduttore a gap indiretto l'elettrone che passa dalla banda di valenza a quella di conduzione oltre ad acquisire energia sufficiente dalla radiazione elettromagnetica deve variare il suo momento attraverso l'interazione con il reticolo.



Gap indiretto : Si

Gap diretto: GaAs

Il gap indiretto del silicio provoca un'inefficiente assorbimento ottico: è necessario uno spessore maggiore di materiale per ottenere la stessa frazione di luce assorbita. Il **Si non è quindi il materiale ideale per la conversione di energia solare in elettricità**

## Caratteristiche delle celle di seconda generazione: celle solari a film sottile

Nelle celle solari a film sottile la quantità di materiale usata è almeno 100 volte inferiore a quella usata per i moduli cristallini ed è una parte trascurabile del costo totale

### Coefficienti di assorbimento nel visibile

| Materiale                                                         | $\text{CuInSe}_2$ | $\text{CdTe}$  | Si amorfo      | Si cristallino |
|-------------------------------------------------------------------|-------------------|----------------|----------------|----------------|
| $\alpha \text{ (cm}^{-1}\text{) } (\lambda = 0,6 \text{ micron})$ | $1,2 \cdot 10^5$  | $1 \cdot 10^5$ | $2 \cdot 10^4$ | $6 \cdot 10^3$ |

Per materiali come diseleniuro di rame ed indio, tellururo di cadmio, silicio amorfo sono sufficienti spessori di circa 1 – 4 micron per assorbire completamente la luce, al contrario del silicio cristallino ove il coefficiente di assorbimento è circa due ordini di grandezza più basso. Per questo la quantità di materiale utilizzato è molto minore, con conseguente minor costo della cella.